REMOVAL OF METHYL MERCAPTAN FROM FOUL GAS BY IN-SITU PRODUCTION OF FERRATE(VI) FOR ODOUR CONTROL

DING LING

Ph.D
The Hong Kong Polytechnic University
2013

The Hong Kong Polytechnic University

Department of Civil and Environmental Engineering

REMOVAL OF METHYL MERCAPTAN FROM FOUL GAS BY IN-SITU PRODUCTION OF FERRATE(VI) FOR ODOUR CONTROL

DING Ling

A thesis submitted in partial fulfilment of
the requirements for the Degree of Doctor of Philosophy

November 2012

CERTIFICATE OF ORIGINALITY

I hereby declare that this thesis is my own work and that, to the best of my knowledge and belief, it reproduces no material previously published or written, nor material that has been accepted for the award of any other degree or diploma, except where due acknowledgement has been made in the text.

____________________(Signed)

DING Ling___________(Name of Student)

ABSTRACT

Offensive odour from sewage treatment works and other municipal waste management facilities generally cause nuisance to the adjacent neighbourhood. The growing awareness of people to odorous emissions has led governments set limits of odour exposures of the neighbouring residents. Methyl mercaptan (CH_3SH) is a representative member of sulphur species with a very low odour threshold of around 0.4 ppb/v. Compared with most dry processes, some wet processes are more suitable for treating these wet odorous gases in sewage treatment works. Ferrate(VI) as a powerful oxidant has a significant selectivity to oxidize sulphur-containing compounds rapidly. Using in-situ produced ferrate(VI) not only saves time and money on ferrate(VI) purification, but also saves steps in the transportation and storage of ferrate(VI) chemicals. This study demonstrated a new odorous gas treatment approach in a wet scrubbing/oxidation system with in-situ generation of ferrate(VI). In this approach, gaseous CH_3SH can be quickly absorbed by aqueous alkaline solution and rapidly oxidized by liquid ferrate(VI) generated through electrochemical synthesis in-situ.

Firstly, the electrochemical generation of ferrate(VI) in aqueous NaOH solution was studied. The related experiments demonstrated that the maximum current efficiency to generate ferrate(VI) occurred in 14 M NaOH solution, with the applied current density of 14.06 mA cm^{-2}. The self-decomposition of ferrate(VI) in such strong alkaline solutions was then studied. The results showed that the behaviour of ferrate(VI) was more stable in the stronger alkaline solution. This was the first time that the reactivity of ferrate(VI) with CH_3SH in the highly-concentrated NaOH solution had been investigated under different reaction conditions. The experimental results confirmed that CH_3SH can be fully oxidized by ferrate(VI) to sulphate ion (SO_4^{2-}) as a final product. It has been confirmed that the second-order reaction model is suitable to describe the kinetics of ferrate(VI) reaction with CH_3SH in the strong alkaline solution. Additionally, stoichiometry of ferrate(VI) reaction with CH_3SH in aqueous solution was determined with a minimum molar ratio of 2.20:1 (Fe(VI):CH_3SH) to fully destruct CH_3SH effectively and a higher molar ratio of 4.53:1 to completely convert CH_3SH to SO_4^{2-}.

Secondly, research effort was further focused on the kinetic models of the process named "In-situ Ferrate(VI) Oxidation (IFO)". Two kinetic models to describe the in-situ ferrate(VI) generation and its reaction with CH_3SH were established mathematically by considering three main reaction mechanisms of ferrate(VI) electrochemical generation, ferrate(VI) self-decomposition and CH_3SH degradation in aqueous strong alkaline solution. The effects of three key factors: (i) NaOH concentration, (ii) applied current density, and (iii) initial CH_3SH concentration on the performance of the IFO process were investigated in three sets of experiments, and the kinetic models were validated by fitting the experimental data. The goodness of the fittings demonstrated that the new models could well describe both the kinetics of ferrate(VI) generation reaction and

CH_3SH degradation reaction. The experimental results confirmed that the higher NaOH concentration and current density applied would be beneficial to ferrate(VI) electrochemical generation and also the elimination of its self-decomposition. The experiments also demonstrated an optimum NaOH concentration to achieve the best CH_3SH degradation performance at 10 M. This is a breakeven balance between the ferrate (VI) oxidation potential and ferrate(VI) generation rate in such an IFO system.

Finally, to evaluate the performance of this wet scrubbing/oxidation process with in-situ electro-generation of ferrate(VI) for removing odour from foul gas, a series of experiments were conducted. In this process, CH_3SH in synthetic gas is removed through absorption and oxidation by contacting the gaseous stream with aqueous NaOH electrolyte that offers in-situ generation of ferrate(VI). The process parameters including electrolyte concentration, applied current density, initial CH_3SH concentration, gas flow rate and gaseous CH_3SH compositions were investigated to conclude on the best operating conditions and design parameters for a scale-up design. Under all the experimental conditions, gaseous CH_3SH was completely removed by the wet scrubbing/oxidation process at room temperature and atmospheric pressure. The process proved to be quite effective for gaseous CH_3SH removal under the optimum experimental conditions at NaOH concentration of 6 M in electrolyte, current density of 2.22 mA cm^{-2} and CH_3SH loading below 30 g m^{-3} h^{-1}. A very short contact time of 0.06 s between the gas and the liquid phases was achieved in this in-situ ferrate(VI) generation reactor.

In summary, this research optimized the electrochemical production of ferrate(VI) and studied the reactivity of ferrate(VI) with CH_3S^- in details. Furthermore, kinetic models were successfully established and validated by the results of CH_3S^- degradation experiments. Based on the above work, gaseous CH_3SH removal was achieved by this wet scrubbing/oxidation process. From this study, we had better understanding of the removal of methyl mercaptan from foul gas by in-situ production of ferrate(VI) for odour control.

LIST OF PUBLICATIONS

Journal Papers

1. **Ding**, **L.,** Liang, H.C. and Li, X.Z. (2012) Oxidation of CH_3SH by in-situ generation of ferrate(VI) in aqueous alkaline solution for odour treatment. *Separation and Purification Technology* 91,117-124.
2. **Ding**, **L.,** Li, X.Z. and Lee, S.C. (2013) Kinetics of CH_3SH reaction with in-situ Ferrate(VI) in aqueous alkaline solution. *Chemosphere in press*.
3. **Ding**, **L.,** Liu, T.X. and Li, X.Z. (2013) Removal of CH_3SH with in-situ generated ferrate(VI) in a wet-scrubbing reactor. *Journal of Chemical Technology and Biotechnology accepted*.

Conference Papers

4. **Ding**, **L.,** Li, X.Z. and Liu, T.X. (2010）A Study of CH3SH removal in a photocatalytic scrubber for odour control. *2nd International Postgraduate Conference on Infrastructure and Environment*, June 1-2, 2010, Hong Kong.
5. **Ding**, **L.,** Li, X.Z. and Liang, H.C. (2010）Electrochemical preparation of ferrate(VI) and its reactivity with methyl mercaptan in aqueous solution for odour control. *The 16th International Conference on Advanced Oxidation Technologies for Treatment of Water*, Air and Soil, November 15-18, 2010, California, USA.
6. **Ding**, **L. and** Li, X.Z. (2010）Development of a new wet process for gaseous odour treatment in sewage treatment works. *TechConnect World 2011*, June 18-21, 2011, Santa Clara, California, USA.

ACKNOWLEDGEMENTS

I would like to express my deepest gratitude to my first supervisor, Professor X. Z. Li, for providing me with the unique opportunity to pursue my PhD and also for his generous support, excellent guidance and valuable discussions throughout the research project. I especially thank him for his selfless help after his retirement regarding problems both scientific and personal. I am also greatly indebted to my current supervisor, Prof. S. C. Lee, for his valuable suggestions. I would also like to express my sincere thanks to technicians, Mr. K. H. Ng, Mr. W. S. Lam and Mr. C.W. Lau, in the Water and Wastes Laboratory for their kind of help in instrumental usage and chemicals provision. I am very grateful to Drs. H.C. Liang, T. X. Liu, S. Y. Yang and other friends for their constant encouragement and valuable advice over the past few years. In addition, the author also wishes to thank Mrs. Elaine Anson for her help in English writing.

I am especially grateful to my parents and my husband for their unwavering and immense support, encouragement and understanding throughout my doctoral studies. Finally, I would like to express my gratitude to the Research Committee of The Hong Kong Polytechnic University for providing me with a PhD scholarship.

TABLE OF CONTENTS

LIST OF FIGURES

LIST OF TABLES

CHAPTER 1 Introduction

1.1 Background

Over the past decades and related to rapid industrial and social development, increasing concerns have been raised globally and regionally over the effectiveness of controlling and preventing odour pollution problems. Volatile sulphur compounds are generally considered to be one of the most obvious contributors to sewage odours from sewage treatment works (Hwang et al. 1994, Mansfield et al. 1992). These sulphur compounds mainly include hydrogen sulphide, methyl mercaptan, dimethyl sulphide, dimethyl disulfide, methanethiol, carbon disulfide, and carbonyl sulphide. Due to their very low odour threshold value (ppb/v range), high toxicity, and potential corrosive effect, the presence of volatile sulphur compounds in waste gases deserves intensive attention. Hong Kong is notable for the atmospheric odour content., An example is provided by the process whereby seawater is used for toilet flushing in most areas. Due to the high sulphate content in the saline sewage, this results in the production of high concentrations of hydrogen sulphide which in turn leads to serious corrosion of sewer pipes and sewer odour (Chen and Leung 2000).

To remove this odour pollutant from the air, a number of technologies have been investigated, including adsorption with activated carbons (Newcombe et al. 2002, Tanada and Boki 1979), oxidation with catalysts (Liu et al. 2008), catalytic incineration (Chu et al. 2001), and biological alternatives (Myung et al. 1999).

However, there are various advantages and disadvantages of these techniques, as well as different degrees of cost effectiveness. Taking the use of adsorbents as an example, adsorbents have to be changed, disposed of or regenerated after certain time intervals. Among the technologies for odour control, the degradation of odorous compounds by advanced oxidation process (AOP) technique has been found to be effective. For example, TiO_2-based photocatalysis shows an effective deodorization behaviour (Kachina et al. 2006, Li et al. 2006), but some toxic by-products gases (such as SO_2 and CO) are always emitted during the photocatalytic process, leading to a negative impact on air quality. Hydrogen peroxide (H_2O_2) has also been employed to remove odorous sulphur compounds (Charron et al. 2004, Feliers et al. 2001), while H_2O_2 can be dangerous to handle and takes time to react. Therefore, the exploration of other effective and environment friendly oxidants are urgently needed for more effective odour control.

Ferrate(VI) species have been known for a long time as very powerful oxidizing agents, with the reduction potentials of 2.20 V at acidic pH and 0.72 V at alkaline conditions (Sharma et al. 2000). The rapid oxidation of ferrate(VI) to the environmentally benign Fe(III) species makes it suitable to be used in a wide range of applications (DeLuca et al. 1996). Ferrate(VI) is also a selective oxidant with a highly efficient oxidation performance for the degradation of a number of sulphur-containing compounds, such as inorganic oxysulphur compounds (Read et al. 2001), thiourea and thioacetamide (Sharma et al. 2000, Sharma et al. 1999),

H_2S (Sharma et al. 1997b). The half-lives for reactions of ferrate(VI) with these contaminants under excess ferrate(VI) conditions are in seconds to minutes with formation of non-hazardous products. Sulphide pollution is a potential risk in Hong Kong. Therefore the application of ferrate(VI), as a powerful chemical oxidant, shows great promise for odour control.

Several techniques have been reported for the synthesis of ferrate(VI) including thermal (Hives et al. 2008), chemical (Thompson et al. 1951) and electrochemical techniques (De Koninck et al. 2003, Licht and Yu 2005). In general, the prepared ferrate(VI) solutions are unstable, and easily undergo the self-decomposition by reduction to the Fe(III) species. Solid ferrate(VI) salts are stable, but they require complex synthesis processes and long synthesis time. In order to solve these problems, the in-situ electro-generated ferrate(VI) approach presents a potential alternative for water and wastewater treatment, particularly the odour treatment strategies. For example, in 2005 Licht and Yu (Licht and Yu 2005) first introduced an in-situ electrochemical formation of ferrate(VI) for water treatment. To the best of the author's knowledge, however, such an approach for odour control has not been previously reported before in the literature. In the present work, odour control of CH_3SH with in-situ electro-generated ferrate(VI) was investigated under high alkaline conditions.

1.2 Aims and Objectives

The aim of this study is to explore a new approach to treat gaseous odours in highly alkaline solution with in-situ production of ferrate(VI) through an electrochemical process for odour control. To maximize odour removal efficiency by this new approach, it is necessary to understand the interaction between in-situ ferrate(VI) generation and the reaction between ferrate(VI) and CH_3SH. Additionally, in this study, in order to optimize the best operating conditions and design parameters for a scale-up design, the efficiency on CH_3SH removal is characterized in a laboratory-scale unit in this study. The specific objectives of this study are given below:

The overall objective is to complete the first steps in the development of a reactor for odour control. Such a reactor should perform effectively and practically in a continuous process. Hence it is necessary to:

- determine the optimum conditions for electrochemical generation of ferrate(VI) under high alkaline condition
- study the characteristics of ferrate(VI) self-decomposing in an alkaline solution
- investigate the kinetics and the reaction mechanism of methyl mercaptan degradation with ferrate(VI) in an alkaline solution
- establish kinetics models to simulate the process of in-situ ferrate(VI)

oxidation

- set-up an absorption/oxidation scrubbing reactor and evaluate its performance by removal of CH_3SH with in-situ electro-generation of ferrate(VI)

1.3. Scope of the Thesis

To achieve the above objectives, the scope of the work includes:

- a comprehensive literature review including odour pollution, current techniques for odour control, ferrate(VI) oxidation technology
- electrochemical production of ferrate(VI) by examining the ferrate(VI) yield and current efficiency with anode materials, cathode materials and dissolved oxygen in a two-unit electrolysis cell
- optimization of electrochemical production of ferrate(VI) by determining the NaOH concentration and current density
- investigation of the characteristics of ferrate(VI) self-decomposition with different initial concentrations in different NaOH concentrations
- study of the kinetics of CH_3S^- reduction by ferrate(VI) in aqueous NaOH solution by stopped-flow technique
- study of the stoichiometry and mechanism of the reaction between CH_3S^- and ferrate(VI) in aqueous NaOH solution through identification and measurement of the main products
- establishment of models for in-situ ferrate(VI) oxidation and validation of the models with the results of the process variables, including NaOH

concentration, current density and initial CH_3S^- concentration

- design, setting-up an absorbance/oxidation scrubbing reactor for gaseous CH_3SH removal in a continuous flow mode and evaluation of its performance

1.4 Organisation of the Thesis

This thesis is divided into eight chapters.

The background information, objectives and scope of the thesis are covered in Chapter 1.

A comprehensive literature review related to this study is given in Chapter 2, including the source, reason and effect of odour pollution, current techniques for odour control, the property, application and preparation methods of ferrate(VI) chemical.

The experimental methods of this study are described in Chapter 3. The materials, preparation methods for in-situ ferrate(VI) generation both in one-cell and two-cell electrolysis reactor and the experiments of CH_3SH degradation by ferrate(VI) are also presented in this chapter. The final part of this chapter shows two experimental set-ups for CH_3SH removal in a continuous flow mode. Experimental details for the determination of ferrate(VI) and CH_3SH concentration are also given.

The work shown in Chapter 4 reports the electrochemical production of ferrate(VI). The effects of various experimental parameters including NaOH concentration, current density, cathode materials and SO_4^{2-} concentration on the ferrate(VI) yield were investigated

In Chapter 5, the oxidation of CH_3SH with ferrate(VI) in aqueous alkaline solution is explored. The kinetics study of ferrate(VI) reaction with CH_3SH is conducted by stopped-flow system. The reaction mechanism and pathway of CH_3SH degradation through the identification of the main intermediate products are proposed.

Modelling of in-situ ferrate(VI) oxidation is discussed in Chapter 6. Two kinetic models to describe the in-situ ferrate(VI) generation and its reaction with CH_3SH are established mathematically by considering the key reaction mechanism. The new models are validated by the experiments of CH_3SH degradation on the effect of current density, NaOH concentration and initial CH_3SH concentration.

In chapter 7, a wet scrubbing process with in-situ electro-generation of ferrate(VI) has been developed for removing odour from foul gas in wastewater treatment plants. In this process, CH_3SH in synthetic gas is removed through absorption and oxidation by contacting the gaseous stream with aqueous NaOH electrolyte that offers in-situ generation of ferrate(VI). The process parameters including electrolyte concentration, applied current density, initial CH_3SH concentration, gas flow rate and gaseous CH_3SH compositions were investigated to find the best operating conditions and design parameters for a scale-up design.

The general conclusions obtained are summarized in Chapter 8 based on the experimental studies and data analyses. The recommendations and suggestions for future research on odour control are proposed.

CHAPTER 2 Literature Review

2.1 Odour Pollution

Odour, which refers to offensive smells, is considered as an important environmental pollution issue. It is a complex mixture of many organic and some inorganic chemicals. Up to 330 different chemicals belonging to a range of chemical classes including volatile fatty acids, aldehydes and ketones, nitrogen, heterocycles, reduced sulphur compounds and phenols were identified in odour samples derived from various sources such as sewage treatment works, refuse transfer stations, landfill sites, stormwater nullars and many other sources in an urban city like Hong Kong, which can cause a nuisance to adjacent populations and contribute significantly to atmospheric pollution. So attention to odour as an environmental nuisance has been growing as a result of increasing industrialization and the awareness of people's need for a clean environment.

Water and wastewater treatment process, as one of the most important contributors, produces odours from the biodegradation of sewage, especially anaerobic degradation. Odours are generated by a number of different wastewater components, the most significant being the sulphur compounds, hydrogen sulphide (H_2S) and mercaptan. Sulphurous compounds are responsible for acid rain and mist, airborne public health concerns, as well as environmental problems. This situation is particularly serious in the coastal cities where seawater infiltration occurs or seawater toilet flushing is practiced. Seawater with high sulphate content and high salinity is finally collected in the municipal wastewater treatment plant. Thus, massive hydrogen sulphide is formed in the plant. For example, serious corrosion of the sewage tunnels occurs in Hong Kong, since seawater toilet flushing is normal practice. Besides Hong Kong, it is also forecast that the use of seawater in other coastal cities of China will reach 55 billion tons per year in 2010 and 100 billion tons per year in 2020, respectively. Therefore, a cost-effective method for sulphurous compounds control in wastewater treatment plant is important both in Hong Kong and the Mainland.

Mercaptans are known as odorous, toxic pollutants which are disagreeable to our environment (Bashkova et al. 2002). In the author's study, methyl mercaptan was chosen as the representative compound with its very low odour threshold of around 0.4 ppb/v, high toxicity, and potential corrosive effect (Bashkova et al. 2002, Kastner et al. 2003, Li et al. 2005c). A long-term exposure to low levels of CH_3SH can result in harmful health effects. So, removing or conversion of these to harmless materials is significantly important. As a consequence, efforts to abate odour problems are necessary in order to maintain the quality of the environment and it is necessary to develop effective and compact deodorization systems.

2.2 Current Techniques for Gaseous Odour Treatment

The most commonly used treatment processes for gaseous odour control include (i) physical processes such as condensation, adsorption (activated carbon), and absorption (clean water scrubbers); (ii) biological processes such as biofilters and bioscrubbers; and (iii) chemical processes such as chemical scrubbers, thermal oxidation, photocatalytic oxidation, ozone oxidation, etc.

2.2.1 Physical Processes

Adsorption is the process whereby the molecules of odorous compounds bind to the solid surfaces. It must be distinguished from absorption, whereby odorous compounds are dissolved in clean water. In the absorption process, the removal efficiency is mainly controlled by the solubility of the substances in water. Here we focus on the adsorption process.

Among the available adsorbents (silica gel, activated carbon, zeolites, activated alumina, synthetic resins, etc.), activated carbon adsorption has been widely employed in the removal of solvents, volatile organic compounds (VOCs), odours and gaseous components due to its large surface area, microporosity, and surface chemistry (Turk et al. 1989). A variety of materials can be the source of activated carbon, which are through dehydration and carbonization under slow heating in the absence of air and lastly activation by oxidation at high temperatures (200℃ to 1000℃). Generally, there are two kinds of activated carbon: granular and powdered. The features of activated carbon play an important role.

Tanada and Boki (Tanada and Boki 1979) investigated the adsorptive capacity of various kinds of offensive odour substances on porous adsorbents. However, physical adsorption is a reversible process. High molecular weight compounds are more easily adsorbed than low molecular weight molecules, which may be displaced by the subsequent adsorption of heavier compounds. Therefore the treatment capacity of AC for an odour mixture depends on its capacity for the least easily adsorbed component. Hwang et al. (Hwang et al. 1994) proved that AC provides a much higher sorption capacity toward volatile sulphur compounds than volatile nitrogen compounds.

Chemical oxidation is usually applied after physical adsorption to enhance the removal capacity, since AC provides a catalytic surface for oxidation. It was reported that methyl mercaptan can be oxidized by oxygen and hydroxyl radicals created on the surface of the activated carbon (Katoh et al. 1995). To optimize odour abatement, it has been pointed out in the literature that different functional groups on the carbon surface (Bansal et al. 1988) or/and metal ions such as iron can catalyze oxidation of mercaptans to disulfides (Dalai et al. 1997, Ziolek and Decyk 1999). Bagreev et al. (Bagreev et al. 2005) reported that the introduction of basic nitrogen groups enhanced the capacity of carbons for methyl mercaptan removal.

2.2.2 Biological Processes

The principle of bio-techniques for odour control is the sorption of volatile contaminants in an aqueous phase or biofilm, where the biodegradation of these sorbed pollutants occur. In general, these systems include biofilters, bioscrubbers, and biotrickling filters (Smet et al. 1998).

In a biofilter, the humidified gas is forced through a bed packed with an organic carrier material (compost, peat, bark, or a mixture of these), where microorganisms are attached as a biofilm. In a bioscrubber, the waste gas is pumped into a wet scrubbing tower and then the contaminated water phase is cleaned in a bioreactor. In a biotrickling filter, the waste gas is forced through a packed bed filled with a chemically inert carrier material allowing microbial colonization. Contrary to biofilters, bioscrubbers and biotrickling filters can only treat contaminated compounds with a low air-water partition coefficient (lower than 0.01 and 1, respectively). Laboratory and field studies are summarised on the biodegradation of a wide range of pollutants in biofilters and biotrickling filters (Iranpour et al. 2005). Compared with H_2S abatement, the removal efficiency for other organic sulphur compounds in biotechnological waste gas treatment systems is rather low and variable (Kasakura and Tatsukawa 1995, Phae and Shoda 1991, Smet et al. 1996, Tanji et al. 1989). Bonnin et al. (Bonnin et al. 1994) employed sea mineral as a biofilter carrier material for H_2S removal at very low gas residence times. Numerous H_2S converting microorganisms can be applied (Cho et al. 1992, Jensen and Webb 1995).

2.2.3 Chemical Processes

The traditional chemical technologies for gaseous odour treatment include thermal oxidation and chemical oxidation. Besides them, UV-treatment, ozone oxidation or non-thermal plasma, have been investigated in the last few years.

2.2.3.1 Thermal Oxidation

Incineration can be basically applied to any gaseous wastes. Typically it is for exhaust air which is highly concentrated in low value combustible vapours. Incineration is a very efficient but expensive waste gas technology when pollutant concentrations are low. Generally, there are two kinds of thermal treatment: catalytic and non-catalytical techniques. The difference between them is that lower temperatures needed in the catalytical processes. That is to say that thermal incineration requires temperatures up to 700 to 1000 ℃ with gas residence times of 0.5 to 1 s, while catalytic incineration can take place at 300 to 450 ℃ (Paillard and Blondeau 1988). The addition of catalyst may considerably result in lower energy demand, while the costs for the catalyst itself have to be taken into account.

Sulphide-containing compounds are commonly combustible molecules, so they can burn in air at temperature above 1000 K. The final product is essentially SO_2, which is also a toxic substance and the main cause of acid rain. Therefore it is obvious to see the drawbacks of thermal waste gas treatment, not only the high operating costs but also the formation of secondary pollutions.

2.2.3.2 Chemical Oxidation

A number of oxidants are available to control odours in chemical scrubbers, including hydrogen peroxide, sodium hypochlorite and so on. Such chemicals have been used successfully for odour control in sewage collection systems and for reducing odour emissions from sludge storage and dewatering processes

Hypochlorite is considered as the most efficient oxidant for the chemical scrubbing (Van Durme et al. 1992). Hypochlorite has three species depending on the pH of the reaction solution, including: hypochlorite (OCl^-, $pH > 6$), hypochlorous acid (HOCl, pH 2-6), or chlorine water (Cl_2, $pH < 2$). The oxidation potential of HOCl with organic sulphur compounds is higher than that of OCl^-. However, hypochlorite oxidation produced strong chlorine and burnt organic odours at too low pH values ($pH < 4.5$). While the use of chlorine dioxide (ClO_2) as an oxidant is more expensive compared with hypochlorite. Moreover, ClO_2 produces toxic chlorine and chlorine dioxide in the exit gas.

In order to avoid the formation of chlorinated species which are harmful for human health, H_2O_2 seems to be a good substitute for NaClO due to its ability to oxidize odorous pollutants without generating harmful oxidation by-products (Feliers et al.

2001). In fact, H_2O_2 is well known to show high decomposition efficiency in basic aqueous solution. The parameters promoting this decomposition contain pH, high temperatures, and transition metal and carbonate ions in solution (Colodette et al. 1988, Galbács and Csányi 1983, Špalek et al. 1982). Charron (Charron et al. 2004) showed a good removal of hydrogen sulphide (up to 98%) using sodium silicate as the stabilizer in the reaction solution, while the best elimination rate for CH_3SH of 45%. Oxidation by H_2O_2 alone is not effective for high concentrations of certain refractory contaminants, such as highly chlorinated aromatic compounds and inorganic compounds (e.g., cyanides), because of low rates of reactions at reasonable H_2O_2 concentrations.

2.2.3.3 Photocatalytical Oxidation

Recently, the degradation of odorous compounds by advanced oxidation processes (AOPs) has attracted much attention because of the complete degradation of toxic and poorly biodegradable organic contaminants into mineral products (Canela et al. 1999, Li et al. 2004). Among AOPs, the photocatalytic oxidation of various organic compounds has been proposed to be an effective process for wastewater treatment and also air purification.

The principle of photocatalytic reactions is based on charge separation, which is induced in large band gap semiconductor by excitation with ultra band gap radiations

(Rideh et al. 1997). When the absorption of light by the photocatalyst is greater than its band gap energy, a positively charged hole in the valence band and an electron in the conduction band are produced (Thompson and Yates 2006). The hole in the valence band may react with water or hydroxide ion absorbed at the surface to form hydroxyl radicals, while the conduction band electron can reduce absorbed oxygen to form peroxide radical anion that can further disproportionate to form hydroxyl radicals through various pathways (Thompson and Yates 2006). Hydroxyl radical, the primary oxidant, is a strong, non-selective oxidant with a high oxidation potential of 2.8 V, which is a powerful oxidant in degrading organics in water. The oxidation processes with OH radicals has been applied successfully to mineralize toxic and hazardous organic micropollutants to inorganic materials or convert them to readily biodegradable intermediates (Alberici and Jardim 1997, Hoffmann et al. 1995, Li and Li 2001).

Studies involving gas-phase photocatalysis are of growing interest because of the potential application to contaminant control in contained air atmospheres as found in aircraft and spacecraft, office buildings and factories. Pichat et al. (Pichat et al. 2000) studied the removal rate of three different pollutants (CO, n-octane, pyridine) using 365 nm UV lamp and a TiO_2-coated fibre glass mesh. Li et al. (Li et al. 2005c) reported that the CH_3SH in foul gas can be successfully degraded by photocatalytic oxidation under UV-A irradiation with TiO_2-based photocatalysts, particularly by NH_4^+-TiO_2 catalyst. Photocatalytic degradation of an odorous chemical, 2-mercaptobenzothiazole (MBT), in aqueous suspension was also investigated using pure TiO_2 and neodymium ion doped TiO_2 (Nd_3^+-TiO_2) catalysts (Li et al. 2005b).

2.2.3.4 Ozone Oxidation

Ozone has been widely applied in the treatment of municipal and industrial wastewaters and the disinfection of drinking water due to its high oxidation potential (2.08eV) (Chu and Ma 2000, Graham et al. 2003, Hoigné and Bader 1983a, b). However, ozonation process is highly selective since high electrophilicity and selectivity of the reaction between O_3 and organic compound lead to organics with electron donor substituent group (e.g. OH and CH_3) showing higher reactivity toward ozone and organics with electron-withdrawing substituents (e.g. Cl and NO_2) having lower ozone reactivity (Hoigné and Bader 1983a). In the water phase, sulphur-containing compounds are efficiently oxidized with ozone (Hwang et al. 1994), while gas phase oxidation reactions are usually too slow to be of interest, except for H_2S (Anderson 1984). As O_3 is a sparingly soluble gas, specialized techniques are required to achieve a high degree of dissolution. For complete H_2S and MeSH removal in emissions of a WWTP, Laplanche et al. (Laplanche et al. 1994) measured an O_3 consumption of 0.8 to 3.5 and 1.5 kg × kg^{-1} VSC, respectively, yielding a significantly lower reagent cost compared with hypochlorite oxidation. Recently, De Guardia et al. (De Guardia et al. 1995) described the use of silicon oil as a scrubbing liquid for the absorption of MeSH and Me_2S_2 from the gas phase. The absorbed sulphur compounds were subsequently oxidized with O_3, while the metabolites of the oxidation process were extracted from the solvent phase by water injection. The silicone oil used was stable toward O_3.

2.2.3.5 Plasma Technology

The basic mechanism of non-thermal plasma technology is by using strong alternating electrical currents or microwave radiation to induce highly activated molecules. Thus, reactive radicals and ions are subsequently formed and degrade the odorous compounds. However, excess ozone, a secondary pollutant, is simultaneously produced either non-thermal plasma or UV radiation process.

The results of applying a RF (radio frequency) cold plasma method showed different removal efficiencies of methanethiol (CH_3SH) at different O_2/CH_3SH ratios (0-4.5), with various input powers (20-90 W), and at constant operating pressure (30 Torr), in which the reaction mechanisms in the decomposition of CH_3SH also involved (Tsai et al. 2001). However, the required electrical power increases strongly with increasing contaminant concentrations, which indicts this technology can only be capable for low concentration range. This result was verified by using a microwave reactor, high efficiencies for the treatment of a gas containing 10% ethanol were only obtained at an electrical power corresponding to 14.5 kWh m^{-3} (I et al. 2004).

2.3 Current Techniques for Odour Elimination in Wastewater

Generally speaking, there are two methods to prevent odour emission from sewer systems. One involves increasing the redox potential by air/oxygen injection or addition of nitrate, thus decreasing sulphur production. The other is chemical removal sulphide by adding chemicals as precipitations or oxidants, such as iron salts, H_2O_2, chlorines and potassium permanganate.

2.3.1 Air or Oxygen Injection

Some studies revealed that the adequate presence of dissolved oxygen in sewers, as an ideal electron acceptor, could be effective in removing organic matter (Boon and Lister 1975, Bryers and Characklis 1990). At anoxic environment dissolved sulphide will convert to dissolved hydrogen sulphide, which is a well-known odour problem (Agency 1985, Tanaka and Takenaka 1995). Therefore, dissolved oxygen cannot only prevent hydrogen sulphide production but also remove organic matters in wastewater treatment.

In general, dissolved oxygen levels should be maintained above 0.5 mg L^{-1} which prevents sulphide formation (Agency 1991), by applying air injection or by pure oxygen to force mains and wet wells (Tanaka et al. 2000). The drawback of air injection is the incomplete dissolving of air in water under normal pressures. (Agency 1992). Pure oxygen is better to achieve higher dissolved oxygen levels than air (Chen and Leung 2000, Delgado et al. 1998). However, pure oxygen is classified as an explosive chemical and pose hazardous risks. Special precautions should be required.

2.3.2 Addition of Nitrate

The inhibition effect of nitrate on sulphide production has been known for many years. In 1932, sodium nitrate was already reported for odour control (Carpenter 1932). The effect of nitrite on both transient and long-term inhibition of sulphide production have been reported (Allen 1949, Beardslay et al. 1958, Poduska and Anderson 1981).

This prevention can be caused by the attribution to the increase in redox potential caused in the presence of nitrate. It was reported that nitrate addition could control sulphide generation in a wastewater lagoon as long as enough nitrate was added initially to raise the redox potential of the lagoon above 300 mV (Poduska and Anderson 1981). Another possible reason have been reported that addition of nitrate in a septic wastewater biologically oxidizes dissolved sulphide via autotrophic denitrification by sulphur-oxidizing denitrifying bacteria such as Thiobacillus denitrificans and Thiomicrospira denitrificans. Under anoxic condition, S^0 can be accumulated as end product in a biological oxidation reactor, with NO_3^- as the electron acceptor (Yang et al. 2005)

2.3.3 Precipitation by Iron Salts

Dosage of iron salts of chloride (Haaning Nielsen et al. 2005, Nielsen et al. 2005) or nitrate (Padival et al. 1995) have been widely used for the abatement of sulphide -associated problems, either in ferric or ferrous forms. The reaction mechanisms of these two forms with sulphide are different. The reaction of ferrous with sulphide is by precipitation of sulphide to ferrous sulphide (FeS), while ferric can remove sulphide by oxidizing it to elemental sulphur while being reduced to Fe(II), which can subsequently produce FeS (Zhang et al. 2008). The main advantage by using iron salts is the low cost, while the drawback is that iron salts are not effective in removing any other odorous compounds except H_2S.

The addition dosage of iron salts in practical application relies heavily on empirical experience and field studies shows a very high dosage of iron salts is recommended for sulphide reduction, much higher than the stoichiometric ratios (Jameel 1989, Padival et al. 1995). It was reported that ferrous chloride to be more than twice as effective in controlling the dissolved sulphide concentration compared to ferric chloride (Jameel 1989), while Tomar and Abdullah (Tomar and Abdullah 1994) reported the iron dosage for complete sulphide control was 20% lower for the ferric salt solution than the ferrous salt solution. Padival et al. (Padival et al. 1995) observed that a mixture of ferric and ferrous iron salts exhibited better sulphide removal efficiency than that of either salt by itself.

2.3.4 Addition of Oxidants

Hydrogen peroxide (H_2O_2) and chlorine have been used to oxidize sulphide to sulphate or to elemental sulphur in wastewater. It was reported that a proper ratio of H_2O_2 at 1.3–4.0 mg H_2O_2 L^{-1} to 1 mg S L^{-1} can achieve 85–100% elimination of sulphide. Due to the short lifetime of H_2O_2 (less than 90 min) (Agency 1991), it may be better to add the chemical at several points along the sewers. The high operation and maintenance costs using hydrogen peroxide should be considered. Chlorine in the form of gas or sodium hypochlorite can oxidize sulphide to sulphate or to elemental sulphur depending on pH in wastewater (Agency 1992). According to chlorine existing form, different ratios of chlorine to sulphide have been required (Agency 1991, Tomar and Abdullah 1994). Due to the possibility of forming chlorinated by products, chlorine is not commonly preferred for odour control. Potassium permanganate ($KMnO_4$), as a strong oxidant, converts sulphide to sulphate. It is recommended that a feeding of 6% solution in water is used for odour control (Agency 1991). The drawback of $KMnO_4$ is still the high cost.

2.4 Summary of Current Techniques

The most important physical, chemical and biological treatment processes for odour are described in detail and their favourable applications, as well as their limits are highlighted in this Chapter. Biological processes seem to be the most potential technique for sulphur-containing compound removal practice. However, the system usually occupies vast space and only limits kinds of pollutants with low concentration can be treated. The additional regeneration processes are badly needed in physical treatment for high concentration pollutants. Traditional chemical processes, such as chemical dosing with nitrate salts or iron salts, or their combination ($FeCl_3$, $FeCl_2$, $Fe(NO_3)_3$, $Fe_2(SO_4)_3$) is wildly used for minimizing the sulphide-associated odour emission in sewer systems. On the other hand, many chemical oxidation technologies have been reported to be efficient for odours control from wastewater and sludge by adding chemical oxidants such as hydrogen peroxide, chlorine, hypochlorite, potassium permanganate. The newly explored techniques, non-traditional chemical processes, exist uncertainties to some extent.

In the view of the Hong Kong situation, chemical oxidation process was employed in this study. However, most chemicals used in the plants have residual odour and there are also concerns of unwanted oxidation products such as toxic chlorinated by-product from chlorination. Therefore it is necessary to seek an alternative chemical oxidation agent with nontoxic by-product. Ferrate(VI), a powerful and green oxidant, has a potential to abate these limits.

2.5 Ferrate(VI) Oxidation Technology

2.5.1 Characteristics of Ferrate(VI)

In common, iron exists in 2^+ and 3^+ oxidation states, however, higher oxidation states could be obtained, such as 6^+. Ferrate(VI) species have been known for a long time as very powerful oxidizing agents, with the reduction potentials of 2.20 V at acidic pH and 0.72 V at alkaline conditions (Lee et al. 2004). The rapid oxidation of ferrate(VI) to the environmentally benign Fe(III) species makes them suitable to be used in a wide range of applications: selectively organic synthesis, water and wastewater treatment, and super-iron batteries. In the area of environmental application, ferrate(VI) plays dual functions in the remediation of pollutants in wastewater treatment as a powerful oxidant and coagulant.

Potassium ferrate(VI) is a black-purple powder and its aqueous solution has a characteristic violet (red purple) colour. The molecular formula of ferrate(VI) ion is FeO_4^{2-}. Ferrate(VI) has a tetrahedral structure, since it shows that four Fe-O bonds are equivalent with covalent character according to an X-ray powder pattern study (Hoppe et al. 1982). Three hybrid resonance structures of ferrate(VI) in aqueous solution were proposed (Fig. 2-1) (Norcross et al. 1997). Thermodynamic constants of potassium ferrate(VI), such as heat, entropy and free energy, were first reported by Wood (Wood 1958).

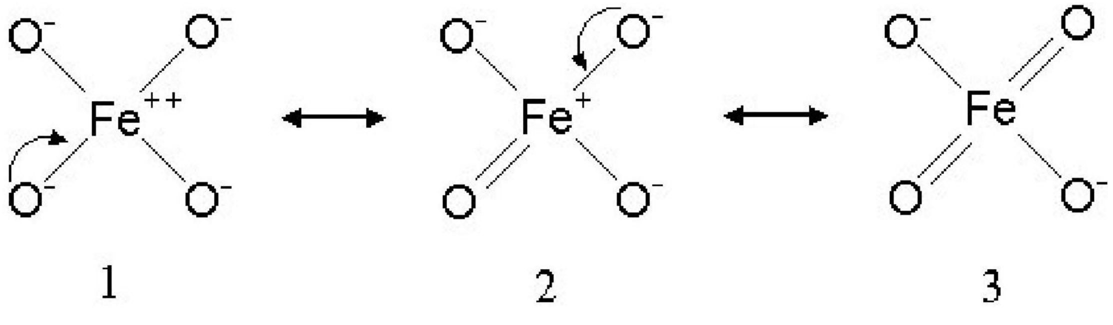

Figure 2-1 Hybrid resonance structures proposed for ferrate(VI) in aqueous solution

(Norcross et al. 1997)

Ferrate(VI) in aqueous solution has four forms depending on pH, Eqs. (1-3) and the fractions of each form as shown in Fig. 2-2. From Fig. 2-2, we can see that $HFeO_4^-$ and FeO_4^{2-} are the dominant species in mildly acidic condition and alkaline condition.

$H_3FeO_4^+ \rightarrow H^+ + H_2FeO_4^{2-}$ pK_a = 1.6 (Licht et al. 2001) (1)

$H_2FeO_4 \rightarrow H^+ + HFeO_4^-$ pK_a = 3.5 (Licht et al. 2001, Sharma 2002) (2)

$HFeO_4^- \rightarrow H^+ + FeO_4^{2-}$ pK_a = 7.3 (Licht et al. 2001, Sharma 2002) (3)

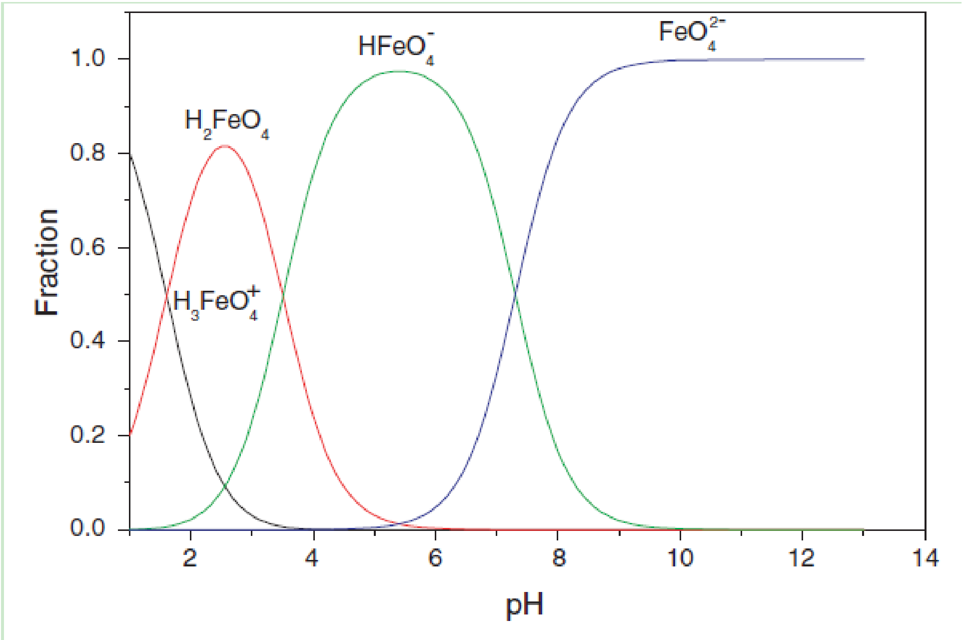

Figure 2-2 Variation of ferrate(VI) species depend on pH (Delaude and Laszlo 1996)

2.5.2 Preparation Methods of Ferrate(VI)

Several techniques have been reported for the synthesis of ferrate(VI) including: thermal, wet chemical and electrochemical techniques.

Wet chemical method

The most commonly employed method of ferrate(VI) production is wet chemical synthesis (Ayers and White 2005, Licht et al. 2002a). It is by oxidizing ferric ions to form ferrate(VI) in the presence of hypochlorite or chlorine. However, the self-decomposition of ferrate(VI) is very rapid in acid and neutral media. The high purity of ferrate(VI) from wet chemical method is difficult to obtain. Considering the less solubility of potassium salt, sodium hydroxide was replaced by potassium hydroxide to precipitate the potassium ferrate(VI) from the solution mixtures. Williams and Riley (Williams and Riley 1974) improved the purity of potassium ferrate to 80~90% in 1974. Li et al. (Li et al. 2005a) reported a high purity (99%) of solid phase potassium ferrate(VI) with a high yield (50–70%) by an improved procedure for preparing. Recently some studies reported that ozone as an alternative oxidizing agent was used to form ferrate(VI) in 5M NaOH solution (Perfiliev et al. 2007). Various iron compounds can be used as a source of Fe^{3+} ions, e.g., β-Fe_2O_3, $Fe_2(SO_4)_3$ or $FeSO_4 \cdot 7H_2O$ (Deininger 1993). The basic chemical reactions involved are as follows:

$$KMnO_4 + 8HCl \rightarrow MnCl_2 + 5/2Cl_2 \uparrow + 4H_2O + KCl \quad (4)$$

$$Cl_2 + 2KOH \rightarrow KClO + KCl + H_2O \quad (5)$$

$$Fe(NO_3)_3.9H_2O + 5KOH + 3/2KClO \rightarrow 3/2KCl + 23/2H_2O + K_2FeO_4 + 3KNO_3 \quad (6)$$

Thermal method

Stahl (Stahl 1715) was the first one to synthesis ferrate(VI) using thermal chemical method. Recently effects have been made by different investigators, where potassium or sodium ferrate(VI) is prepared by heating/melting iron or iron oxide (Fe_2O_3 or Fe_3O_4) to a range of 500–650℃ with strong alkali metal oxide, peroxide, or nitrate salt under oxygen flow (Thompson 1983, 1985). The resulting product is considered to contain FeO_5^{4-} anions which are instantaneously hydrolyzed when dissolved in water to form a tetrahedral ion FeO_4^{2-}, resulting in a red-violet solution.

$$FeO_5^{4-} + H_2O \rightarrow FeO_4^{2-} + 2OH^- \quad (7)$$

Fe^{3+} salts can be oxidized to ferrate(VI) by K_2O_2 producing from the reaction between molten KOH and ambient atmosphere. The principle of the reaction is as follows:

$$4KOH + O_2 \rightarrow 2K_2O_2 + 2H_2O \quad (8)$$

In addition, solid sodium peroxide can only be employed directly to form ferrate(VI) in a muffle furnace at 800℃.

$$Fe_2O_3 + 3Na_2O_2 \rightarrow 2Na_2FeO_4 + Na_2O \tag{9}$$

Electrochemical method

Many studies have been carried out on the mechanism of ferrate(VI) generation and the optimization of ferrate(VI) yield. The basic principle of generation is shown in Eqs. (10-12) (Bouzek and Roušar 1993, Jiang and Lloyd 2002, Lapicque and Valentin 2002, Licht et al. 2001).

Anode reaction: $Fe + 8OH^- \rightarrow FeO_4^{2-} + 4H_2O + 6e$ (10)

Cathode reaction: $3H_2O \rightarrow 3H_2 + 6OH^- - 6e$ (11)

Overall reactions: $Fe + 2OH^- \rightarrow FeO_4^{2-} + 3H_2 + H_2O$ (12)

Various synthesis parameters have been systematically studies on preparing ferrate(VI) salts, including: (1) anode materials; (2) separator; (3) alkaline electrolyte; (4) anodic current density; (5) temperature and (6) electrolysis time etc.

Electrolyte solution may include a hydroxide selected from sodium hydroxide, potassium hydroxide, lithium hydroxide, cesium hydroxide, barium hydroxide and combinations between them. As previously reported, NaOH electrolytes support higher solution ferrate(VI) production rates and current yields (Bouzek and Roušar 1993) at low temperature. Therefore, in most solution phase ferrate(VI) generation studies at low temperature and NaOH was generally used as the alkaline electrolyte (De Koninck and Belanger 2003, De Koninck et al. 2003, He et al. 2006, Licht et al.

2002b, 2004).

Some researchers (Bouzek et al. 1999b, Bouzek et al. 1996b) studied the effect of anode material composition on the ferrate(VI) solution phase generation. They used raw iron, steel and cast iron as anode materials, which contains different carbon contents at a current density 10 A m^{-2} and NaOH concentration of 16.5 M. The results showed that the highest current yield was obtained using a cast iron anode containing 3.16% C in the form of iron carbide (Fe_3C), T=20℃ and 14 M NaOH. Another study showed that high silicon content in the gray cast iron improved current yields to be in the range of 20–40% depending on the applied current density (Lescuras-Darrou et al. 2002).

The geometry of the anode, especially its specific surface, can yield a significant enhancement of production rates. Some studies (De Koninck and Belanger 2003, Denvir and Pletcher 1996, Lescuras-Darrou et al. 2002) reported the utilization of three-dimensional iron anodes in the form of iron wool (Castle 1954), cast iron chunks (Lescuras-Darrou et al. 2002), and pressed iron powder pellets (De Koninck and Belanger 2003) in order to increase the surface area available for the reaction. Another reason for the increase of the current yield by using pure iron powder (pellet), it could positively influence the formation of passive layer. Ding et al. (Ding et al. 2004) further studied the important of porosity in the ferrate(VI) generation using a porous magnetite (Fe_3O_4) electrode.

Anodic passivation involves a firm film developed on the surface of the anode which prevents the pathways of electrons flow and then stops the electrolytic process. The following methods have been proposed for pre-treatment of electrode: (i) mechanical polishing of the electrode before experiments, (ii) chemical etching of the electrode (Beck et al. 1985, Bouzek and Roušar 1993) and (iii) cathodic pre-polarization (Toušek 1962).

2.5.3 Application of Ferrate(VI) in Environment and Industry

Potassium ferrate(VI), an environmentally friendly oxidant, has properties such as oxidizing power, selectivity, and a non-toxic by-product. Many of the contaminants in wastewater can be removed by ferrate(VI) in seconds to minutes with formation of non-hazardous products. Ferrate(VI) is also a selective oxidant for a large number of organic compounds. Fe(III), as the by-product of ferrate(VI) has a role in cleaner technology for coagulation. Other application of ferrate(VI) include 'super-iron' batteries. Hence, ferrate(VI) is a disinfectant, oxidant, coagulant, and therefore a promising multi-purpose wastewater treatment chemical. Due to the topic of my study, this paper focus on ferrate(VI) as a chemical oxidant in environmental and industrial removal of contaminants.

Oxidation with ferrate(VI)

Ferrate(VI) is a powerful oxidizing agent throughout the entire pH range. Under acidic condition, it is potentially the strongest of all the oxidants realistically applicable to water and wastewater treatment shown in Table 2-1 (Lee et al. 2004)

Table 2- 1 Reduction potential of ferrate(VI) and other oxidants used in water treatment (Lee et al. 2004)

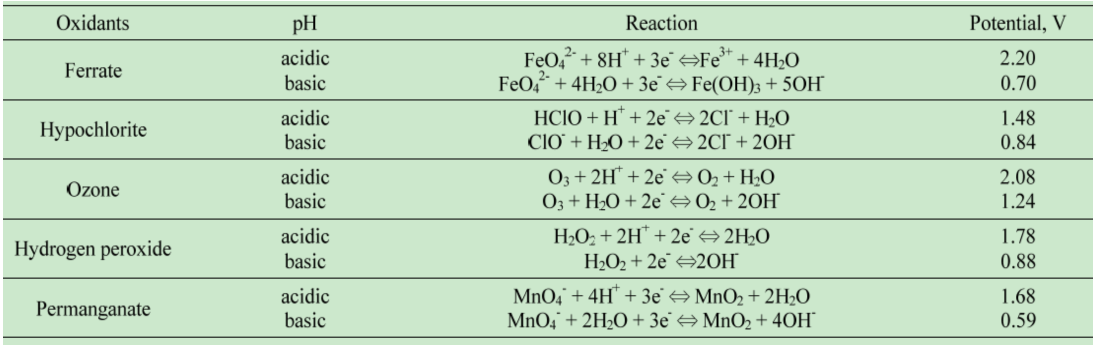

Oxidants	pH	Reaction	Potential, V
Ferrate	acidic	$FeO_4^{2-} + 8H^+ + 3e^- \Leftrightarrow Fe^{3+} + 4H_2O$	2.20
	basic	$FeO_4^{2-} + 4H_2O + 3e^- \Leftrightarrow Fe(OH)_3 + 5OH^-$	0.70
Hypochlorite	acidic	$HClO + H^+ + 2e^- \Leftrightarrow 2Cl^- + H_2O$	1.48
	basic	$ClO^- + H_2O + 2e^- \Leftrightarrow 2Cl^- + 2OH^-$	0.84
Ozone	acidic	$O_3 + 2H^+ + 2e^- \Leftrightarrow O_2 + H_2O$	2.08
	basic	$O_3 + H_2O + 2e^- \Leftrightarrow O_2 + 2OH^-$	1.24
Hydrogen peroxide	acidic	$H_2O_2 + 2H^+ + 2e^- \Leftrightarrow 2H_2O$	1.78
	basic	$H_2O_2 + 2e^- \Leftrightarrow 2OH^-$	0.88
Permanganate	acidic	$MnO_4^- + 4H^+ + 3e^- \Leftrightarrow MnO_2 + 2H_2O$	1.68
	basic	$MnO_4^- + 2H_2O + 3e^- \Leftrightarrow MnO_2 + 4OH^-$	0.59

As discussed in the characteristic of ferrate(VI), ferrate(VI) in aqueous solution has four species with pH variation. In accordance with that, the redox potential for each form is summarized by the Pourbaix diagram in Fig. 2-3 (Wulfsberg 2000). It can be seen that a high oxidation potential of ferrate(VI) was found in acidic conditions. That is the reason why the self-decomposition of ferrate(VI) is faster with lower pH.

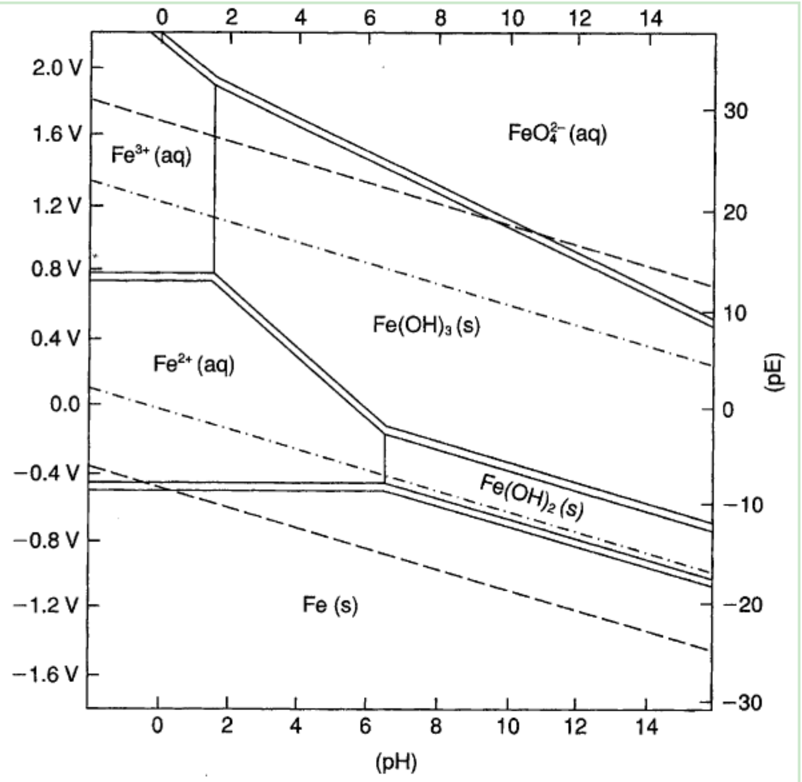

Figure 2-3 Pourbaix diagram for 1 M iron solution (Wulfsberg 2000)

It has been shown that ferrate(VI) has a high efficient oxidation performance for the degradation of a number of organic compounds. The investigated organic compounds included nitrogen-containing compounds, sulphur-containing compound and other organic compounds. Nitrogen-containing compounds were summarized by Sharma (Sharma 2010a), including amino-acids (Sharma and Bielski 1991), hydroxylamines (Johnson and Hornstein 2003), hydrazines (Johnson Michael et al. 2008), azide (Carr James 2008), amines (Carr James 2008) and anilines (Johnson and Hornstein 1996). Sulphur-containing compounds were also investigated (Sharma et al. 2011). The other organic compounds were nitrosamines compounds (Bartzatt and Nagel 1991), recalcitrant organics (Gulyas 1997), carboxylic compounds (Bielski et al. 1994), phenol and chlorophenol (Graham et al. 2004), endocrine disrupting chemicals (EDCs)

(Jiang et al. 2005). All of these compounds strongly depends on the dose of ferrate(VI) and the pH values of the solution. Moreover, the maximum oxidation efficiency was achieved when the molar ratios of the ferrate(VI) to organic impurities were in the range of 3:1-15:1 (Jiang and Lloyd, 2002).

Many studies also showed the oxidation of inorganic pollutants with ferrate(VI). Cyanide (Osathaphan et al. 2009, Sharma et al. 1997a, Sharma et al. 1998b) can be oxidized in few minutes in aqueous wastewater (Tiwari et al. 2007). More than 22% of ammonia (Sharma et al. 1998a) can be removed when the molar ratio of ferrate(VI) to ammonia is greater than one. 99.9% of hydrogen sulphide (He et al. 2009, Sharma et al. 1997b) is removed by ferrate(VI) from groundwater and wastewater. Arsenite (Jain et al. 2009) is oxidized to As(V) by aqueous solutions of ferrate(VI).

Disinfection with ferrate(VI)

Chlorination is the most famous and the frequently used disinfectant in water treatment technology. Other disinfectants, including bromine, iodine, chlorine dioxide, and ozone, also have been employed to kill the harmful organisms and to control/remove the odour precursors. However, the formation of by-products, which are toxic to some extent to the human population and to aquatic life, was discovered in succession. Therefore, other alternative disinfectants are needed, not only to achieve higher treated water quality but also to be environmental friendly.

The disinfecting properties of ferrate(VI) were first reported by Murmann and Robinson in 1974 (Murmann and Robinson 1974), who found that ferrate(VI) could completely destroy bacteria with a lower content in water. Therefore the application of ferrate(VI), as a great potential disinfectant, was extensively investigated for final purifying of municipal water. Many studies showed that ferrate(VI) can inactivate effectively Escherichia coli (E. coli), coliforms and viable bacteria (Gilbert et al. 1976, Waite 1979). Studies of the effect of the ferrate(VI) on virus removal were also investigated, such as f2 virus and coliphage Qß (Kazama 1995, Schink and Waite 1980). In addition, the disinfection ability of ferrate(VI) seems less sensitive to the variations in temperature, pH and the organic content of the disinfecting medium than chlorine or bromine.

Coagulation with ferrate(VI)

Ferrate(VI) also have been proven an efficient coagulant, since Fe(III) ions or ferric hydroxide are produced during the oxidation of organic matter and microorganisms in water.

Compared with the most common coagulants, including ferric sulphate, aluminium sulphate, and ferric chloride, the coagulation performance of ferrate(VI) has been studied in the following areas. Firstly, the performance of turbidity removal with ferrate(VI) was better than ferrous sulphate and ferric nitrate (Gray and Waite 1983, Solo and Waite 1989). Many studies showed that ferrate(VI) can remove a range of metals (e.g., Fe^{2+}, Fe3+, Mn^{2+}, and Cu^{2+}) and toxic heavy metals (e.g., Pb^{2+}, Cd^{2+}, Cr^{3+}, and Hg^{2+}) to a low level (Bartzatt et al. 1992, Murmann and Robinson 1974). In addition, ferrate(VI) also can be applied for reducing radioactive wastes in wastewater (Potts and Churchwell 1994, Stupin and Ozernoi 1995). Finally, the same colour removal percentage can be achieved at relatively lower dosages of ferrate(VI) compared with the ferric coagulant (Jiang and Lloyd 2002).

Other application with ferrate(VI)

Ferrate(VI) is also a selective oxidant which can be used in the field of organic synthesis. Recent studies have shown that it can selectively oxidize some functional groups of organic compounds successfully. For example, ferrate(VI) can synthesis aldehydes and ketones from alcohols and aldehydes from amines (Audette et al. 1972, Tsuda and Nakajima 1978, Williams and Riley 1974). The development of ferrate(VI) as an selectively oxidant can replace the traditional toxic oxidants, such as managanate, chromate and ruthenate oxides, for a green technology for organic synthesis.

The storage capacities of the commonly batteries, comprising alkaline (KOH) and metal hydride (MnO_2), are largely limited, due to the lower discharge capacity of cathode. The field of solid ferrate(VI) compounds called 'super-iron', as high capacity batteries, are first introduced in 1999 (Licht et al. 1999). Since this kind of battery produces three electrons via reduction, which enabled the battery provide 50% more energy capacity than the conventional alkaline batteries. It was also reported that 'super-iron' batteries have better conduction of electricity and recharge ability. In addition, the super-iron batteries are based on environmentally benign compounds.

2.5.4 Potential of Ferrate(VI) Oxidation for Gaseous Odour Control

As mentioned at the beginning of this Chapter, high level of sulphate is usually contained in local sewage in Hong Kong due to seawater is used for toilet flushing. More sulphur in sewage leads to produce more hydrogen sulphate under de-oxygenated condition. Ferrate(VI) is a desirable agent to removal odour, not only its high reactivity and nontoxic by-product, but also selectivity over traditional oxidants. Because ferrate(VI) has a significant selectivity to oxidize sulphur-containing compounds rapidly.

Solid ferrate(VI) salts are stable, but they are costly as they require multiple chemical reagents and long synthesis time. This makes it difficult to be used in industry. In order to solve the problems of instability and the high cost of using ferrate(VI), it would be an ideal approach to generate ferrate(VI) in-situ and apply the generated ferrate(VI) directly. However, ferrate(VI) can only be electrochemically generated in extremely high alkaline solution, which is not easy to apply in wastewater treatment due to high influence to wastewater pH. Foul gas containing odorous compounds such as H_2S or mercaptans can be quickly absorbed by alkaline aqueous solution and immediately oxidized by ferrate(VI) in the solution. Therefore in-situ electrochemical production of ferrate(VI) would be a suitable technique for gaseous odour control.

CHAPTER 3 Methodology

3.1 Introduction

In this chapter, the methodology regarding the whole study is described, where the detailed descriptions of experimental set-ups and reactors for in-situ ferrate(VI) generation and CH_3SH removal are given. Some important chemicals and reagents used in this study are listed. The sampling and analytical methods of probe compound can be found in this chapter. In addition, some other instruments used to determine the solution parameters (e.g. ORP and pH) are also provided

3.2 Materials

3.2.1 Chemicals

All the chemicals used in this study are summarized in Table 3-1. The stock solutions were prepared in deionized and distilled water with a resistivity of 18.2 MΩ from a Bamstead NANO pure water treatment system (Thermo Fisher Scientific Inc., USA).

Methyl mercaptan gas from a certified gas cylinder with a traceable concentration of 2000 ppm/v balanced in nitrogen was supplied by BOC Gases and used as an odour source. Pure iron sheet with Fe content of >99% plus 0.3% Mn, 0.1% Si, 0.08% C, 0.04% P, 0.05% S was bought from Goodfellow Cambridge Limited.

Table 3-1 List of chemicals used in this study

Chemicals	MW, g mol^{-1}	Formula	Purchased from
Sodium methanethiolate (95%)	70.09	CH_3SNa	Sigma Aldrich Inc.
Ellman's regent	396.35	$C_{14}H_8N_2O_8S_2$	Pierce Biotechnol. Inc.
EDTA	292.24	$(HO_2CCH_2)_2NCH_2CH_2N(CH_2CO_2H)_2$	Sigma Aldrich Inc.
Potassium chromate	194.19	K_2CrO_4	Aldrich
Barium chloride dihydrate	244.26	$BaCl_2 \bullet 2H_2O$	Sigma Aldrich Inc.
Ammonia	35.05	$NH_3.H_2O$	Aldrich
Disodium hydrogen phosphate	141.96	Na_2HPO_4	Aldrich
Sodium dihydrogen phosphate	119.98	NaH_2PO_4	Aldrich
Sodium Sulfate (99%)	142.04	Na_2SO_4	Sigma Aldrich Inc.
Sulfuric acid	98.08	H_2SO_4	Tedia
Nitric acid	63.01	HNO_3	Tedia
Potassium ferrate(VI) (97%)	198.04	K_2FeO_4	Aldrich
Sodium hydroxide (99%)	40.00	$NaOH$	Sigma Aldrich Inc

3.2.2 Buffer Solution

Phosphate buffer solutions were prepared for ferrate(VI) measurement. The buffer solution was prepared by dissolving disodium phosphate (Na_2HPO_4), sodium dihydrogen phosphate (NaH_2PO_4), and sodium phosphate (Na_3PO_4) in DDW. All the chemicals are commercially available from Aldrich. The properties of these phosphate salts are given in Table 3-2. The stock phosphate buffer composition is given in Table 3-3.

Table 3-2 Dissociation constants of phosphoric acid in aqueous solutions (Beynon and Easterby 1996)

Chemical name	T, ℃	Ka	pKa
H_3PO_4	25	7.5×10^{-3}	2.12
NaH_2PO_4	25	6.2×10^{-8}	7.21
Na_2HPO_4	18	2.2×10^{-13}	12.67

Table 3-3 0.1 mol/L phosphate buffer composition (25℃)

pH	1mol/L Na_2HPO_4 (ml) per liter	1mol/L NaH_2PO_4 (ml) per liter	Remarks
7.6	84.5	15.5	
7.8	89.6	10.4	
8.0	93.2	6.8	1 mM EDTA

3.3 Equipment and Experimental Procedures

3.3.1 Electrochemical Synthesis of Ferrate(VI)

The electrochemical synthesis of solution-phased ferrate(VI) was carried out in a two-cell unit with an effective volume of 80 mL for each cell, in which an iron sheet was used as the anode and a platinum sheet/stainless steel was applied as the cathode. It has been reported that aqueous NaOH solution is a more preferred electrolyte for rapid production of ferrate(VI) than equimolar KOH or LiOH solution under the same electrical conditions (Bouzek et al. 1999a). An explanation may be the different solubilities of ferrate(VI) and its intermediates such as Fe(II) and Fe(III) in the different electrolytes (Yu 2008). Therefore, aqueous NaOH solution was prepared in our experiments. The production of ferrate(VI) was operated by applying a current density in the range of 1.56-52.08 mA cm^{-2} at room temperature. Prior to the electrolysis, the iron sheet was first polished with abrasive paper and then washed with distilled water. The electrolysis process with constant current intensity in the NaOH solution was well controlled by a potentiostat/galvanostat power supply (ZF-9 DC, Zhengfang Electronics Company, China).

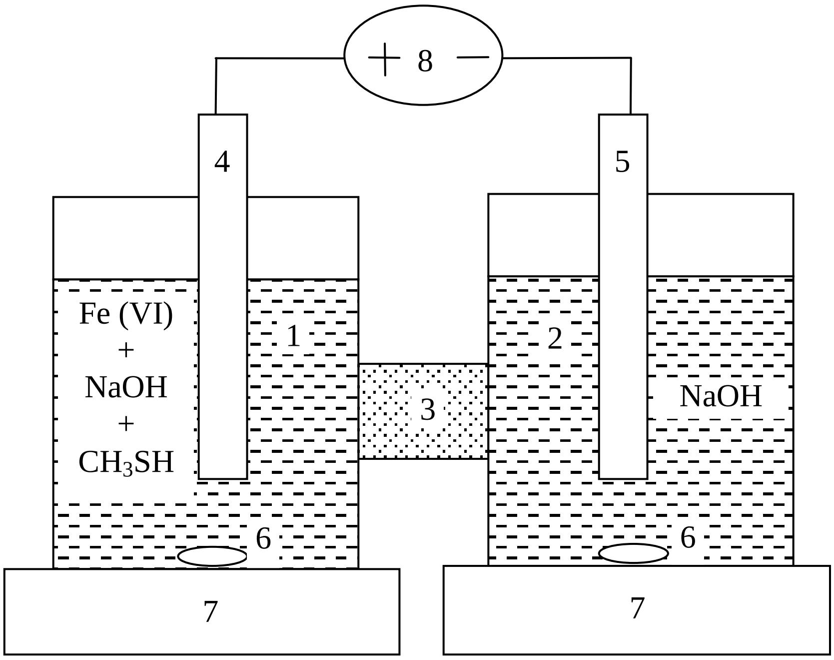

Figure 3-1 Electrochemical synthesis of ferrate(VI) in H cell: 1. Anodic compartment (a half cell); 2. Cathodic compartment (a half cell); 3. Glass frit; 4.Iron plate; 5. Platinum plate; 6. Stirring bar; 7. Magnetic stirrer; 8. DC power supply.

3.3.2 Experiments to Determine the Stability of Ferrate(VI)

To determine the stability of ferrate(VI) in the concentrated NaOH solution, a set of experiments was conducted to investigate the self-decomposition of ferrate(VI) in aqueous NaOH solutions at 20±1 ℃. The first experiment was conducted to investigate the effect of ferrate(VI) concentration on its self-decomposition in 3 M NaOH solution. The second experiment of the self-decomposition of ferrate(VI) was performed to investigate the effect of NaOH concentration in the range of 1.5-14 M. The aqueous NaOH solution, with an initial ferrate(VI) concentration of 0.145 mM, was obtained by electrochemical synthesis. The decline of Fe(VI) concentration in the solutions against time was monitored to determine the rates of ferrate(VI) self-decomposition at different NaOH concentrations.

3.3.2 Experiments of Kinetics Study Using a Stopped-Flow System

The stopped-flow instrument is a rapid mixing device, which is used to study the chemical kinetics of a reaction in solution. A stopped-flow spectrophotometer (SF-61DX2, Hi-Tech KinetAsyst Stopped-Flow System, UK) purchased from TgK Scientific equipped with a photomultiplier (PM) detector was used to perform the kinetic measurements under pseudo-first-order conditions with methyl mercaptan in excess. The stopped-flow unit comprised two syringes, one filled with ferrate(VI) solution the other with methyl mercaptan solution. The solutions entering the flow cell are only milliseconds old. Reactions were monitored by measuring the absorbance of ferrate(VI) at 510 nm wavelength as a function of time. The concentrations of methyl mercaptan in the experiments were more than 1.0~3.6 mM, while the ferrate(VI) concentrations ranged from 0.035 to 0.12 mM. Quadruplicate tests were conducted for each reaction and the reaction rate constants were calculated from the average values.

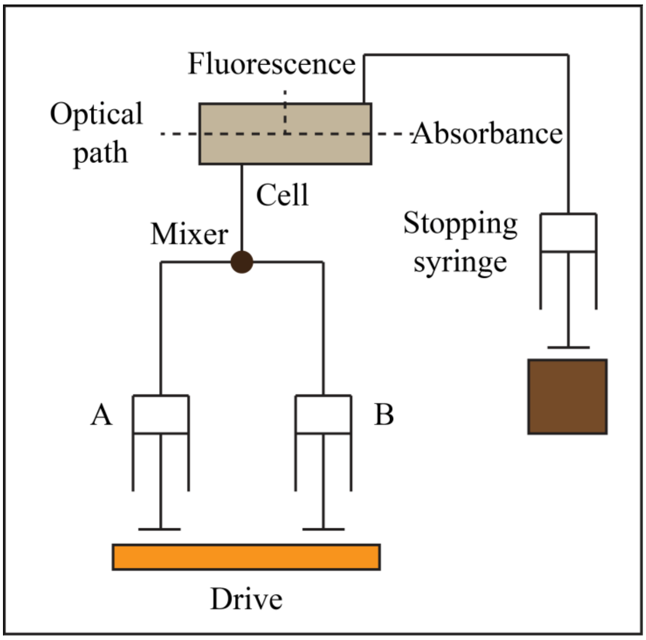

(a)

(b)

Figure 3-2 (a) Diagram of the Single mixing stopped flow (b) Photo of the stopped-flow spectrophotometer (SF-61DX2, Hi-Tech KinetAsyst Stopped-Flow System, UK).

3.3.3 Experiments of Stoichiometry Study

The stoichiometry of the ferrate(VI) oxidation with CH_3SH was examined in aqueous 10 M NaOH solution where the self-decomposition of ferrate(VI) could be neglect, because of a long half-life time of nearly 19 h. A series of experiments with the molecular ratios of $[Fe(VI)]/[CH_3SH] = 0$~4.72 were conducted, respectively, in which the prepared ferrate(VI) and CH_3SH solutions were mixed rapidly and completely.

3.3.4 Experiments of CH_3SH Degradation by Ferrate(VI)

The experiments of CH_3SH degradation by IFO were also conducted in the two-compartment cell containing aqueous NaOH solution, in which, a saturated mercury oxide electrode was applied as the reference electrode. Both the anode and reference electrode were placed in one compartment, while the cathode was placed in another compartment. Aqueous CH_3SH solution with an initial concentration in the range of 0.09-1.71 mM was prepared by adding CH_3SNa chemical into aqueous NaOH solution from 5 M to 14 M. When a constant electrical current of 1.56-5.63 mA cm^{-2} was supplied, ferrate(VI) was electrochemically generated in-situ and then diffused to the bulk solution and reacted with dissolved CH_3S^-. During the experiments, the reaction solution was continuously agitated by a magnetic stirrer to ensure its homogeneity throughout the reactor. Samples were withdrawn from the solution at predetermined time intervals for analysis to determine CH_3SH concentration against reaction time.

3.3.5 Experiments of CH_3SH Removal in a Continuous Gas Flow Mode

The experimental set-up was shown in Fig. 3-3. CH_3SH gas and air from cylinders at different ratios were simultaneously pumped into a surge flask, where they were mixed well with the required concentrations. Two mass flow controllers from the Sevenstar company were used to synthesize different CH_3SH concentrations. Two methyl mercaptan sensors from Detcon Inc. were equipped to monitor the inlet and outlet CH_3SH concentrations. A cylindrical reactor containing NaOH electrolyte was used as the wet scrubbing-oxidation reactor, in which an iron anode and a stainless steel cathode were positioned at its centre. The reactor has an effective volume of 120 mL. The synthetic CH_3SH gas was continuously pumped into the aqueous NaOH solution through an air diffuser from the bottom, and the solution was magnetically stirred to ensure good contact between the dispersed gas bubbles and the solution. The electrolysis process with a constant current intensity in the NaOH solution was well controlled by a potentiostat/galvanostat power supply (ZF-9 DC, Zhengfang Electronics Company, China).

In order to achieve shorter contact time between the gas and the liquid phases, an absorption scrubbing column was positioned before the oxidizing reactor in Fig. 3-5.

The aim of the pre-absorption column is to clarify the effect of CO_2 on NaOH consumption. As there is such a short gas-liquid phase residence time, the reaction between CO_2 and NaOH can be avoided.

The experiments for gaseous CH_3SH treatment were carried out in a wet scrubbing-oxidation reaction system equipped with two electrodes and filled with aqueous NaOH solution for simultaneous ferrate(VI) generation and CH_3SH degradation. The synthetic CH_3SH gas was prepared by mixing CH_3SH gas with air, nitrogen, and oxygen from the gas cylinders at different ratios and continuously pumped into aqueous NaOH solution through an air diffuser from the bottom, and the solution was magnetically stirred to ensure good contact between the dispersed gas bubbles and the solution.

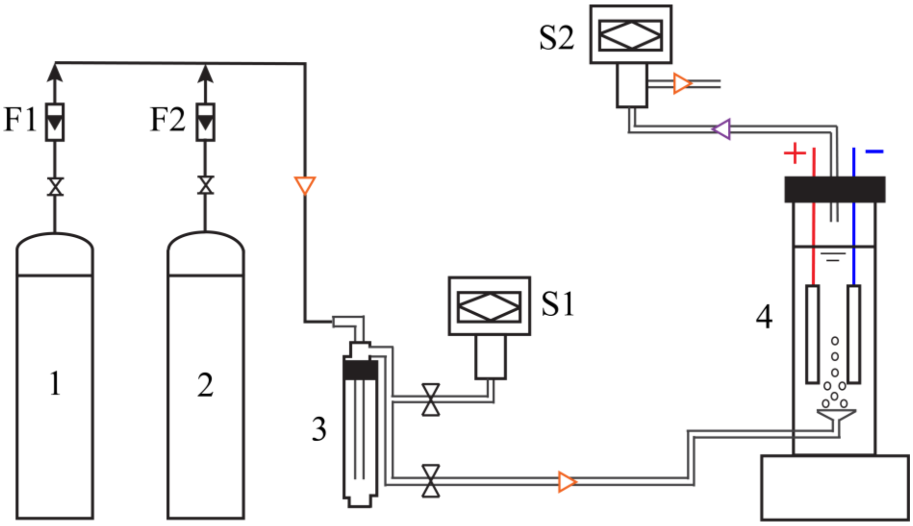

(a)

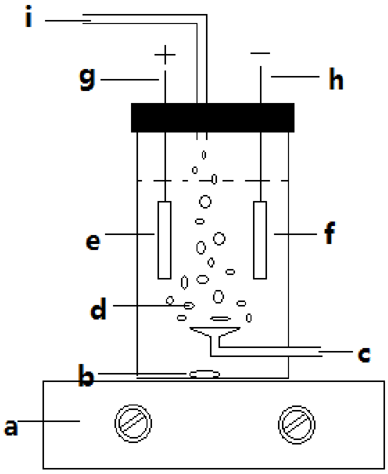

(b)

Figure 3-3 (a). Experimental setup of the gaseous CH_3SH removal in the in-situ ferrate(VI) generation reactor: (1) CH_3SH gas cylinder; (2) air cylinder; (3) surge flask; (4) wet scrubbing reactor; F1–F2. Mass flow controller; S1–S2. CH_3SH sensor. (b): Diagram of the wet scrubbing reactor: a, stirring machine; b, stirring bar; c, gas inlet with an air diffuser; d, gas bubbles; e, iron sheet; f, stainless bar; g, anode contact; h, cathode contact; i, gas outlet.

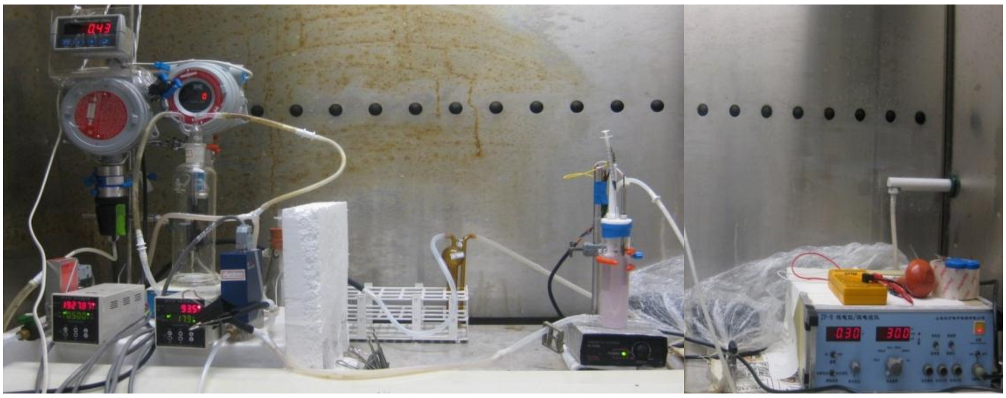

Figure 3-4 Photo of the Experimental setup of the gaseous CH_3SH removal in the in-situ ferrate(VI) generation reactor.

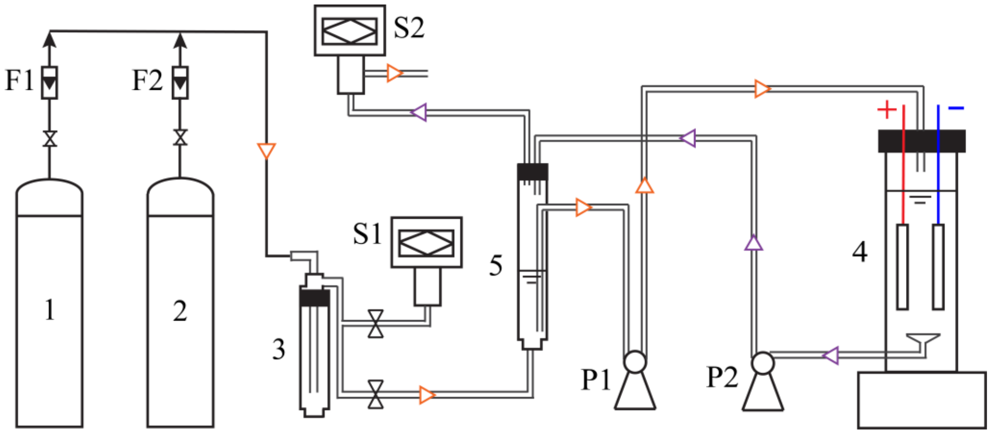

Figure 3-5 Improved experimental setup of the gaseous CH_3SH removal in the in-situ ferrate(VI) generation reactor: (1) CH_3SH gas cylinder; (2) air cylinder; (3) surge flask; (4) oxidization reactor; (5) absorption scrubbing column ; F1–F2. Mass flow controller; S1–S2. CH_3SH sensor; P1-P2. Peristaltic pump.

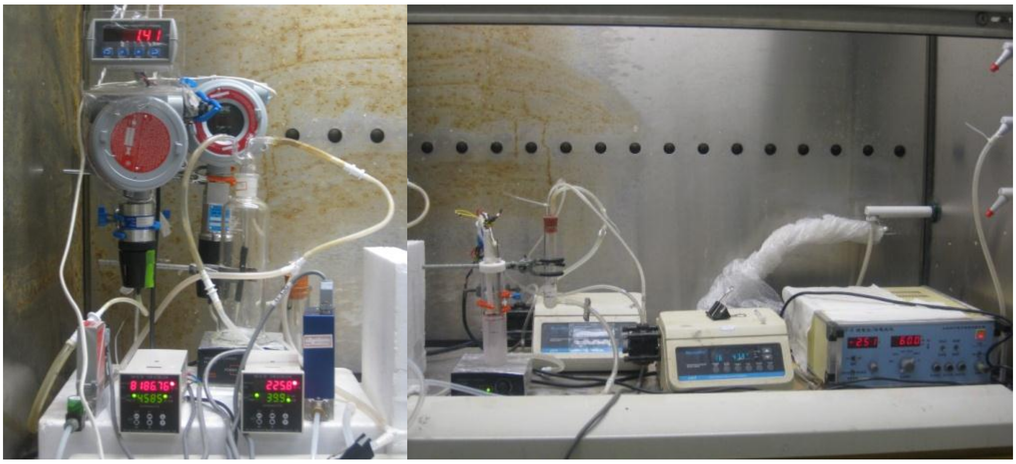

Figure 3-6 Photo of improved experimental setup of the gaseous CH_3SH removal in the in-situ ferrate(VI) generation reactor.

The two mass flow controller with flow ranges up to 0.1 L min^{-1} and 5 L min^{-1} should be calibrated before use.

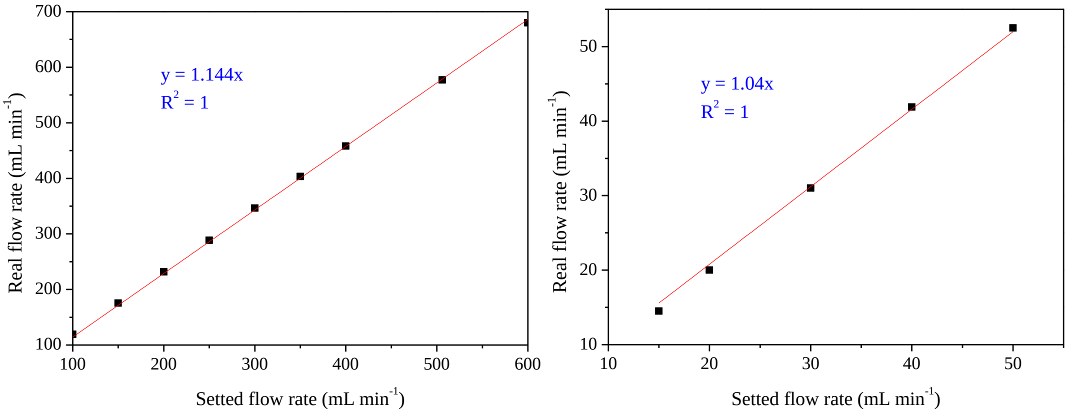

(a) (b)

Figure 3-7 Calibration curves for mass flow controllers (a) 5 L min^{-1} (b) 0.1 L min^{-1}

3.4. Characterization and Analytical Methods

3.4.1 Ferrate(VI) Measurement

In this study, ferrate(VI) concentration in aqueous solution was determined by a UV/Vis spectrophotometer (Libra S35, Biochrom) according to the molar absorptivity of 1150 $M^{-1}cm^{-1}$ at λ = 510 nm (Luo et al. 2011), where the measured ferrate(VI) solutions were buffered at 0.1 M phosphate buffer. In this analysis, colloidal ferric oxide interference can be minimized by a 385 nm baseline correction (Licht et al. 2001). Other phosphate iron(II) and iron(III) of Fe(VI) end-products have no interference at 510 nm (Huang et al. 2001). This UV-Vis spectrophotometer with WinSpec software was used. The concentration of potassium ferrate, decomposed in the solution, was measured and recorded every 10 seconds, using WinSpec software. The computer automatically recorded the absorbance of potassium ferrate at 510 nm.

Calibration curves for ferrate(VI) measurement directly in 14 M NaOH were prepared in Fig. 3-8. Different concentrations of ferrate(VI) were prepared in 14 M NaOH, which were exactly measured in buffer solutions at 510 nm to calculate their concentrations. Simultaneously, the corresponding absorbance of ferrate(VI) for each prepared concentration was directly measured at 510 nm. Thus the calibration curves were plotted.

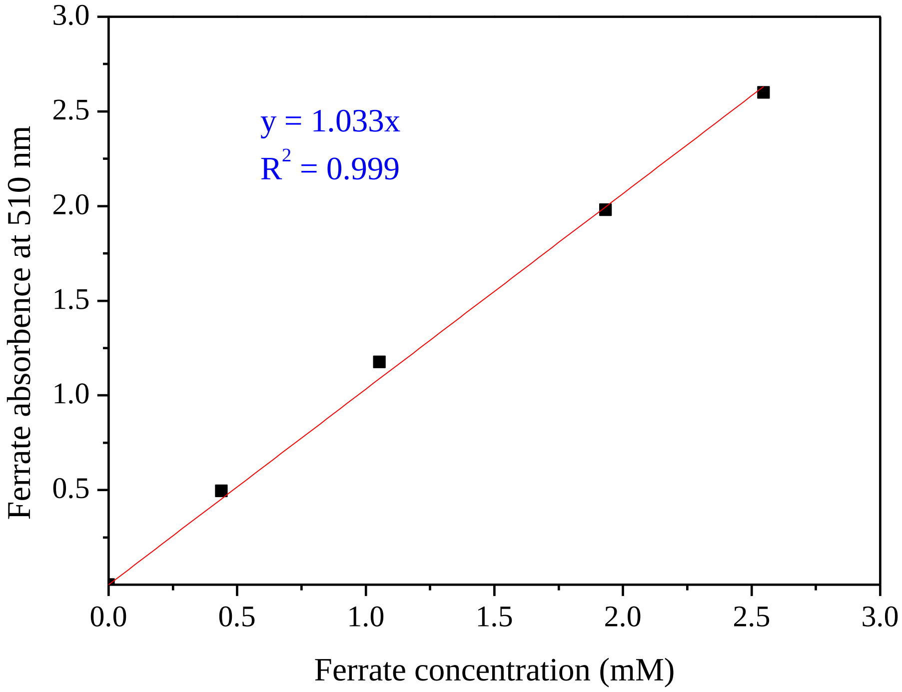

Figure 3-8 Calibration curve of ferrate (VI) measurement in 14 M NaOH

The concentration of generated ferrate(VI) was determined by diluting 0.5 or 1 ml of the ferrate(VI) electrolyte in 2 or 3 ml of pure electrolyte of the same concentration used in the experiment, and then, the absorbance was measured at 510 nm using a spectrophotometer. The measurements were duplicated and the average was taken and used to work out the corresponding concentration of ferrate(VI), using the calibration curves prepared in advance for this purpose.

3.4.2 Gaseous CH_3SH Measurement

Gaseous CH_3SH concentrations in inlet and outlet were monitored by two CH_3SH sensors (Detcon DM-100-CH_3SH). Detcon Model DM-100-CH3SH is a gas detection sensor designed to detect and monitor methyl mercaptan in air over the range of 0-100 ppm/v (±2%) using electrochemical sensor technology. Method of detection is by diffusion adsorption. Air and gas molecules diffuse through a porous membrane contacting an electrolyte solution which creates a change in electrical conductance between a reference and measure electrode. This change in conductance is conditioned by internal electronic circuitry to provide a linear 4-20 milliamp signal proportional to the gas concentration (www.detcon.com).

Figure 3-9 Photo of gaseous CH_3SH sensor (Detcon DM-100-CH_3SH)

3.4.3 Aqueous CH_3SH Measurement

The CH_3SH concentration in aqueous solution before and after the reactions were determined by the Ellman's reagent method with the details described by Riener et al (Riener et al. 2002). Briefly of the standard procedures, 250 μl of the prepared sample was added to the test tube which contained 50 μl of Ellman's Reagent solution and 2.5 ml of reaction buffer. Finally, the light absorbance at 412 nm was measured using the spectrophotometer after incubation of 15 min. As a blank, 250 μl of reaction buffer replaced the prepared sample was added to a separate tube.

Due to the high concentration of the NaOH solution used in our study, the reaction buffer would not be able to maintain the solution at working pH 8.0. Therefore, pre-dilution of the samples with diluted HCl solution was needed before measurements. The calibration curves are presented below.

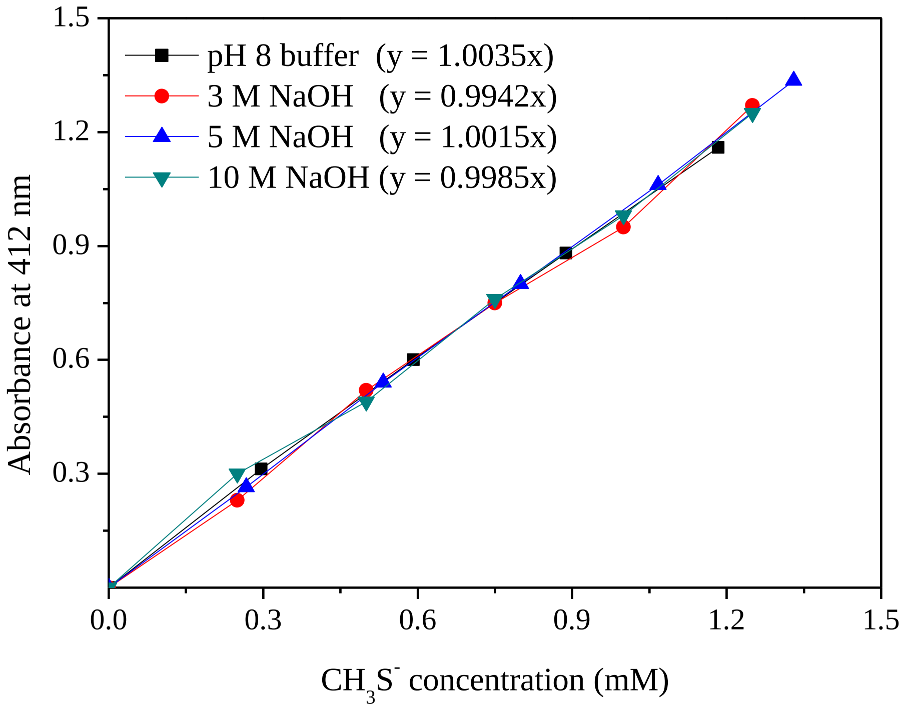

Figure 3-10 Calibration curve of aqueous CH_3SH measurement

3.4.4 pH and ORP Measurements

Solution pH was adjusted by the addition of diluted HCl, H_2SO_4 or NaOH. Measurement was carried out by the WPA-CD 510 pH meter and thorough mixing was ensured by magnetic stirrer. The oxidation-reduction potential (ORP) was also measured using an ORP Model.

3.4.5 Sulphate Measurement

The concentration of sulphate ion as a final product of CH_3SH degradation by ferrate(VI) oxidation was determined using a barium chromate spectrophotometry method. This method involves the formation of a barium sulphate precipitate in a weak acid solution, and the measurement of the absorbance of the precipitate using a spectrophotometer at 420 nm wavelength (APHA 1985). The calibration curve was first obtained to calculate sulphate concentrations in sample solutions.

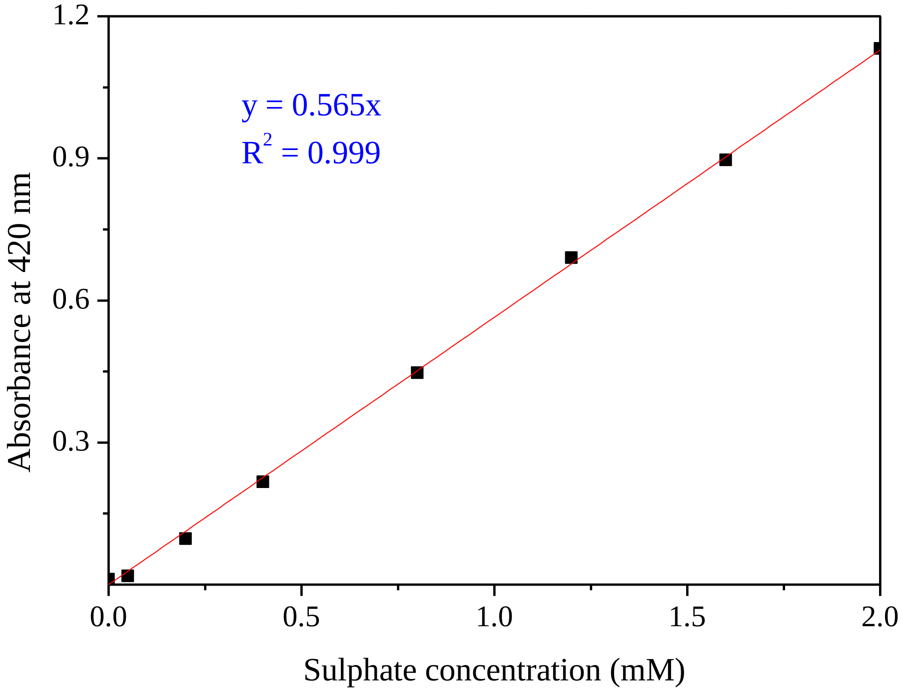

Figure 3-11 Calibration curve of sulphate measurement

CHAPTER 4 Electrochemical Production of Ferrate(VI)

4.1 Introduction

Generally, there are two basic approaches for ferrate(VI) production: chemical (Ayers and White 2005, Ockerman and Schreyer 1951, Thompson et al. 1951) and electrochemical (Bouzek and Roušar 1996, Bouzek et al. 1998, Licht et al. 1999, Licht et al. 2002b) methods.

The Chemical method is the most commonly employed for ferrate(VI) preparation. The wet chemical approach is based on contacting iron compounds, such as iron(III) nitrate and iron oxides, with an oxidizing reagent in an aqueous alkaline environment. Although this method has the advantages of high purity and yield, the technological process is complicated and the cost is high. Worst of all, chlorine used in the operation has deleterious effects on the environment. The dry chemical method, also called the thermal method, consists in oxidation of a Fe(III) salt in a molten mixture of nitrate salts with potassium hydroxide under extreme temperatures in a controlled atmosphere. The advantages of this method are that it is simple and easy to operate, although the temperature needed is extremely high and the reaction is potentially explosive.

Alternatively, the electrochemical approach to synthesize ferrate(VI), as a green technology, is a hypochlorite-free and safe process and easy to operate.

Electrochemical synthesis proceeds in a concentrated solution of alkali metal hydroxides or their melts, where either an iron anode or Fe^{3+} ions can be directly oxidized at sufficient anodic potentials. In general, the process of electrochemical generation of ferrate(VI) is carried out in a two compartment electrolysis cell separated with an anion impermeable membrane, where usually consists of a sacrificial iron anode and a steel cathode in a strongly alkaline solution with an electric current. The basic principle of ferrate(VI) synthesis in aqueous alkaline solution by electrolysis is shown by Eqs. (1-3) (Licht et al. 2004).

Anode: $\mathrm{Fe + 8OH^{-} \rightarrow FeO_4{}^{2-} + 4H_2O + 6e}$ (1)

Cathode: $\mathrm{6H_2O \rightarrow 6OH^{-} + 3H_2 - 6e}$ (2)

Net: $\mathrm{Fe + 2OH^{-} + 2H_2O \rightarrow FeO_4{}^{2-} + 3H_2}$ (3)

Ferrate(VI) yield strongly depends on various synthesis parameters including: (1) anode materials; (2) membrane of the electrolysis cell; (3) alkaline electrolyte; (4) anodic current density; (5) temperature and (6) electrolysis time etc. Optimization of the electrochemical generation of solution phased ferrate(VI) has recently been systematically studied (De Koninck and Belanger 2003, De Koninck et al. 2003, He et al. 2006, Licht et al. 2002b, 2004).

This chapter aims at the determination of the optimum operating conditions for ferrate(VI) generation in our laboratory, which is required for the design of a continuous flow reactor for further study. In our study, the effects of the three main parameters, current density, electrolyte concentration and SO_4^- concentration, were investigated on the performance of the efficiency of ferrate(VI) generation in the same electrochemical reactor. The self-decomposition of ferrate(VI) in such strong alkaline solutions was then also studied.

4.2 Electrochemical Generation of Ferrate(VI)

4.2.1 Effect of Anode Materials

The efficiency of electrochemical ferrate(VI) production is very sensitive to reaction conditions. Obviously, anode material as an iron source, is very important for ferrate(VI) production electrochemically. Bouzek et al. (Bouzek and Roušar 1996, 1997, Bouzek et al. 1996a) investigated different kinds of anode materials on ferrate(VI) production and found that the content of carbon in the anode material had a crucial impact in the anode dissolution process, especially the form of Fe_3C in white cast iron (WCI).

Cyclic voltammetry (CV) curves showed that current densities, on the dissolution of a WCI electrode, were the highest among the employed anode materials (Mácová et al. 2008). It was reported that the presence of carbon in the form of Fe_3C readily dissolved in the concentrated NaOH solution during anodic polarization and thus exposed a fresh anode surface to the anolyte (Bouzek et al. 1996a). That meant Fe_3C suppressed the anode surface deactivation and enhanced deterioration of the protective properties of the oxide layer. Silicon in the anode materials had a similar effect on enhancing ferrate(VI) production with carbon (Lescuras-Darrou et al. 2002). Moreover, the recent study on both WCI and SRS also showed a similar temperature dependence in NaOH anolyte.

To develop the pilot study using in-situ production of ferrate(VI) for odour control, the aim of this work was to identify an appropriate anode material with the highest production yield. Two kinds of iron anodes were compared in our study, including commercial iron sheet with high silicon content, which is used in transformers to increase magnetic permeability, and pure iron sheet with Fe content of >99%, plus 0.3% Mn, 0.1% Si, 0.08% C, 0.04% P, 0.05% S bought from Goodfellow Cambridge Limited. The experiments were conducted in aqueous 14 M NaOH solution by applying the same current density at $j = 3.13$ mA cm^{-2}. From Fig. 4-1, it can be seen that the ferrate(VI) concentration is much higher when using commercial iron sheet than pure iron, the same results as reported by Bouzek (Macova et al. 2009a). It was reported that pure iron became passive more easily than other anode materials, which meant the anode surface of pure iron sheet was protected from further dissolution (Bouzek and Roušar 1997). While the commercial iron sheet has the potential of formation oxy-hydroxide layer covering the anode surface. As a result, commercial iron sheet was chosen as the anode material for ferrate(VI) production in the continuous study.

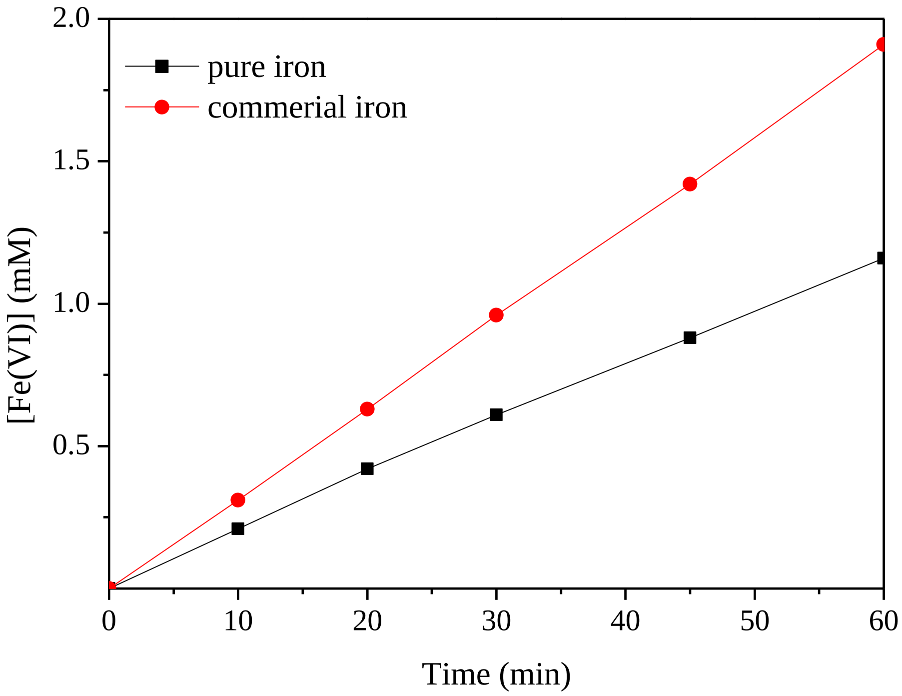

Figure 4-1 Variation of the ferrate(VI) concentration with the anode materials at 14 M NaOH in H cell with the current density of 3.33 mA cm^{-2}.

4.2.2 Effect of Cathode Materials

To our best knowledge, there is no published study on the effect of different cathode materials used in ferrate(VI) production electrochemically. Since the potential difference on the surface of the anode is controlled by the system thermodynamics (Rabald 1954), this may vary with different cathode materials during the electrolysis process. It has been reported that using different cathode materials affects the dissolution kinetics of the Ti anode due to differences in their overvoltages, in turn controlling the activity of the electrolyte and morphology of the formed architectures (Allam and Grimes 2008). That is to say that selecting different electrode influences the rates of certain reaction steps and then influences the overall performance.

Considering the above, the aim of this work was to indentify alternative less-expensive cathode materials to replace the conventional platinum cathode, while maintaining the high production yield of ferrate(VI). However, due to the caustic solution employed in our experiments, the number of available cathode materials was very limited. Finally, the five materials, Pt, Cu, Ti, Ni and stainless steel, were chosen as cathodes and the experimental results are shown in Figure 4-2. It can be observed that ferrate(VI) concentration with the Pt cathode was slightly lower than with other cathode materials, which can be taken as experimental error. Thus there was no significant difference in ferrate(VI) yield among these cathode materials under the same conditions.

Mass losses of the tested cathode materials in the electrolyte were also measured after 5 h of electrosynthesis. All of the tested materials showed good stability in the electrolyte, as shown in Table 4-1. The above results indicate that these four materials can be efficiently used as cathodes to produce ferrate(VI). Stainless steel has been intensive used (Alsheyab et al. 2010, Stanford et al. 2010), most likely because it is relatively cheap and a typical material in commonly available cathode materials. Therefore, stainless steel was chosen as the cathode material for ferrate(VI) production in the continuous study.

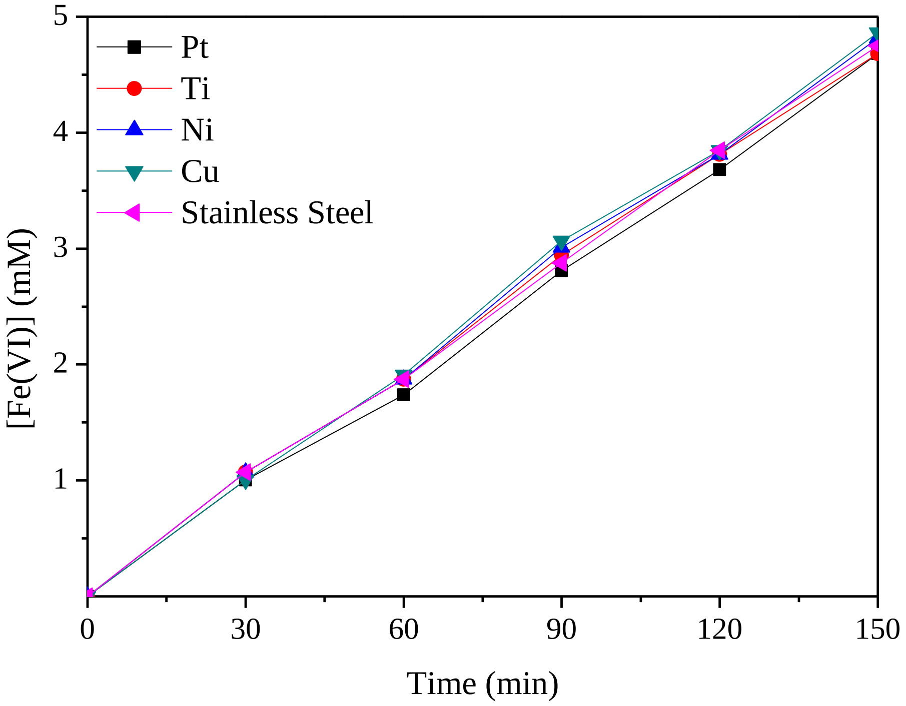

Figure 4-2 Variation of the ferrate(VI) concentration with the cathode materials at 14 M NaOH in H cell with the current density of 3.33 mA cm^{-2}.

Table 4- 1 The rate of mass loss of the tested cathode materials in aqueous electrolyte after 5 h of electrosynthesis

Cathode materials	Rate of mass loss ($mg^{-1}cm^{-2}h^{-1}$)
Pt	0
Ti	0
Ni	0.0015
Cu	0.0018
Stainless steel	0

4.2.3 Effect of Dissolved Oxygen

Recently, the results of cyclic voltammograms of Pt electrode have shown that O_2^- forms on the anode surface during the oxidation of melt, Eq. (4) (Hives et al. 2006), which was one of the intermediates in the ferrate(VI) generation process. Shao's study (Shao et al. 2006) showed that O_2^- can also be produced from the reaction between atmospheric O_2 and OH^-. This phenomenon indicates that oxygen might enhance the ferrate(VI) yield by converting the intermediate iron species to final ferrate(VI). Therefore, the effect of oxygen on ferrate(VI) generation was carried out in a 14 M NaOH solution with the current density of 3.33 mA cm^{-2}.

$$4OH^- = O_2^- + 2H_2O + 3e^- \qquad (4)$$

The experiments were conducted by continuously bubbling O_2, air and N_2 gases into NaOH solutions during the electrolysis and the results are shown in Fig. 4-3. It can be clearly observed that ferrate(VI) concentration was 4.52 mM at 150 min with N_2 bubbling, while ferrate(VI) concentration was up to 4.75 and 4.86 mM with air and O_2 bubbling. Moreover, under the N_2 condition, ferrate(VI) concentration was always the lowest during the whole reaction period. These results indicate that oxygen has a slight influence on ferrate(VI) generation. However, it was interesting to find that ferrate(VI) concentration was almost the same, when comparing the air and O_2 case. This result may be caused by the low solubility of oxygen in a concentrated NaOH solution

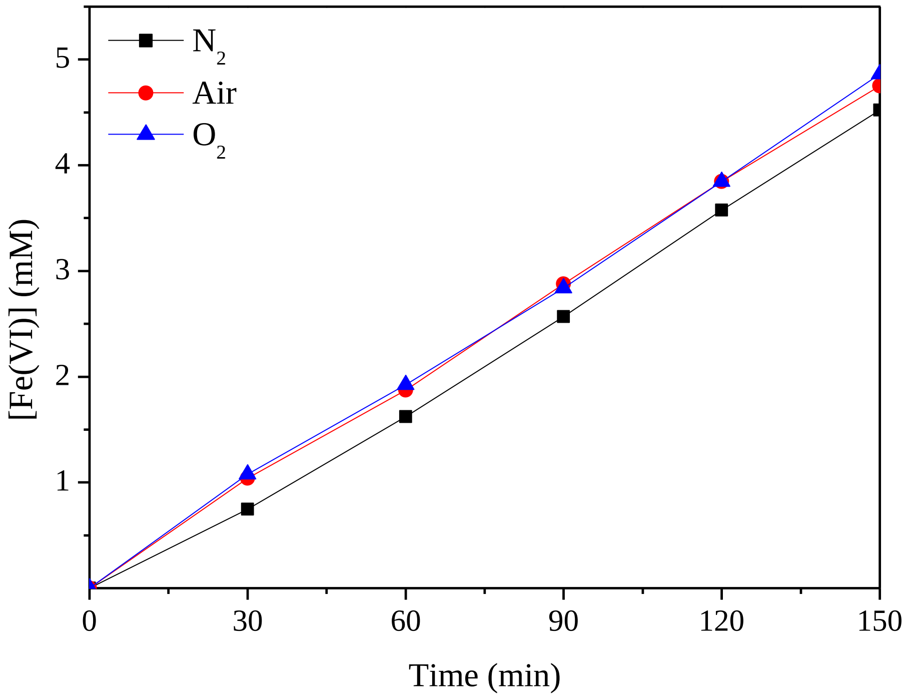

Figure 4-3 Effect of oxygen on the ferrate(VI) generation in 14 M NaOH solution with the current density of 3.33 mA cm^{-2}.

4.2.4 Effect of Electrolysis Time

Current efficiency is a reference parameter referring to the optimum conditions of ferrate(VI) production electrochemically. However, the thickness of the iron oxide film on the surface of the iron anode increases over time and then the surface of the iron anode will deactivate during a continuous electrosynthesis of ferrate(VI). Moreover, the rate of ferrate(VI) decomposition will also increase due to the increasing amount of hydrous ferric oxide and temperature of the electrolyte (Denvir and Pletcher 1996). The current efficiency of ferrate(VI) over a short electrolysis duration may lead to larger analysis errors and so it is necessary to chose a suitable electrolysis duration when calculating current efficiency of ferrate(VI) under different experimental conditions. The experimental results on the effect of the duration of continuous electrolysis is shown in Fig. 4-4.

The experimental results demonstrate that the current efficiency decreases with increased electrolysis time and that the highest current efficiency was obtained in the first hour. Therefore, it is reasonable to adopt a duration of 1 h when determining the current efficiency of ferrate(VI) production.

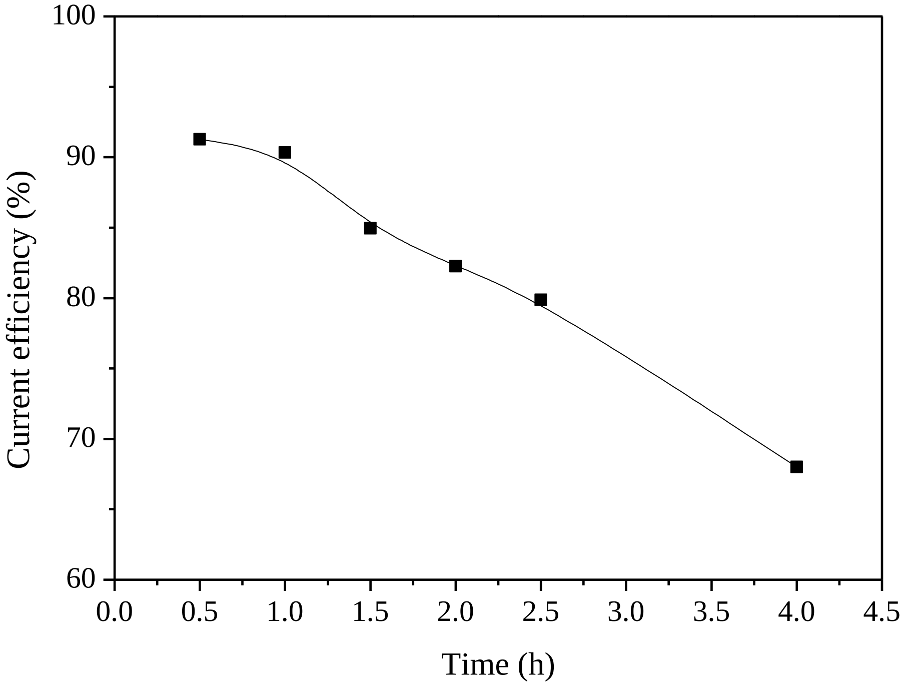

Figure 4-4 Effect of continuous electrolysis time on the current efficiency of ferrate(VI) in 14 M NaOH solution with the current density of 6.67 mA cm^{-2}.

4.3 Optimization of Ferrate(VI) Production

4.3.1 Effect of NaOH Concentration

The first set of experiments was conducted in aqueous NaOH solution by applying the same current density at j = 3.13 mA cm^{-2}, but with different NaOH concentrations in the range of 1-18 M. Each experiment lasted for 60 min and the accumulated ferrate(VI) concentrations in the solutions vs. NaOH concentrations are shown in Fig. 4-5a. It was interesting to observe that a light purple colour, as a feature of ferrate(VI), appeared on the surface of iron anode in the 1 M NaOH electrolyte or below, even though the ferrate(VI) concentration in the bulk solution was not detectable. This demonstrates that the rate of ferrate(VI) generation was slower than that of ferrate(VI) self-decomposition in the 1 M (or below) NaOH solution. A significant amount of ferrate(VI) in the bulk NaOH solution at 4 M and above was easily detected due to a faster rate of ferrate(VI) generation and increased with an increased time steadily. For example, the ferrate(VI) concentration in the 4 M NaOH solution gradually rose up to 0.235 mM after 60 min. The higher concentration of ferrate(VI) up to 1.85 mM was also found in the more concentrated NaOH solution from 4 to 18 M. The enhancement of ferrate(VI) formation in the highly concentrated NaOH electrolytes is attributed to the increasing hydroxide which leads to shift the equilibrium of Eq. (1) towards the right. The polarization curve of iron in the passive potential region also confirmed that the anodic current density of the iron electrode at high NaOH concentration is higher than that at low NaOH concentration (He et al. 2006). This implies that the extent of passivation decreases with increase of alkaline concentration, where high alkalinity is used to ensure iron species dissolves easily. Furthermore, the parasitic decomposition can also increase the loss of ferrate(VI) at the lower NaOH concentration. On the other hand, when NaOH concentration approaches to its saturated value of around 20 M in water, the electrolyte solution will become very viscous and the solution conductivity will decline significantly resulting in a lower rate of electron transfer on the anode surface. In this study, the conductivity of aqueous NaOH solutions in the range 1-16 M was measured and the results are presented in Fig. 4-5b. It was found that the maximum value of conductivity in NaOH solutions occurred at around 5 M. From the results of ferrate(VI) generation as shown in Fig. 4-5a, it can be seen that the accumulated ferrate(VI) concentration in the NaOH solution increased quickly with increased NaOH concentration from 1 to 5 M and further increased at a gradually reduced rate until a maximum value of [Fe(VI)] = 1.85 mM was achieved at 14 M after 60 min. At the higher NaOH concentration of 18 M, a lower ferrate(VI) concentration was found. These results indicate that at NaOH concentrations below 5 M, the ferrate(VI) generation was effectively accelerated by increases in both hydroxide ion strength and electrolyte conductivity, and at the higher NaOH concentration between 5-14 M, the ferrate(VI) generation was still dominated by the increase of hydroxide ion strength rather than the decrease of electrolyte conductivity. However, at NaOH concentrations beyond 14 M, the adverse effect of lower conductivity became dominant resulting in a slower rate of ferrate(VI) generation.

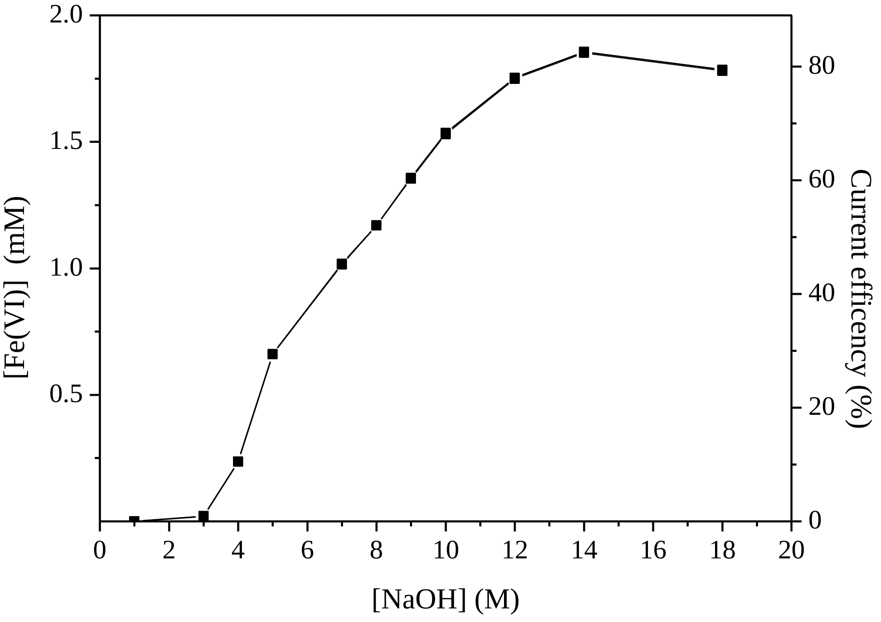

(a)

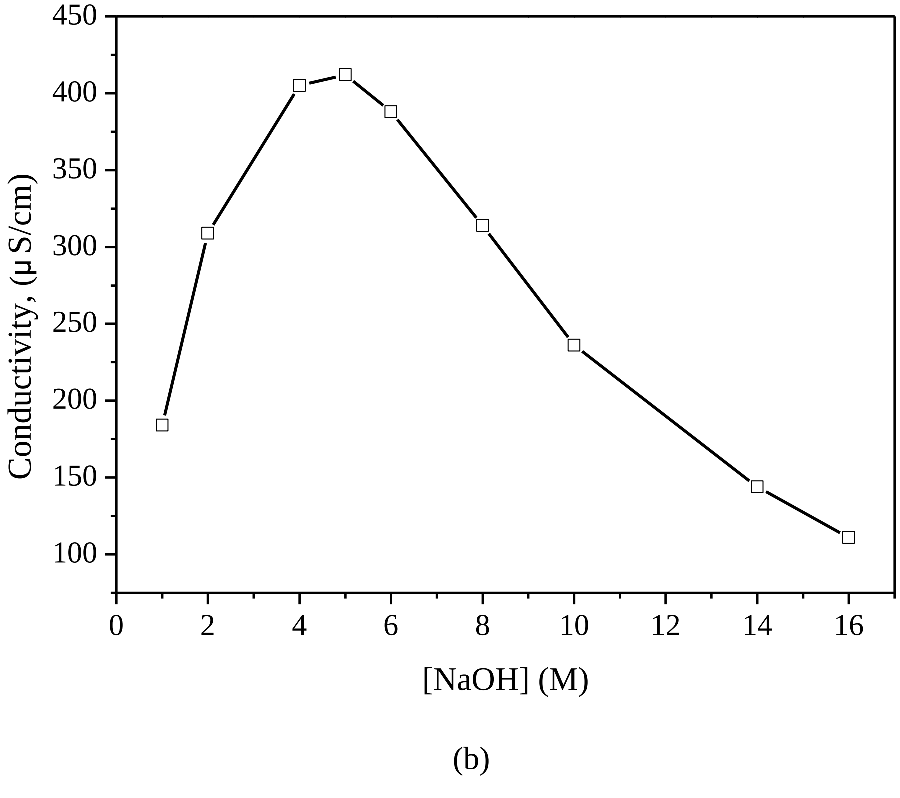

(b)

Figure 4-5 (a): Variation of the accumulated ferrate(VI) concentration and current efficiency vs. NaOH concentration at j = 3.13 mA cm^{-2}: (b): The conductivity of aqueous NaOH electrolyte solution at 20 ℃.

The experiments discussed above, showed that 14 M NaOH with the highest current efficiencies is the optimum NaOH concentration for ferrate (VI) production. As discussed above, ferrate(VI) also can be generated in 1 M NaOH electrolyte or below, although the ferrate(VI) concentration in the bulk solution was not yet detectable. It was interesting to investigate which is the lowest NaOH concentration for ferrate(VI) generation. The experiments were carried out by preparing a series of NaOH solutions from 0.05 to 1 M. A light purple colour, a feature of ferrate(VI), can be observed on the surface of the iron anode even down to as low as 0.074 M NaOH electrolyte. Below 0.074 M NaOH, the light purple colour was invisible to the naked eye. A long electrolysis duration test in 1 M NaOH solution was also conducted to investigate the colour variation in the ferrate(VI) solution. First, the ferrate(VI) solution showed up as a very pale purple. Thereafter, the electrolyte turned a faint yellow and finally, the solution became orange. After 2 plus hours of electrolysis, a black oxide coating on the surface of the anode was seen. The main reason for this phenomenon is that ferrate(VI) is so unstable that it decomposes in a magnitude of from seconds to minutes.

In this study, the current efficiency of ferrate(VI) generation was further evaluated using the ratio of C_{exp}/C_{theor}, in which C_{theor} is the calculated ferrate(VI) concentration according to Eq. (5), and C_{exp} is the experimentally measured ferrate(VI) concentration.

$$C_{theor} = \frac{It}{6FV} \tag{5}$$

where I is the current intensity (A), t is the reaction time (s), F is the Faraday’s constant (96,500 C mol^{-1}) and V is the volume of the electrolyte (L)

On the basis of experimental data, the current efficiency of ferrate(VI) generation in different NaOH solutions was calculated and the results are shown in Fig. 4-5a. It can be seen that the current efficiency gradually increased with increased NaOH concentration significantly until its maximum value of 83% was achieved in the 14 M NaOH solution at j = 3.13 mA cm^{-2}. These results demonstrate that 14 M would be an optimum NaOH concentration for electrochemical generation of ferrate(VI) in aqueous solution under our experimental condition, which is similar to those reported in other studies (Licht et al. 2004).

4.3.2 Effect of Current Density

The second set of experiments was conducted in the 14 M NaOH solution by applying different current densities in the range 1.56-52.08 mA cm^{-2}. The results as summarized in Table 4-1 showed that the maximum current efficiency of 90.4% occurred at the current density of 14.06 mA cm^{-2}. At lower current densities, such as 1.56 mA cm^{-2} or below, the rate of ferrate(VI) formation might be limited by insufficient anodic potential to remove lower valence iron species away from the anode surface (De Koninck et al. 2003, Macova et al. 2009b). However, a cell with higher current density could increase the cell potential and then accelerate the ferrate(VI) synthesis. But very high current densities, such as 52.08 mA cm^{-2}, could also result in IR heat, raising internal cell temperature and accelerating the rate of ferrate(VI) self-decomposition. Therefore, the optimum current density is a compromise between these phenomena. However, further fundamental research on the effect of current density on ferrate(VI) formation is still needed before it is fully understood.

Table 4-2 Dependence of current density on the ferrate generation in 14 M NaOH solution.

Current density (mA cm^{-2})	Ferrate(VI) concentration		Current efficiency (%)*
	C_{exp} (mM)	C_{theor} (mM)	
1.56	0.72	1.17	61.6
3.13	1.93	2.33	82.8
4.69	2.91	3.50	83.0
9.38	6.28	7.11	88.3
14.06	9.49	10.50	90.4
23.44	15.50	17.49	88.6

52.08	32.54	38.86	83.7

The current efficiency of ferrate(VI) generation was calculated according to the accumulated ferrate(VI) concentration in the electrolyte solution.

4.3.3 Effect of Sulphate Ion

After full oxidation of CH_3SH with excess ferrate(VI), SO_4^{2-} ions are produced which accumulate in the aqueous alkaline solution. Therefore, there is a need to gain insight into the effect of SO_4^{2-} ions on ferrate(VI) generation during the electrolysis process. Experiments were carried out by adding Na_2SO_4 into the reaction solution with different concentrations in steps of 5 mM, 10 mM, till supersaturation. The results are shown in Fig. 4-6.

It can be observed that the ferrate(VI) concentration without SO_4^{2-} was achieved by ~4.75 mM after 150 min reaction at 14 M NaOH, while it was achieved by 4.04 mM only at $[SO_4^{2-}]$ = 5 mM, and further down to 3.28 mM with SO_4^{2-} saturation. This indicates that the presence of SO_4^{2-} in the electrolyte solution has a significant inhibiting effect on the rate of ferrate(VI) generation. A possible reason may be the competition absorption of SO_4^{2-} and metal oxides in the interfacial diffusion layer formed on the anodic electrode (Yang et al. 2012), since the metal oxides (mainly Fe(III) species) converted to the final product ferrate (VI) at the active sites of the anodic electrode (Shao et al. 2005). As a consequence, the competitive absorption will decrease the covering density of the initial Fe(III) species on the anodic electrode, thus slowing down the rate of ferrate production.

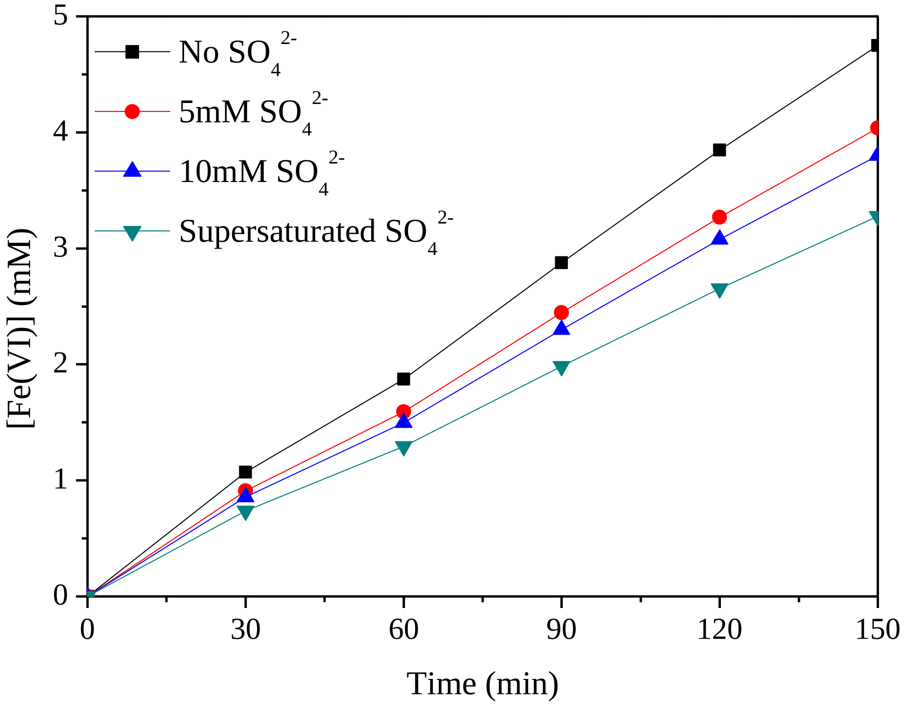

Figure 4-6 Variation of the ferrate(VI) concentration with the SO_4^{2-} ions in 14 M NaOH with the current density of 3.13 mA cm^{-2}

4.4 Stability of Ferrate(VI) in Highly-Concentrated NaOH Solution

Self-decomposition of ferrate(VI) in aqueous solution is an important phenomenon affecting its utilization in the ferrate(VI) oxidation process. Most studies on ferrate(VI) decomposition have been conducted in the normal pH range between 1-14, but the decomposition of ferrate(VI) in a concentrated NaOH solution has not been well investigated so far. In general, under a highly alkaline condition, ferrate(VI) ions occur as the FeO_4^{2-} species only, and undergo the spontaneous decomposition described by the following reaction (Eq. (6)).

$$2FeO_4^{2-} + 5H_2O \rightarrow 2Fe(OH)_3 + 4OH^- + 3/2O_2 \uparrow \qquad (6)$$

A set of experiments to investigate the decomposition of freshly generated ferrate(VI) in aqueous NaOH solutions in the range of 1.5-14 M was conducted at 20 ℃ with an initial ferrate(VI) concentration of 0.145 mM. The decline of Fe(VI) concentration in the solutions against time was monitored to determine the rates of Fe(VI) self-decomposition at different NaOH concentrations. A relationship between the rate constant of Fe(VI) decomposition and NaOH concentration is presented in Fig. 4-7. It is assumed that the kinetics of ferrate(VI) decomposition in the concentrated NaOH solution follows a first-order reaction. The decomposition rate constant (k_d) and the half-life times of ferrate(VI) decomposition in different NaOH solutions were calculated and the results are summarized in Table 4-2. It is clear that the rate of ferrate(VI) decomposition significantly declined with increased NaOH concentration. For example, a half-life time of ferrate(VI) decomposition at 1.5 M was found to be 0.48 h, but this was greatly extended to 43 h at 14 M. It can also be seen in Fig. 4-7 that the rate of ferrate(VI) decomposition was reduced rapidly with increased NaOH concentration in the lower range below 3 M, and was further reduced gradually in the higher range of 4-14 M. These results demonstrate the great effect of NaOH concentration on the aqueous decomposition of ferrate(VI) in accordance with Eq. (6), in which free water activity in NaOH solution from 1.5 M to 14 M decreases and inhibits the redox reaction of FeO_4^- with H_2O (Licht 1985).

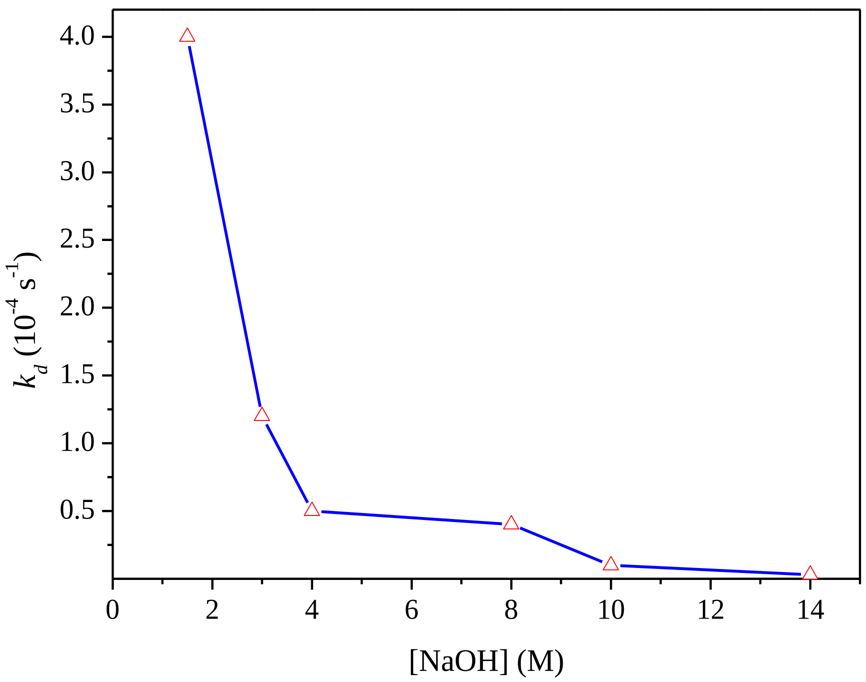

Figure 4-7 Rate constant, k_d, of Fe(VI) decomposition ($[Fe(VI)]_0$ = 0.145 mM) vs. NaOH concentration

Table 4-3 Variation of rate constant (k_d) and half-life time of ferrate (VI) decomposition vs. NaOH concentration.

NaOH Conc. (M)	Rate constant (s^{-1})	Half life (h)
$10^{-4.89*}$	0.7×10^{-4}	2.75
1.5	4×10^{-4}	0.48
3	1.2×10^{-4}	1.6
4	0.5×10^{-4}	3.9
8	0.4×10^{-4}	4.8
10	0.1×10^{-4}	19

14	0.045×10^{-4}	43

*This case contained phosphate buffer.

In addition, ferrate(VI) decomposition was also conducted in a phosphate buffer solution. Since phosphate can chelate the ferric iron from ferrate(VI) decomposition, which prevents interference to optical monitoring of ferrate(VI) concentration. A phosphate buffer has been widely used in studying the reaction kinetics of ferrate(VI) in normal pH solutions. In a pH 9.11 buffer solution, the rate of ferrate(VI) decomposition was 0.7×10^{-4} s^{-1}, which is even faster than that with the 4 M NaOH solution. This result indicates that the stability of ferrate(VI) in 4 M or above NaOH solution is quite high.

4.5 Summary

In this chapter, the electrochemical generation of ferrate(VI) in aqueous NaOH solution was studied and a commercial iron steel and a stainless steel were separately chosen as anode and cathode. Meanwhile, the results showed that the cathode materials used had no obvious effect on the ferrate(VI) yield under the same experimental conditions. The experimental result showed that O_2 provided a slight enhancement on ferrate(VI) generation electrochemically. In addition, 1 h of electrosynthesis duration was determined as the appropriate time for calculating current efficiency of ferrate(VI) production during electrolysis.

The experiments demonstrated that a maximum current efficiency to generate ferrate(VI) occurred at 14 M NaOH concentration, with an applied current density of 14.06 mA cm^{-2}. The presence of SO_4^{2-} in the electrolyte solution significantly inhibited the rate of ferrate(VI) formation. In addition, the self-decomposition of ferrate(VI) in strong alkaline solutions was studied. The results showed that ferrate(VI) behaved more stably in stronger alkaline solutions.

CHAPTER 5 Oxidation of CH_3S^- with Ferrate(VI) in Aqueous Alkaline Solution

5.1 Introduction

Offensive odours from sewage treatment works and other municipal waste management facilities such as refuse transfer stations and landfill sites have caused a great number of complaints in urban areas such as Hong Kong (Gostelow et al. 2001, Sioukri and Bandosz 2005). Volatile sulphur compounds are generally considered to be one group of the most important contributors to sewage-related odours (Mansfield et al. 1992). Hong Kong's sewage has more significant odour problems than other cities, as seawater, with its high natural content of sulphate, is usually used for toilet flushing, resulting in a high content of sulphur-containing compounds such as hydrogen sulphide in the sewage (DSD 2009). These sulphur compounds mainly include hydrogen sulphide (H_2S), methyl mercaptan, dimethyl sulphide, dimethyl disulphide, methanethiol, carbon disulphide, and carbonyl sulphide. Methyl mercaptan (CH_3SH) is one representative of odorous compounds with significant toxicity and a very low threshold of odour detection at around 0.4 ppb/v. Long-term exposure to an even lower levels of CH_3SH can have adverse effects on human health.

Ferrate(VI) chemical (FeO_4^{2-}, Fe(VI)) has long been known for its strong oxidizing power (Anquandah et al. 2011, Sharma 2010a, Sharma 2011). The rapid reduction of ferrate(VI) to the environmentally benign Fe(III) species makes it suitable to be used in a wide range of applications (Delaude and Laszlo 1996, Licht et al. 2002c, Sharma et al. 2000). Furthermore, ferrate(VI) has significant selectivity to rapidly degrade a number of sulphur-containing compounds, such as inorganic sulphur compounds (Sharma 2010b) and organosulphur compounds (Sharma et al. 2011) in seconds to minutes with formation of non-hazardous products. Recently, some research groups reported the on-line production of ferrate(VI) in strong alkaline solution by electrochemical synthesis as a new approach to sewage treatment (Jiang et al. 2009, Licht and Yu 2005). Generally, this approach consists of two separate parts: (i) preparation of ferrate(VI) in an extremely concentrated alkaline solution (10-16 M NaOH solution) and (ii) reduction of ferrate(VI) in the contaminated sewage stream. Simultaneous treatment of multiple contaminants in an effluent flow with ferrate(VI) on-line remediation was found to be effective. Using fresh ferrate(VI) especially, can not only save time and money on ferrate(VI) purification, but also saves steps on the transportation and storage of ferrate(VI) chemical. However, increasing of pH in the sewage stream is a big concern in practice, due to adding such highly concentrated alkaline solution into sewage stream.

Recently continuous feeding of ferrate(VI) chemical was used for the simultaneous removal of NO and SO_2 from the flue gas in a wet-scrubbing process and the flue gas circulating fluidized bed system (Xia et al. 2011, Zhao et al. 2011). The influencing factors and possible reaction mechanisms were investigated. The results demonstrated that ferrate(VI) chemical could be an effective agent for flue gas cleaning. However, the demand for the ferrate(VI) chemical would create practical difficulties.

In fact， we believe that in-situ electro-generation of ferrate(VI) to treat odorous gases by passing through a strong alkaline solution would be more suitable than treating wastewater. Odorous pollutants such as hydrogen sulphide or mercaptans in foul gas can be easily absorbed by the aqueous alkaline solution and rapidly oxidized by the in-situ generation of ferrate(VI) through electrochemical synthesis. Actually, in-situ chemical oxidation has been studied for years and the most common oxidants are hydrogen peroxide (Do and Chen 1993), permanganate (Schroth et al. 2001) and hypochlorite (Do et al. 1997). To the best of our knowledge, the in-situ generation of ferrate(VI) for odour treatment has not been reported. Hence, this study is aimed at exploring this new approach to the treatment of gaseous odours in highly alkaline solution with in-situ production of ferrate(VI) through an electrochemical process for odour control. The objectives of the work described in this chapter were to investigate: (i) the kinetics of ferrate(VI) reaction with CH_3SH in an aqueous solution with concentrated alkali, (ii) stoichiometry, and (ii) the feasibility of treating synthetic odorous gas containing CH_3SH in a continuous gas flow mode.

5.2 Reaction Mechanism

5.2.1. Reaction Kinetics

The reaction between ferrate(VI) and CH_3S^-, and its reaction rate can be expressed by

Eqs. (1) and (2), respectively:

$$\mathrm{mFe(VI) + nCH_3S^- \rightarrow mFe(III) + products} \quad (1)$$

$$\mathrm{-d[Fe(VI)]/dt = k[Fe(VI)]^m[CH_3S^-]^n} \quad (2)$$

where [Fe(VI)] and $[CH_3S^-]$ are the concentrations of ferrate(VI) and CH_3S^-, m and n are the orders of the reaction, and *k* is the overall reaction rate constant.

Actually, the accumulated ferrate(VI) concentrations observed in the NaOH solution should be equivalent to its net generation (prime generation - self-decomposition). As discussed in Chapter 4.4, the self-decomposition of ferrate(VI) in an NaOH solution at high concentrations beyond 10 M can be largely reduced to very low levels. This would be a beneficial condition for practical application. Therefore, one set of experiments with an initial ferrate(VI) concentration of ~0.1 mM and an initial CH_3S^- concentration in the range of 1.0~3.6 mM was conducted in aqueous 10 M NaOH solution at the room temperature of 20 ℃. Due to the very low molar ratio of $[Fe(VI)]/[CH_3S^-]$, the pseudo-first-order rate law is appropriate for modelling the ferrate(VI) reaction with CH_3S^- and Eq. (2) can thus be rewritten below:

$$\mathrm{-d[Fe(VI)]/dt = k_1[Fe(VI)]^m} \quad (3)$$

where $\mathrm{k_1 = k[CH_3S^-]^n}$ (4)

Before each reaction, both CH_3S^- and ferrate(VI) solutions were rapidly mixed in a stopped-flow spectrophotometer system (SF-61DX2, Hi-Tech KinetAsyst Stopped-Flow System, UK) and then the variation of ferrate(VI) concentration was monitored at $\lambda = 510$ nm as a function of time. Four repeat tests were conducted for each reaction. The values of k_1 with different initial CH_3S^- concentrations were determined under the same experimental condition. The plots of k_1 versus $[CH_3S^-]$ in Fig. 5-1a show a linear relationship, suggesting that the kinetics of this reaction follows a second order model with a rate constant of $k = 791.45 \pm 40$ $M^{-1}s^{-1}$. Fig. 5-1b also shows that the profile of light absorbance by ferrate(VI) against reaction time well follows the first-order model. The half-life times of ferrate(VI) reduction in the CH_3S^- concentrations (1.0~3.6 mM) were found to be between 0.25~0.93 s (less than 1 s), indicating very high reaction rates of CH_3S^- degradation by ferrate(VI). He et al. summarized the reactivity of ferrate(VI) with most sulphur-containing compounds at pH 9.0 and 25 ℃ (He et al. 2009). Therefore, it indicates that ferrate(VI) has high reactivity with major sulphur-containing odorous compounds even when in a concentrated alkaline solution. Compared with the commonly used oxidizing reagents to limit odour emission such as chlorine and sodium hypochloride, ferrate(VI) is an effective reagent for odour control. Although ozone (O_3) and hydroxyl radical (OH) also have high reactivity, they have much shorter lifetimes due to their more rapid self-decomposition in water than ferrate(VI) (Westerhoff et al. 1999).

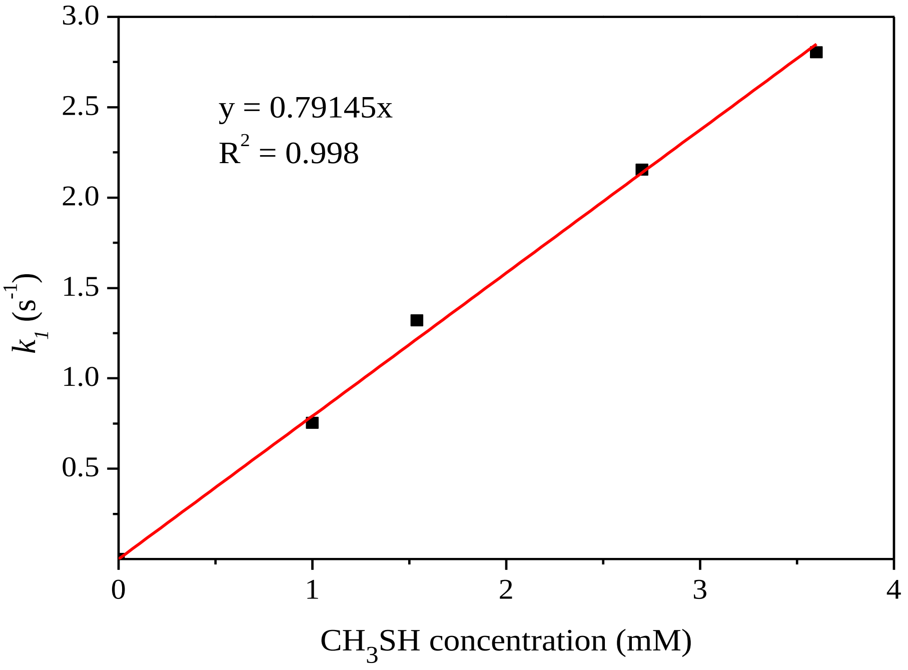

(a)

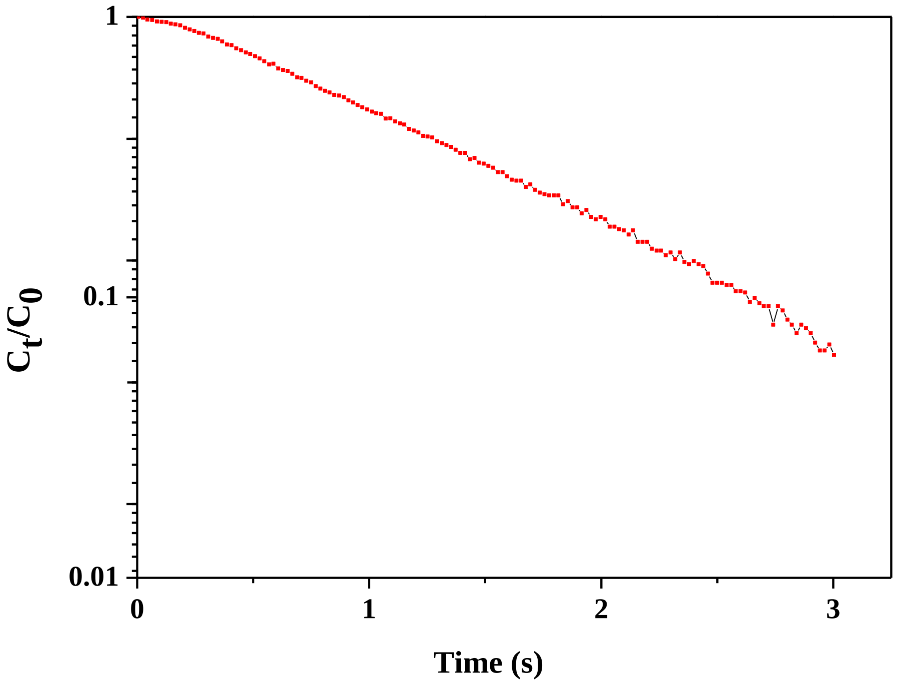

(b)

Figure 5-1 (a) Values of k_1 (s^{-1}) vs. CH_3S^- concentration for the reduction of ferrate(VI) by CH_3S^- at 10 M NaOH and temp = 20 ℃; (b) The first-order decay of ferrate(VI) at 510 nm by CH_3S^- vs. reaction time.

5.2.2 Stoichiometry Study

The stoichiometry of the reactions between ferrate(VI) and CH_3S^- was determined by conducting one set of reactions in a 10 M NaOH solution by rapidly mixing ferrate(VI) and CH_3S^- solutions with different molar ratios, in which while an initial CH_3S^- concentration of 3.1 mM was fixed for all reactions, different initial concentrations of ferrate(VI) from 1.49 to 15 mM with molar ratios of 0.5-4.8 were applied. The amounts of CH_3S^- reduced and sulphate ions formed were determined by counting the difference before and after each reaction. The results are presented in Fig. 5-2.

To confirm the formation of sulphate as a final product, barium chromate was added into the reacted mixture and a white precipitate occurred immediately. Fig. 5-2 showed that the CH_3S^- reaction with ferrate(VI) in the 10 M NaOH reaction solutions was achieved to different degrees with different stoichiometric ratios. It can be seen that while the ratio of [Fe(VI)]/[CH_3S^-] was increased, the concentration of CH_3S^- was gradually decreased and the concentration of SO_4^{2-} was steadily increased. It was found that the complete destruction of CH_3S^- was achieved at a ratio of 2.20 and the complete conversion of sulphur to sulphate was achieved at a ratio of 4.53. These results indicate that the ratio of 2.20 would be a minimum dosage of ferrate(VI) to remove CH_3S^- and the ratio of 4.53 would be a sufficient dosage to convert CH_3S^- to sulphate ions completely. These data should be valuable for designing a prototype ferrate(VI) reactor system to work in continuous flow mode to degrade CH_3S^- from foul gases for odour control.

Considering the rate law and stoichiometry determined in this study, the mechanism of the CH_3S^- reaction with ferrate(VI) may be represented by Eqs (5-10). Although ferrate(VI) could have four different species ($H_3FeO_4^+$, H_2FeO_4, $HFeO_4^-$, and FeO_4^{2-}) against pH (Sharma 2010a), FeO_4^- was the only dominant species in such highly alkaline solution and CH_3SH with pKa = 9.7 fully dissociated into CH_3S^- in aqueous NaOH solution. CH_3S^- is a good electron donor and can react with FeO_4^{2-} (Eq. (6)) via one-electron-transfer mechanism to give the thiol radical ($CH_3S\bullet$) (Sharma et al. 2011). The breakage of the S-H bond, resulting in the formation of $CH_3S\bullet$, has been reported to occur much faster than that of the C-H bond (Masgrau et al. 2003). The $CH_3S\bullet$ further reacts with ferrate(VI) or Fe(V) to form $CH_3SO_3^-$ and $Fe(OH)_3$. The reaction of Fe(V) with sulphur compounds are 3-5 orders of magnitude faster than ferrate(VI) (Sharma and Cabelli 2009). Therefore, $CH_3SO_3^-$ and CH_3S^- further react preferentially with Fe(V) to form reaction products in Eqs. (8) and (9).

$$CH_3SH + OH^- \rightarrow CH_3S^- + H_2O \qquad (5)$$

$$FeO_4^{2-} + CH_3S^- \rightarrow Fe(V) + CH_3S\bullet \qquad (6)$$

$$FeO_4^{2-} + CH_3S\bullet + H_2O \rightarrow Fe(V) + CH_3SO_3^- \qquad (7)$$

$$Fe(V) + CH_3S^- + H_2O \rightarrow Fe(OH)_3 + CH_3SO_3^- \qquad (8)$$

$$Fe(V) + CH_3SO_3^- + H_2O \rightarrow Fe(OH)_3 + SO_4^{2-} \qquad (9)$$

$$\textbf{Net:}\ 14FeO_4^{2-} + 3CH_3SH + 23H_2O \rightarrow 14Fe(OH)_3 + 3SO_4^{2-} + 3CO_3^{2-} + 16OH^- \qquad (10)$$

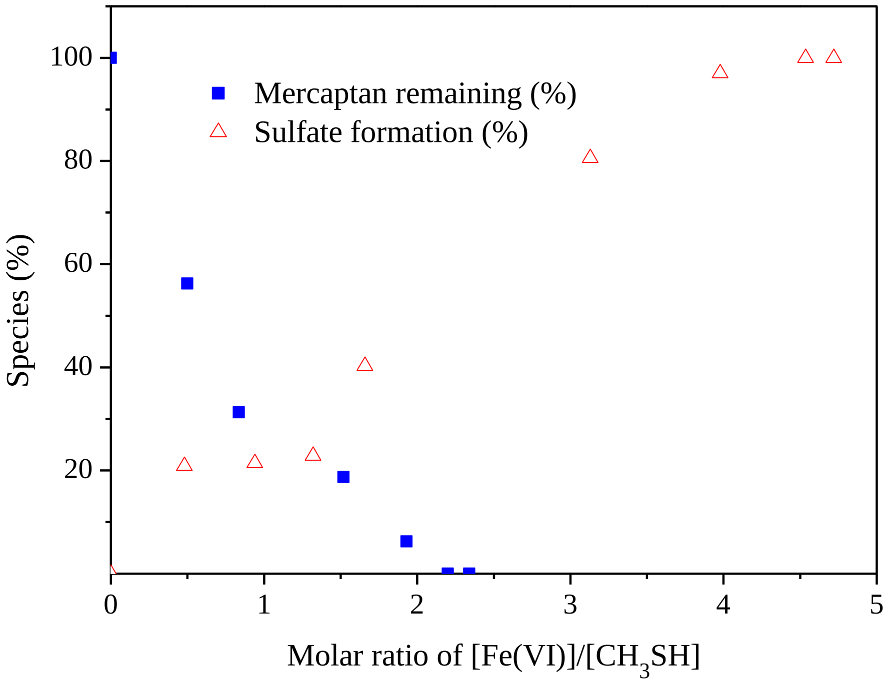

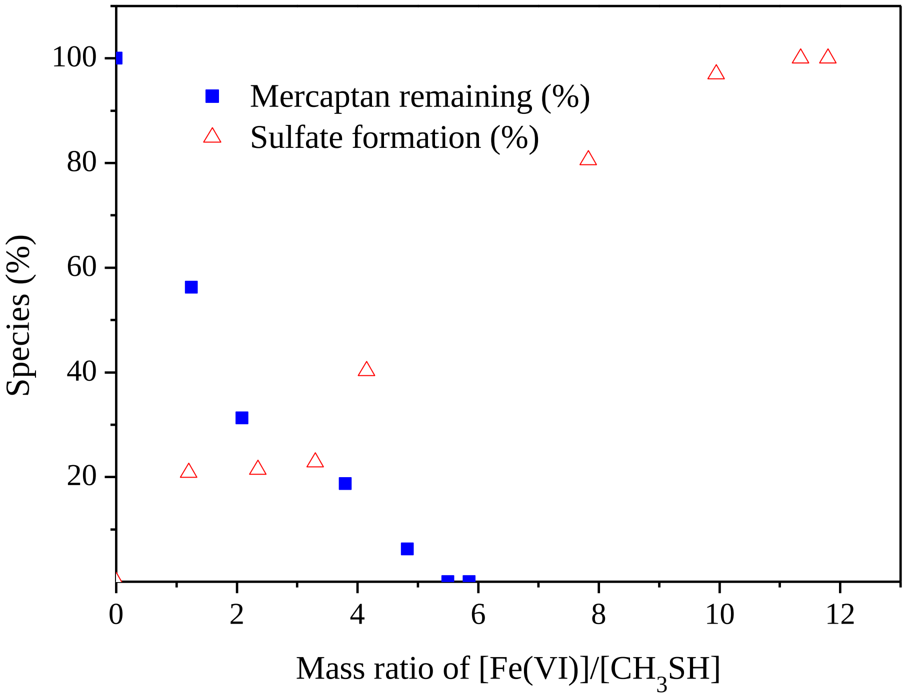

Figure 5-2 Percentage of mercaptan remaining and sulphate formation as a function of [Fe(VI)]/[CH_3S^-].

5.3 Effect of NaOH concentration on the CH_3SH degradation

As one of the most important operating parameters, the NaOH concentration in aqueous solution would greatly affect both the ferrate(VI) generation rate and its oxidation potential. Therefore, the influence of NaOH concentration on CH_3S^- degradation in a two-cell unit was investigated with the same initial CH_3S^- concentration of 0.2 mmol L^{-1} at 3.13 mA cm^{-2}, but different NaOH concentrations in the range of 1-14 M. The results are shown in Fig. 5-3 with an inset showing the pseudo first-order rate constants of CH_3S^- decay versus NaOH concentration. It was found that the rate of CH_3S^- degradation increased gradually from 1 to 3 M and more quickly beyond 4 M until a maximum value of $k = 0.236$ min^{-1} was achieved at 8 M. It was also found that at the higher NaOH concentration from 8 to 14 M, the degradation rate declined gradually. These results indicate that at NaOH concentrations below 8 M, CH_3S^- degradation was effectively dominated by the increase in ferrate(VI) generation rather than the decrease in oxidation potential of ferrate(VI). However, when the NaOH concentration was higher than 8 M, the adverse effect of the further lower oxidation potential of ferrate(VI) greatly reduced its reaction activity with CH_3S^- and resulted in a reduced rate of CH_3S^- degradation. It was important to note that the efficiency of CH_3S^- removal in such a system can be achieved by at least 60% after 15 min even in 1 M NaOH， where ferrate(VI) is not stable at all. Even under such a condition, the reaction rate between ferrate(VI) and CH_3S^- was still much faster than the rate of ferrate(VI) self-decomposition with H_2O. Moreover, this phenomenon in such a system demonstrates that at lower NaOH concentration, ferrate(VI) has a higher oxidation potential which is favourable to reaction with CH_3S^-, but not beneficial to the ferrate(VI) production. Therefore, there must be an optimum NaOH concentration (such as at 8 M under our experimental conditions), at which a breakeven balance between the ferrate (VI) oxidation potential and ferrate(VI) generation rate. This optimum NaOH concentration for CH_3S^- degradation found in this study is different from the optimum concentrations at 10 and 16 M for the ferrate(VI) generation only reported by Licht and Yu (Licht and Yu 2005), and Jiang et al. (Jiang et al. 2009), respectively as mentioned above in the introduction.

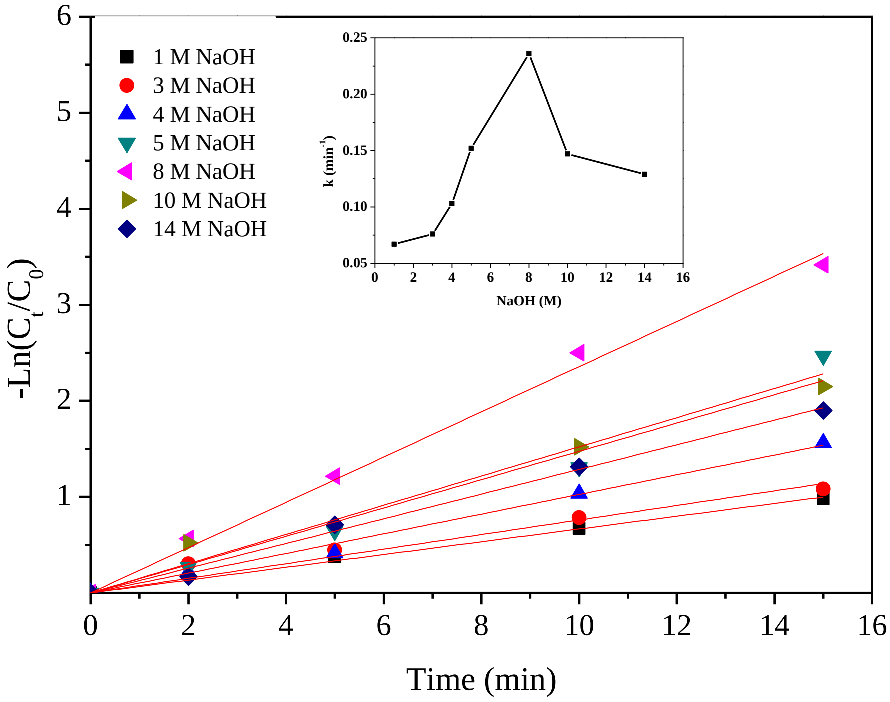

Figure 5-3 Effect of NaOH concentration on CH_3S^- degradation by in-situ generation of ferrate(VI) Insert: Variation of CH_3S^- decay rate constants (*k*) vs. NaOH concentration (Current density = 3.13 mA cm^{-2})

From an electrical energy consumption point of view, the electrical energy required for degrading 0.2 mM CH_3S^- at various NaOH concentrations and the constant current of 30 mA by online generation of ferrate(VI) was calculated in terms of kWh M^{-1} using Eq. (11) shown as follows:

$$E = \frac{UIt}{M} \times 10^{-3} \tag{11}$$

Where U is the applied voltage during the reaction (volt), I is the applied current intensity (A), t is the electrolysis time (h), and M is the mole of degraded CH_3S^- (M) (Khataee et al. 2009).

The calculated values are summarized in Table 5-1. It can be seen that the energy consumption per mole of degraded CH_3S^- gradually decreased with an increased NaOH concentration and the lowest value of 0.0854 kWh M^{-1} CH_3S^- was achieved at 8 M. With a further increase of NaOH beyond 8 M, the energy consumption increased gradually. These results indicate that the reaction at the optimum NaOH concentration can achieve not only the maximum rate of CH_3S^- degradation, but also the lowest rate of energy consumption with both technical and economic benefits.

Table 5-1 The energy consumption to degrade one mole of CH_3S^- with an initial concentration of 0.2 mM at I = 30 mA after 15 min affected by NaOH concentration.

NaOH	Degradation	Operating	Energy consumption per

Concentration (M)	efficiency (%)	voltage (V)	mole of degraded CH_3S^- (kWh M^{-1} CH_3S^-)
1	60.7	2.5	0.1544
3	64.1	2.4	0.1404
4	69.1	2.3	0.1248
5	91.5	2.3	0.0943
8	96.6	2.2	0.0854
10	87.5	2.2	0.0943
14	74.3	2.2	0.1110

5.5 Summary

This chapter described investigations into the reactivity of ferrate(VI) with methyl mercaptan in an aqueous highly alkaline solution. The experimental results indicate that the second-order reaction model suitably describes the kinetics of CH_3S^- reaction with ferrate(VI) in a strong alkaline solution. Meanwhile, the experimental results demonstrated that the ratio of $[Fe(VI)]/[CH_3S^-] = 2.20$ would be a minimum additional dosage for ferrate(VI) to fully destroy CH_3S^- and the ratio of 4.53 would be a sufficient dosage to completely convert CH_3S^- to sulphate ions. Considering the CH_3S^- degradation efficiency and energy consumption, there must be an optimum

NaOH concentration at which a breakeven balance between the oxidation potential of ferrate (VI) and the rate of ferrate(VI) generation to reach the maximum reaction rate with CH_3S^- is achieved. This chapter provides an essential understanding of the reactivity of ferrate(VI) with CH_3S^-, useful knowledge for developing a new odour control process involving the in-situ electrochemical production of ferrate(VI) for removal of gaseous sulphur-containing odours.

CHAPTER 6 Kinetic Models

6.1 Introduction

In this chapter, we present a new approach named "in-situ ferrate(VI) oxidation (IFO)" which applies the freshly generated ferrate(VI) to oxidize the odorous compounds in aqueous sodium hydroxide (NaOH) solution, in which, odorous contaminants are instantly absorbed first by the aqueous alkaline solution and then rapidly oxidized by the ferrate(VI) continuously generated from an iron anode by electricity. Chapter 4.4 confirmed that the self-decomposition of ferrate(VI) in a concentrated NaOH solution such as at 4 M and above is very slow. Hence, the ferrate(VI) reaction rate with contaminants is much faster than its self-decomposition rate and the actual proportion of fresh ferrate(VI) reacting with contaminants almost approaches the whole amount of its prime generation. The IFO process, therefore could achieve the maximum use of ferrate(VI) for contaminant purification.

As the mentioned in Chapter 5, three key factors involved in the IFO process include (i) prime generation of ferrate(VI), (ii) self-decomposition of ferrate(VI) in aqueous solution, and (iii) the rate of reaction between ferrate(VI) and CH_3S^-. Actually, there is a lack of information on the efficiency of the ferrate(VI) prime generation by the electrochemical method so far. Although Licht (Licht et al. 2004) demonstrated the ability to electrochemically synthesize solid ferrate(VI) salts using sodium/barium hydroxide co-electrolyte, in which the $NaOH/Ba(OH)_2$ concentration must be higher than 10 M due to the dissolution limitation. To the best of our knowledge, the efficiency of prime ferrate(VI) electrogeneration in lower NaOH concentrations (< 10 M) has not been reported in details. As the prime production of ferrate(VI) is a main driving force accelerating its reaction rate with contaminants in the IFO system, investigation of the key factors affecting prime ferrate(VI) generation is critical to the understanding of such as a system.

Methyl mercaptan (CH_3SH) is one representative odorous compound with significant toxicity and a very low odour detection threshold at around 0.4 ppb/v in air. CH_3SH reacts with NaOH very rapidly in concentrated alkaline solution. Hence, CH_3SNa was selected in this study as a probe to study its removal in an IFO system. The objectives of this study were (i) to establish a kinetic model describing the prime ferrate(VI) production and its reaction with CH_3SNa based on an empirical equation developed by He (He et al. 2006) and (ii) to further verify the model with the data obtained in the CH_3SNa degradation experiments with ferrate(VI) as affected by the three key factors of applied current density, initial CH_3SNa concentration, and NaOH concentration.

6.2 Kinetic Modelling Development

In principle, three key reactions are involved in such an IFO system, including (1) the generation of ferrate(VI) from the iron anode (Alsheyab et al. 2009, Licht et al. 2002b), (2) the self-decomposition of ferrate(VI) with H_2O (Jiang and Lloyd 2002), and (3) the reduction of ferrate(VI) by CH_3S^- (Ding et al. 2012, He et al. 2009) as shown below. To investigate the interactive effects between ferrate(VI) electrogeneration and consumption reactions, two sets of experiments were carried out in aqueous solution with and without CH_3S^-, respectively.

(1). Fe(VI) formation:

$$\mathrm{Fe(s)} + 8\mathrm{OH}^- \rightarrow \mathrm{FeO_4}^{2-} + 4\mathrm{H_2O} + 6\mathrm{e}$$

(2). Fe(VI) self-decomposition:

$$2\mathrm{FeO_4}^{2-} + 5\mathrm{H_2O} \rightarrow 2\mathrm{Fe(OH)_3} + 4\mathrm{OH}^- + 3/2\mathrm{O_2} \uparrow$$

(3). Fe(VI) reaction with CH_3S^-:

$$14\mathrm{FeO_4}^{2-} + 3\mathrm{CH_3S}^- + 26\mathrm{H_2O} \rightarrow 14\mathrm{Fe(OH)_3} + 3\mathrm{SO_4}^{2-} + 3\mathrm{CO_3}^{2-} + 19\mathrm{OH}^-$$

6.2.1 A Kinetic Model for In-situ Ferrate(VI) Generation

As is known, the accumulative concentration of ferrate(VI) in the production process depends on the competition between its electrochemical generation rate (reaction 1) and self-decomposition rate (reaction 2). It has been identified that the ferrate(VI) yield rate is strongly related to various synthesizing parameters including: (1) anode material; (2) one or two chambers; (3) electrolyte composition and strength; (4) applied current density; and (5) reaction temperature (Macova et al. 2009b, Yu 2008). In our study with a confined experimental arrangement, the two parameters of applied current density (j), and hydroxide concentration $[OH^-]$ are the key factors affecting the ferrate(VI) generation. The dependences of ferrate(VI) yield on applied current density and the hydroxide concentration were obtained by plotting ln[Fe(VI)] vs. lnj and ln[Fe(VI)] vs. $\ln[OH^-]$ in Figs. 6-1,6-2 and Table 6-1. Therefore, it is assumed that the rate of ferrate(VI) generation is proportional to the applied current density (j^m) and the hydroxide concentration $[OH^-]^n$ in the range of 5-14 M with the same anode and NaOH electrolyte. Based on our previous study, ferrate(VI) self-decomposition in highly concentrated alkaline solutions from 1.5 M to 14 M NaOH follows the first-order decay pattern (Ding et al. 2012). Thus, the accumulative concentration of ferrate(VI) can be expressed by Eq. 1,

$$\frac{\mathrm{d[Fe(VI)]}}{\mathrm{dt}} = k_1 j^m [OH^-]^n - k_2 [\mathrm{Fe(VI)}] \qquad (1)$$

where k_1 (mM min^{-1}) is the rate constant of ferrate(VI) generation, k_2 (min^{-1}) is the rate constant of ferrate(VI) self-decomposition

For a short duration of electrolysis (< 2 h), the iron electrode has light passivation

(Bouzek and Roušar 1997, Bouzek et al. 1996a, De Koninck et al. 2003) which may be ignored as within experimental error. Eq. 1, therefore, can be considered to represent an ideal rate of ferrate(VI) net generation and the accumulative concentration of ferrate(VI) in the electrolyte solution vs. time can be expressed as follows:

$$[\mathrm{Fe(VI)}] = \frac{k_1 j^m [OH^-]^n}{k_2}(1 - e^{-k_2 t}) \qquad (2)$$

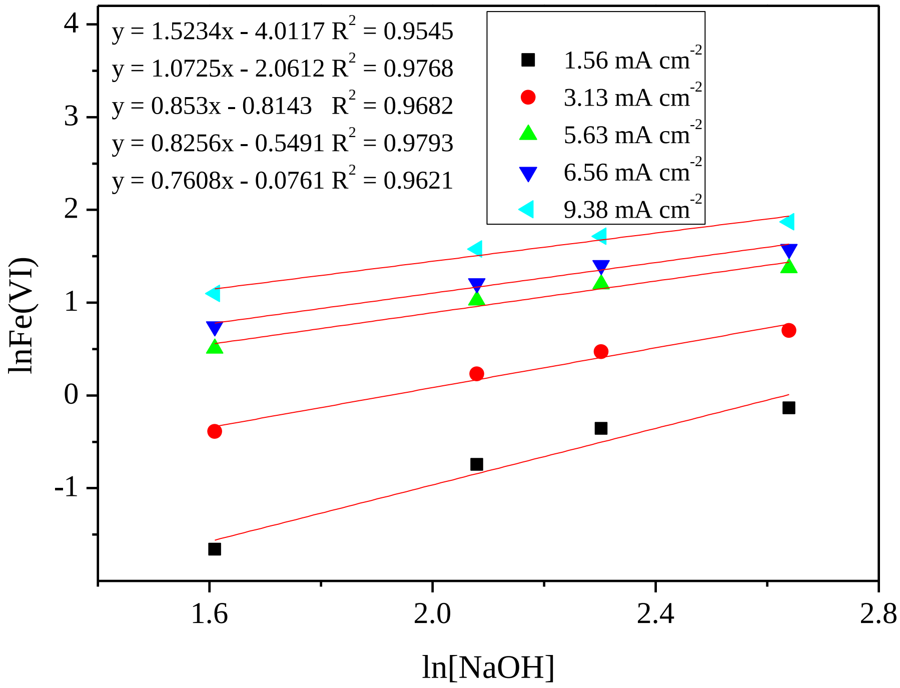

Figure 6-1 Dependence of ln[OH-] vs. ln[Fe(VI)] at various current density

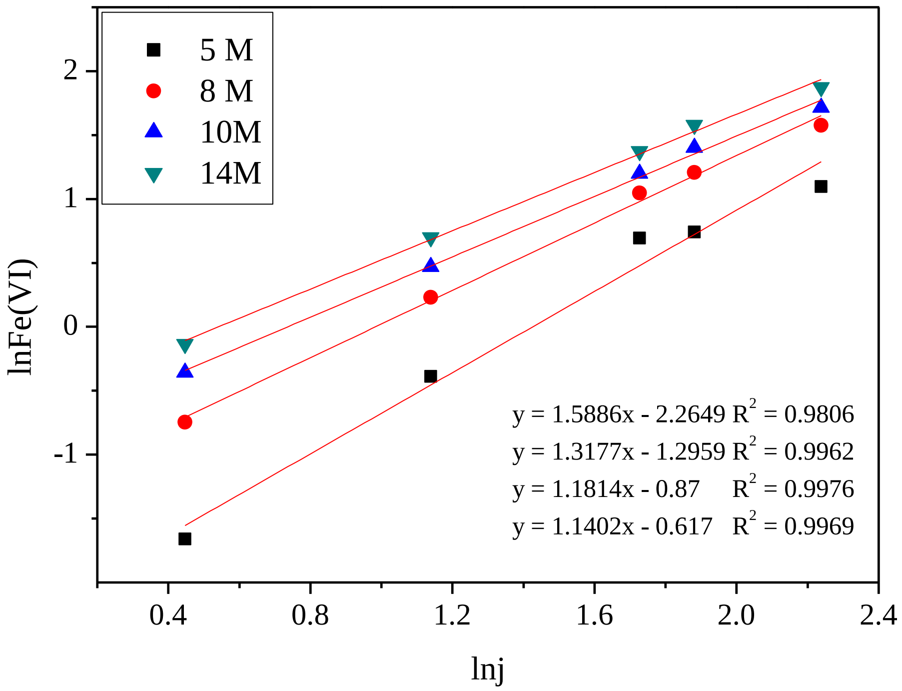

Figure 6-2 Dependence of lnj vs. ln[Fe(VI)] at various NaOH concentration

Table 6-1 The dependence of ferrate(VI) yield (mM) on anodic current density (j) and NaOH concentration

NaOH (M) j (mA cm^{-2})	5	8	10	14
1.56	$k_1(j^{1.59})[OH^-]^{1.52}$	$k_1(j^{1.32})[OH^-]^{1.52}$	$k_1(j^{1.18})[OH^-]^{1.52}$	$k_1(j^{1.14})[OH^-]^{1.52}$
3.13	$k_1(j^{1.59})[OH^-]^{1.07}$	$k_1(j^{1.32})[OH^-]^{1.07}$	$k_1(j^{1.18})[OH^-]^{1.07}$	$k_1(j^{1.14})[OH^-]^{1.07}$
5.63	$k_1(j^{1.59})[OH^-]^{0.85}$	$k_1(j^{1.32})[OH^-]^{0.85}$	$k_1(j^{1.18})[OH^-]^{0.85}$	$k_1(j^{1.14})[OH^-]^{0.85}$
6.56	$k_1(j^{1.59})[OH^-]^{0.83}$	$k_1(j^{1.32})[OH^-]^{0.83}$	$k_1(j^{1.18})[OH^-]^{0.83}$	$k_1(j^{1.14})[OH^-]^{0.83}$
9.38	$k_1(j^{1.59})[OH^-]^{0.76}$	$k_1(j^{1.32})[OH^-]^{0.76}$	$k_1(j^{1.18})[OH^-]^{0.76}$	$k_1(j^{1.14})[OH^-]^{0.76}$

6.2.2 A Kinetic Model for CH_3SH Reaction with In-situ Ferrate(VI)

To establish a new kinetic model for describing the reaction between in-situ ferrate(VI) and CH_3SH, we may assume that CH_3S^- is primarily degraded by ferrate(VI). The reaction between ferrate(VI) and CH_3S^- is regarded as a second-order reaction (Ding et al. 2012), so the kinetics for CH_3S^- reacting with ferrate(VI) can be expressed by Eq. 3 according to the reaction 3.

$$-\frac{\mathrm{d}[\mathrm{CH_3S^-}]}{\mathrm{dt}} = k_3'[\mathrm{Fe(VI)}][\mathrm{CH_3S^-}] \qquad (3)$$

where k_3' (mM^{-1} min^{-1}) is the rate constant of CH_3S^- reaction with ferrate(VI)

While ferrate(VI) is constantly generated from the iron anode into the bulk solution (reaction 1), it is continuously consumed by its self-decomposition (reaction 2) and reaction with CH_3S^- (reaction 3). Therefore, the net increasing rate of ferrate(VI) concentration in the alkaline solution can be expressed by Eq. 4:

$$\frac{\mathrm{d[Fe(VI)]}}{\mathrm{dt}} = k_1\mathrm{j}^{\mathrm{m}}[OH^-]^n - k_2[\mathrm{Fe(VI)}] - k_3[\mathrm{CH_3S^-}][\mathrm{Fe(VI)}] \qquad (4)$$

where k_3 (mM^{-1} min^{-1}) is the rate constant of ferrate(VI) with CH_3S^-

Our previous work (Ding et al. 2012) confirmed that the rate of self-decomposition of potassium ferrate(VI) at 4~14 M NaOH is much slower than the rate of ferrate(VI) reaction with CH_3S^-. Therefore, under this condition, the overall rate expression of ferrate(VI) concentration can be simplified by Eq. 5:

$$\frac{\mathrm{d[Fe(VI)]}}{\mathrm{dt}} = k_1 \mathrm{j}^{\mathrm{m}}[OH^-]^n - k_3[\mathrm{CH_3S^-}][\mathrm{Fe(VI)}] \tag{5}$$

Actually, this experiment was conducted by pre-dissolving an amount of CH_3S^- in aqueous NaOH solution with no ferrate(VI) in the solution when t = 0. Then a constant electrical current was supplied, ferrate(VI) was constantly in-situ generated electrochemically and consumed by the reaction with the dissolved CH_3S^-. Therefore, under the condition of $[CH_3S^-]$ much more than [Fe(VI)], $[CH_3S^-]$ during the reaction was considered to be relatively constant for [Fe(VI)].

To simplify the model development from a mathematical point of view, it was assumed that $[CH_3S^-]$during the reaction is proportional to its initial concentration of $[CH_3S^-]_0$ with a fixed ratio of λ in order to integrate Eq. 5 to obtain Eq. 6 as an expression of [Fe(VI)] against reaction time. According to the initial condition when t = 0, [Fe(VI)] = 0, [ferrate(VI)] can be eventually expressed as Eq. 6.

$$[\mathrm{Fe(VI)}] = \frac{k_1 \mathrm{j}^{\mathrm{m}}[OH^-]^n}{k_3 \lambda [\mathrm{CH_3S^-}]_0}(1 - e^{-(k_3 \lambda [\mathrm{CH_3S^-}]_0)t}) \tag{6}$$

If Eq. 6 is used to replace the [Fe(VI)] in Eq. 3, the rate of CH_3S^- degradation can be further expressed as follows:

$$-\frac{\mathrm{d}[\mathrm{CH_3S^-}]}{\mathrm{dt}} = k_3' \frac{k_1 \mathrm{j}^{\mathrm{m}} [OH^-]^n}{k_3 \lambda [\mathrm{CH_3S^-}]_0} (1 - e^{-(k_3 \lambda [\mathrm{CH_3S^-}]_0) t}) [\mathrm{CH_3S^-}] \tag{7}$$

After integration, the CH_3S^- concentration becomes a function of experimental time (t) as described by Eq. 8.

$$Ln \frac{[\mathrm{CH_3S^-}]_0}{[\mathrm{CH_3S^-}]} = \frac{k_3' k_1 \mathrm{j} [OH^-]^n}{k_3 \lambda [\mathrm{CH_3S^-}]_0} (t - \frac{1 - e^{-k_3 \lambda [\mathrm{CH_3S^-}]_0 t}}{k_3 \lambda [\mathrm{CH_3S^-}]_0}) \tag{8}$$

To simplify Eq. (8), letting a = $k_1 j^m [OH^-]^n$, b = $k_3 \lambda [CH_3S^-]_0$, the above equation can be re-arranged in the more simplified form below:

$$Ln \frac{[\mathrm{CH_3S^-}]_0}{[\mathrm{CH_3S^-}]} = \frac{a k_3'}{b} (t - \frac{1 - e^{-bt}}{b}) \tag{9}$$

It can be concluded that the above pair of equations (Eqs. 2 and 9) have been established as the main kinetic models describing the IFO reaction system giving the profile of ferrate(VI) concentration and CH_3SH concentration in aqueous alkaline solution vs. reaction time.

6.3 Experimental Results and Model Validation

6.3.1 The Kinetic model for in-situ ferrate(VI) generation

Based on the experimental data of electrochemical ferrate(VI) synthesis, the in-situ ferrate(VI) generation model (Eq. 2) was first validated by ferrate(VI) concentrations obtained over a wide range of NaOH concentration from 5 to 14 M and current densities from 1.56 to 9.38 mA cm^{-2}. The curve fitted results are shown in Fig. 6-3and 4. It can be clearly seen that the new model simulated the measured data well in all experiments. The rate constants k_1 and k_2 were also determined by the least-square method via the Matlab R2010b program (MathWorks, Inc) as listed in Tables 6-2 and 6-3.

The preceding experimental results indicate that the high NaOH concentration of 14–16 M proved capable of achieving the highest net ferrate(VI) yield by pushing reaction (1) towards the right side (Ding et al. 2012, He et al. 2006, Licht et al. 2004, Yu 2008). Furthermore, the parasitic decomposition (k_2) can also increase the reduction of ferrate(VI) in the lower NaOH concentration. From Table 6-2, it was interesting to find that the prime electrochemical generation rate of ferrate(VI), k_1, linearly increased from 5 to 10 M [OH$^-$] and then slightly decreased from 10 to 14 M [OH$^-$]. Actually, the polarization curve of iron in the passive potential region showed that the anodic current density of iron electrode at high NaOH concentration is higher than that at low NaOH concentration (He et al. 2006). For the kinetic trend, however, the model results underestimated the rate of ferrate(VI) generation at 14 M NaOH. Since ferrate(VI) concentration was measured from the bulk solution in the study, k_1 exactly represents a two-step rate of ferrate(VI) generation from the iron anode and diffusion into bulk solution, while the polarization curve demonstrated the reactions occurred on the electrode surface. The diffusion coefficient of ferrate(VI) in aqueous NaOH electrolyte decreased with increasing NaOH concentration, due to the NaOH electrolyte becoming more and more viscous. It is speculated, therefore, that a delay in the mass transfer of the generated ferrate(VI) might be the reason why k_1 declined slightly at 14 M [OH^-].

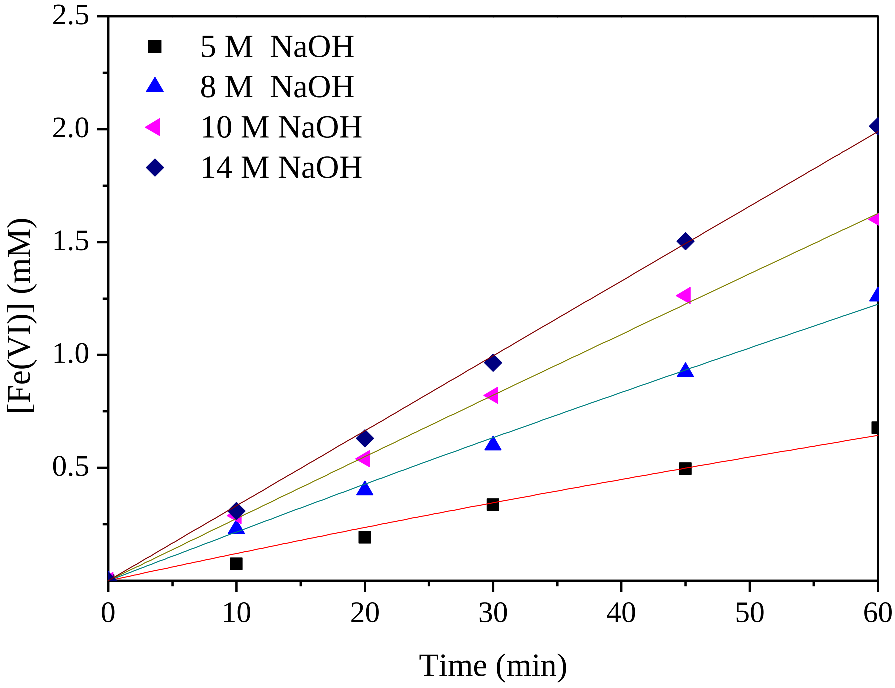

Figure 6-3 Dependence of ferrate(VI) yield (mM) on NaOH concentration ([OH^-]) at 3.13 mA cm^{-2} fitted by the kinetic model for in-situ ferrate(VI) generation

Table 6-2 Regression results of ferrate(VI) yield (mM) on NaOH concentration

($[OH^-]$) at 3.13 mA cm^{-2} using the ferrate(VI) concentration model

NaOH concentration (M)	5 M	8 M	10 M	14 M
a	0.013	0.022	0.028	0.033
k_1 (*10^{-3} mM min^{-1})	0.379	0.527	0.62	0.534
k_2 (*10^{-3} min^{-1})	4.9	2.5	0. 67	0.11

The rate of ferrate(VI) decomposition, k_2, decreased rapidly with increased $[OH^-]$ from 4.9 x 10^{-3} min^{-1} at 5 M to 0.67 x 10^{-3} min^{-1} at 10 M and then gradually further decreased to 0.11 x 10^{-3} min^{-1} at 14 M, which corresponds to the experimental results of our previous work (Ding et al. 2012). From the above fitted values of k_1 and k_2, it may be implied that self-decomposition of ferrate(VI) in different NaOH concentration was a more influential factor than the prime generation of ferrate(VI) on controlling the ferrate(VI) yield. Nevertheless, the model predicts the overall trend of ferrate(VI) yield in the course of time very well, as shown in Fig. 6-3 and 4.

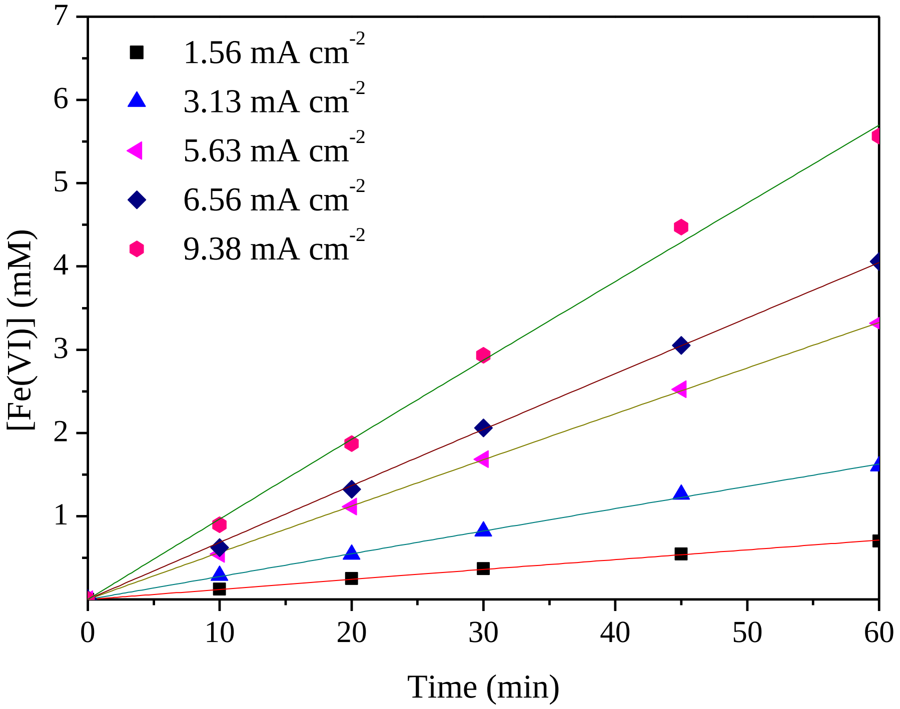

Figure 6-4 Dependence of ferrate(VI) yield (mM) on anodic current density (j) at 10 M NaOH fitted by the kinetic model for in-situ ferrate(VI) generation

Table 6-3 Regression Results of ferrate(VI) yield (mM) on current density (j) at 14 M NaOH using the ferrate(VI) concentration model

Current density (j)	1.56 mA cm^{-2}	3.13 mA cm^{-2}	5.63 mA cm^{-2}	6.56 mA cm^{-2}	9.38 mA cm^{-2}
a	0.015	0.033	0.065	0.077	0.107
k_1 (*10^{-3} mM min^{-1})	0.164	0.534	0.962	1.009	1.122
k_2 (*10^{-3} min^{-1})	0.11	0.11	0.13	0.13	0.14

The results in Table 6-3 show the effect of current density on the ferrate(VI) generation. It can be seen that while the value of k_1 increased rapidly from 0.164 x

10^{-3} mM min^{-1} at 1.56 mA cm^{-2} to 0.962 x 10^{-3} mM min^{-1} at 5.63 mA cm^{-2} and then gradually increased from 1.009 x 10^{-3} mM min^{-1} at 6.56 mA cm^{-2} to 1.122 x 10^{-3} mM min^{-1} at 9.38 mA cm^{-2}, that of k_2 also gradually increased from 0.11 x 10^{-3} min^{-1} at 1.56 mA cm^{-2} to 0.14 x 10^{-3} min^{-1} at 9.38 mA cm^{-2}. These results confirm that the higher current density increases cell potential and then accelerates the rate of ferrate(VI) synthesis, but also raises internal cell temperature and accelerates the rate of ferrate(VI) self-decomposition in aqueous alkaline solution.

Eq. 2 indicates the trend that ferrate(VI) concentration has an initial increase resulting from the gap between prime generation rate and self-decomposition rate, and then gradually rise up to a steady state when the self-decomposition rate catches up with the generation rate. To further confirm this, one experiment was conducted at 4 M NaOH with a relatively high self-decomposition rate and a current density of 1.56 mA cm^{-2} with a relatively low generation rate in order to shorten the time period required to reach the steady state. The experimental results in Fig. 6-5 shows the same pattern as indicated by Eq. 2 that ferrate(VI) concentration increases quickly during the first 20 min and then increases slowly until a nearly steady state was reached at 60 min.

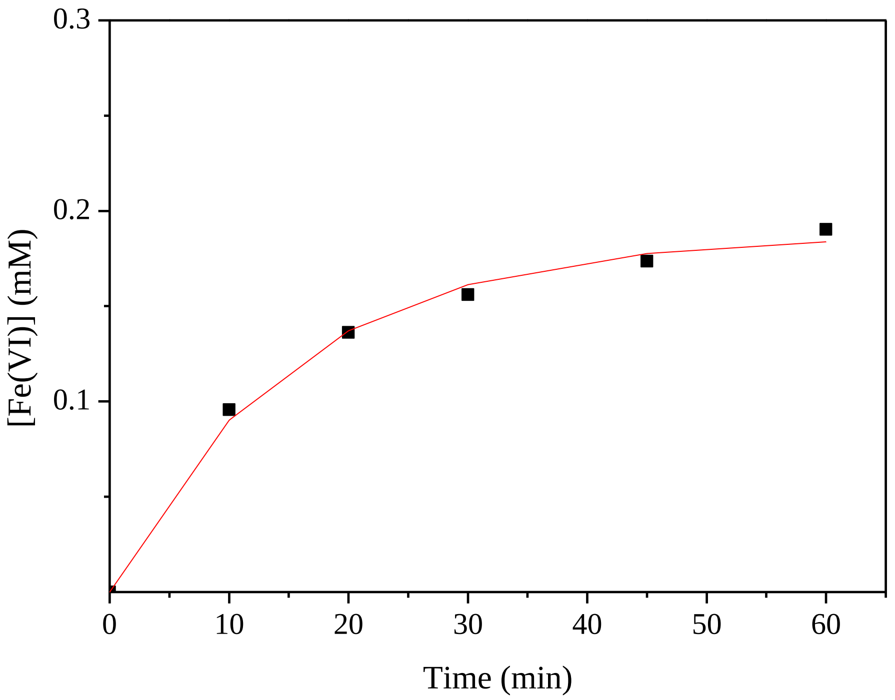

Figure 6-5 Dependence of ferrate(VI) yield (mM) at 4 M NaOH with the current density of 1.56 mA cm^{-2} fitted by the kinetic model for in-situ ferrate(VI) generation

6.3.2 The Kinetic Model for CH_3SH Reaction with In-situ Ferrate(VI)

In this novel process, CH_3SH is first absorbed by aqueous alkaline solution and rapidly oxidized by the ferrate(VI) continuously generated from an iron anode by electricity. As the rate of ferrate(VI) reaction with CH_3SH is much faster than that of its self-decomposition, the freshly generated ferrate(VI) in this IFO system can be almost fully utilized to react with CH_3SH. To validate the new model for application in the IFO system, three sets of experiments were carried out, respectively varying the three key factors of current density, NaOH concentration and initial CH_3SH concentration to study the effects on CH_3SH degradation. Each set of experiments with an initial CH_3SH concentration of 0.09-1.71 mM, a current density of 0.73-5.63

mA cm^{-2} and an NaOH concentration of 5-14 M, was run to investigate CH_3SH concentration against reaction time

6.3.2.1 Effect of current density

The oxidation of organic pollutants in the IFO system is achieved by the in-situ ferrate(VI) produced by the electrochemical reaction (reaction 3) from the iron anode. As reported by many authors (Macova et al. 2009b, Yu 2008), the rate of ferrate(VI) generation on the iron anode is affected by the applied current density and the rate of ferrate(VI) reduction is mainly a consequence of the reaction with CH_3S^-. Hence, the effect of current density on the CH_3S^- degradation reaction was investigated in a set of experiments performed in 14 M NaOH solution with initial CH_3S^- concentration of ~0.2 mM. As shown in Fig. 6-6, the rate of CH_3S^- degradation increased with increased current density in general. It was also found that the CH_3S^- degradation in such a process was very effective and rapid. For example, at the current density = 5.63 mA cm^{-2}, 90% of CH_3S^- was reduced in 14 M NaOH solution within in 10 min.

It can be seen that the kinetics of CH_3S^- degradation with in-situ generated ferrate(VI) in such a system is well fitted by this new model with good correlation coefficients (R^2 = 0.95-0.99) as shown in Table 6-4. The values of the composite parameter (ak_3') were determined to be 0.024 min^{-2} at 0.73 mA cm^{-2} and 0.249 min^{-2} at 5.63 mA cm^{-2}, respectively. Since ak_3' is a product of the rate of ferrate(VI) electrochemical generation and the rate of ferrate(VI) reaction with CH_3S^- in the alkaline solution, the variation is due to these factors. Under this condition, the faster rate of CH_3S^- degradation by ferrate(VI) at the higher current density could be ascribed to the acceleration of ferrate(VI) formation according to Eq. 2. However, the kinetics of CH_3S^- degradation did not fit well with this new model when the current density was below 0.73 mA cm^{-2} (data not shown in Fig. 6-6.). A possible reason is that the rate of ferrate(VI) formation might be limited by the insufficient anodic potential and thus CH_3S^- degradation by ferrate(VI) was quite slow at the beginning. The ak_3' are clearly linear-proportional to the increased current density with a slope of 1.156 on the ln–ln scale for the IFO experiments,

$$\ln(ak_3') = 1.156 \ln j - 3.250 \quad (R^2 = 0.98) \qquad (10)$$

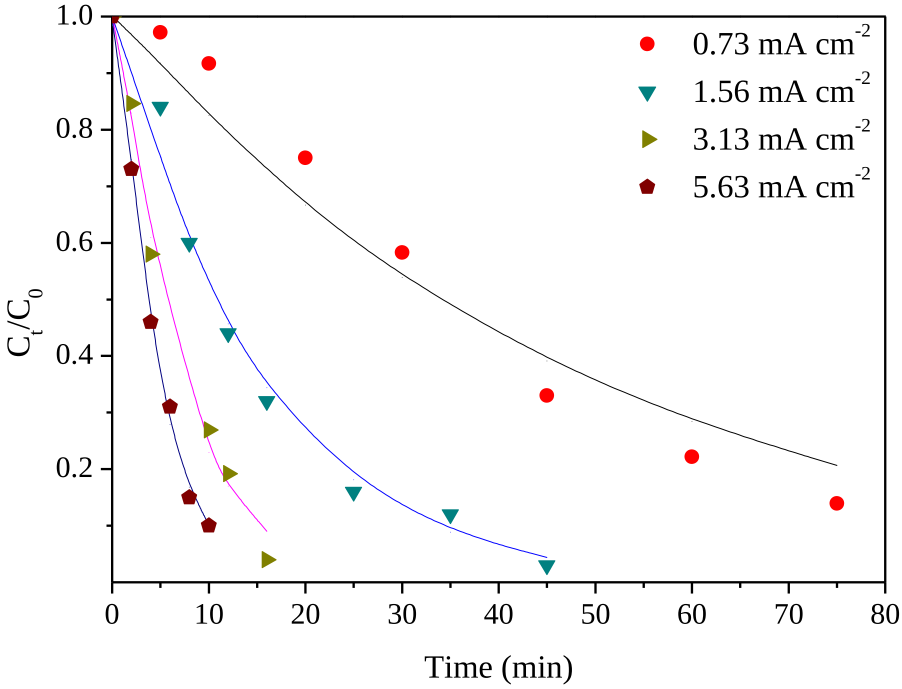

Figure 6-6 CH_3S^- degradation by IFO at different current density, fitted by the kinetic model for in-situ ferrate(VI) oxidation of CH_3S^-

Table 6-4 Regression results of CH_3S^- degradation kinetics with an initial concentration of ~0.2 mM at different current density (j) in 14 M NaOH solution

j (mA cm^{-2})	ak_3' (min^{-2})	R^2
0.73	0.024	0.9597
1.56	0.074	0.9881
3.13	0.165	0.9924
5.63	0.249	0.9974

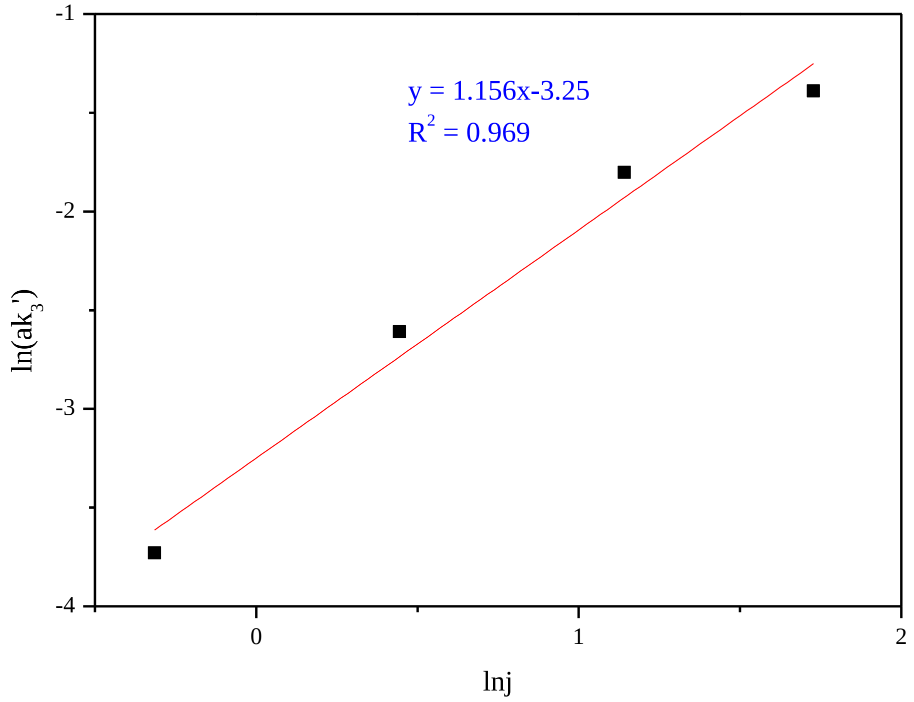

Figure 6-7 Plotting the lnj versus $\ln ak_3'$

6.3.2.2 Effect of NaOH concentration

In such a process, NaOH concentration is a crucial parameter to significantly affect the three rates of (i) ferrate(VI) generation, (ii) ferrate(VI) self-decomposition, and (iii) ferrate(VI) reaction with CH_3S^-. The effect of NaOH concentration on the ferrate(VI) reaction with CH_3S^- was investigated in a set of experiments with an initial CH_3S^- concentration of ~0.1 mM at the current density of 3.13 mA cm^{-2}. The results are shown in Fig. 6-8. It can be seen that the degree of CH_3S^- degradation significantly increased with an increased NaOH concentration from $ak_3' = 0.164$ min^{-2} at 5 M to 0.319 min^{-2} at 7 M and further enhanced to reach a maximum value of 0.398 min^{-2} at 10 M. Moreover, it was also found that the CH_3S^- degradation reaction gradually slowed down at NaOH concentrations beyond 10 M. These results indicate that there is an optimum NaOH concentration which leads the best CH_3S^- degradation performance in such a process.

The overall efficiency of CH_3S^- degradation in this process can be expressed by an apparent rate constant, ak_3', as shown in Table 6-5, which depends on both the rates of ferrate(VI) generation and the CH_3S^- reaction with ferrate(VI) in the alkaline solution. As we know that the rate of ferrate(VI) electrochemical generation increases with an increased NaOH concentration. From Fig. 6-8, it indicates clearly that 10 M NaOH was an optimum concentration to remove ~0.1 mM CH_3S^- at 3.13 mA cm^{-2} in this process. Therefore, the adverse effect of the higher NaOH concentration on the CH_3S^- removal can be explained by a decreased rate of the reaction occurring between ferrate(VI) and CH_3S^-. Since the ferrate(VI) species exist as FeO_4^{2-} in the concentrated alkaline solution, the species involved in these reactions did not change with solution changes from 5 M to 14 M NaOH. Therefore the oxidation potential of ferrate(VI) may be affected by increasing the NaOH concentration according to the Nernst equation (Stephanson and Flanagan 2003). The lower oxidation potential of ferrate(VI) greatly reduced its reaction activity with CH_3S^- resulting in a reduced rate of CH_3S^- degradation.

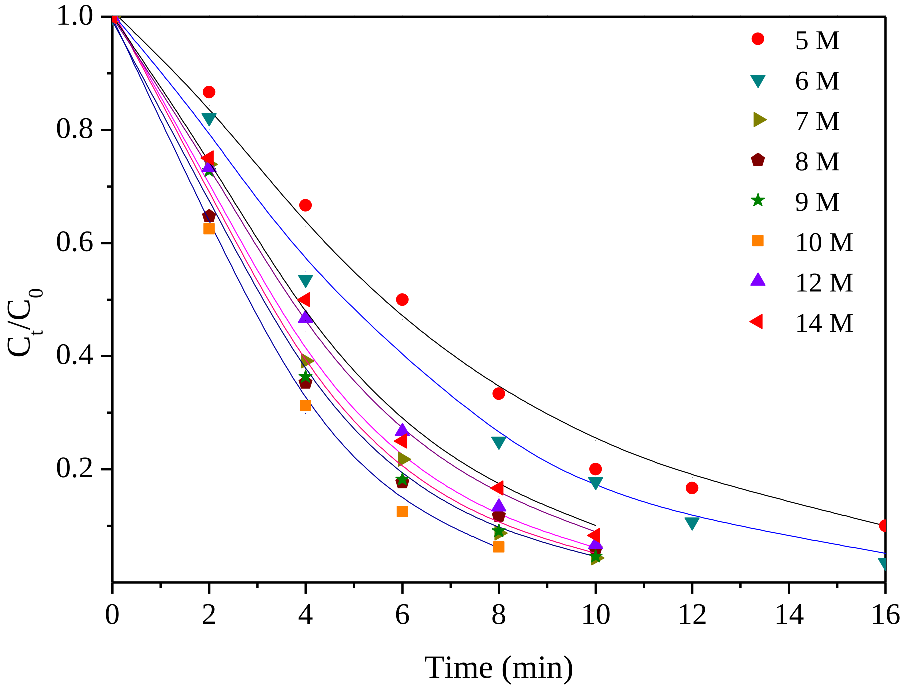

Figure 6-8 ~0.1 mM CH_3S^- degradation by IFO at different NaOH concentration with 3.13 mA cm^{-2}, fitted by the kinetic model for in-situ ferrate(VI) oxidation of CH_3S^-

Table 6-5 Regression results of CH_3S^- degradation kinetics with an initial concentration of ~0.1 mM at different NaOH concentrations at the current density of 3.13 mA cm^{-2}

NaOH (M)	ak_3' (min^{-2})	R^2
5	0.164	0.9915
6	0.204	0.9857
7	0.319	0.9967
8	0.336	0.9974
9	0.340	0.9973
10	0.398	0.9996
12	0.267	0.9975
14	0.257	0.9961

To further understand the effect of the concentrated NaOH solution, two profiles of ORP variation vs. NaOH concentration with and without ferrate(VI) are shown in Fig. 6-9. It can be seen that negative values of ORP were detected in the NaOH solution without ferrate(VI) and these slightly decreased with an increased NaOH concentration from 3 to 12 M. Alternatively, quite positive ORP values of above +250 were detected in the NaOH solution with ferrate(VI) at 0.075 mM and these also slightly decreased with increased NaOH concentration in the same range. Therefore, the increasing NaOH concentration was capable of lowering ORP values and creating reducing conditions, even in the presence of a strong oxidizing agent. The observed ORP values in this system might not be indicative of the true redox potential, but ORP could be useful in an empirical way to indicate whether the system is in an oxidizing or reducing conditions.

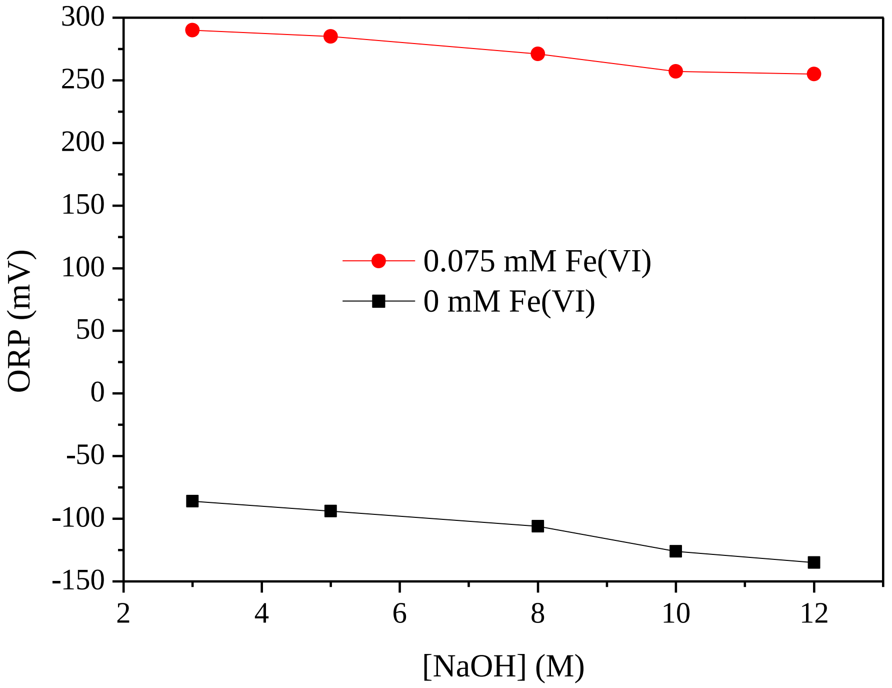

Figure 6-9 Variations of electrolyte ORP with or without ferrate(VI) at different NaOH concentration.

6.3.2.3 Effect of Initial CH_3S^- Concentration

The effect of CH_3S^- concentration from 0.09 to 1.71 mM on its decay kinetics in 14 M NaOH solution was investigated in the IFO process at a current density of 3.13 mA cm^{-2}. The profiles of CH_3S^- concentration vs. reaction time are well fitted by Eq. 9 as shown in Fig. 6-10. Along with the increase of CH_3S^- concentration, the rates of CH_3S^- degradation accelerated, but the reaction time for the complete removal of CH_3S^- was extended as the rate constant, ak_3', decreased quickly with increased CH_3S^- concentration (Table 6-6). The plot between the ak_3' and CH_3S^- concentration on the ln–ln scale again showed a straight line with a slope of 1.046, hence, the reaction rate equation became

$$\ln(ak_3') = -3.709 - 1.046\ln[\mathrm{CH_3S^-}]_0, \quad (R^2 = 0.99) \tag{11}$$

The half-life of CH_3S^- ($t_{1/2}$) degradation can be derived from the kinetic model Eq. 9 as follows:

$$t_{1/2} = \frac{1}{\mathrm{k_3\lambda[CH_3S^-]_0}} + \frac{0.693(\mathrm{k_3\lambda[CH_3S^-]_0})}{ak_3'} \tag{12}$$

Values of $t_{1/2}$ for different initial concentrations of CH_3S^- are listed in Table 6-6. A plot of $\ln(t_{1/2})$ versus $\ln(CH_3S^-)$ shows that there is a good linear correlation between them:

$$\ln(t_{1/2}) = 3.255 + 0.863\ln[\mathrm{CH_3S^-}]_0, \ (R^2 = 0.99) \tag{13}$$

From Eq. (13), it can be seen that the coefficient of $\ln(CH_3S^-)$ is 0.8628, less than 1, which indicates that the initial concentration of CH_3S^- increases at a higher rate than the half-life of CH_3S^-. More CH_3S^- will be degraded by the IFO in high concentration solutions than in dilute solutions for a given time period. High concentrations of CH_3S^- can enhance its ability to compete with its by-products.

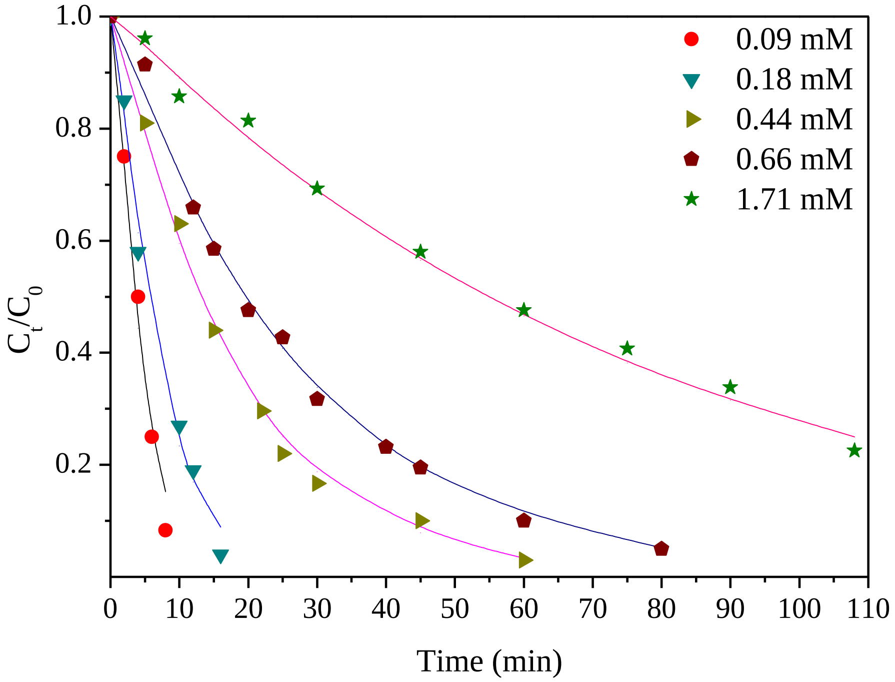

Figure 6-10 CH_3S^- degradation by IFO with different initial CH_3S^- concentration in 14 M NaOH solution at 3.13 mA cm^{-2}, fitted by the kinetic model for in-situ ferrate(VI) oxidation of CH_3S^-

Table 6-6 Regression results of CH_3S^- degradation kinetics with different initial CH_3S^- concentration at current density of 3.13 mA cm^{-2} in 14 M NaOH solution

CH_3S^- (mM)	ak_3'	R^2	$t_{1/2}$ (min)
0.09	0.275	0.9851	3.52
0.18	0.165	0.9924	5.20
0.44	0.058	0.9964	12.91
0.66	0.039	0.9961	18.77
1.71	0.013	0.9931	41.19

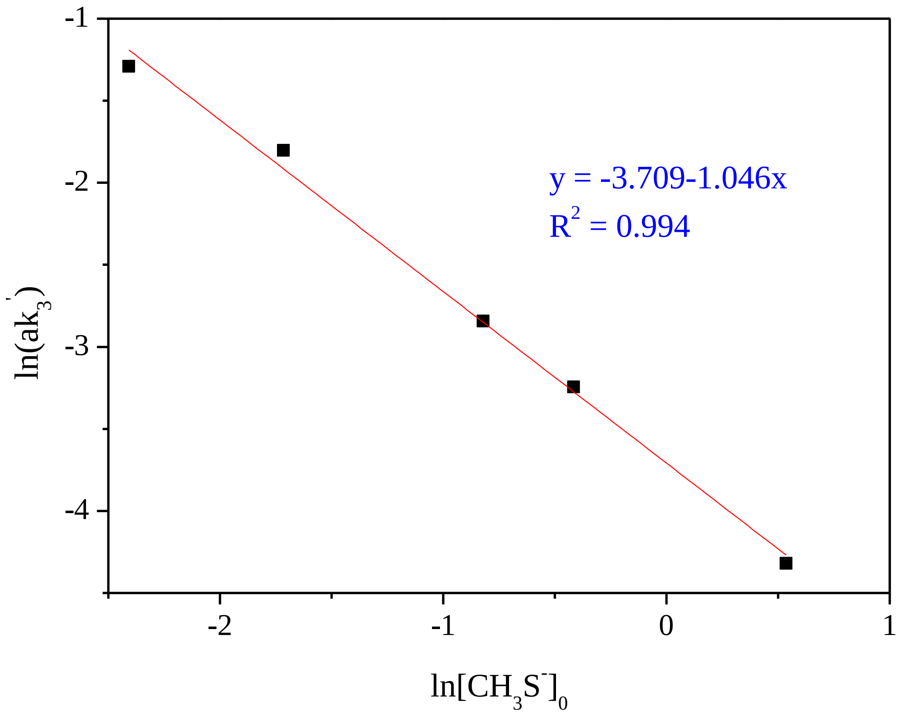

Figure 6-11 The plot between the ln(ak_3') and ln[CH_3S^-]$_0$

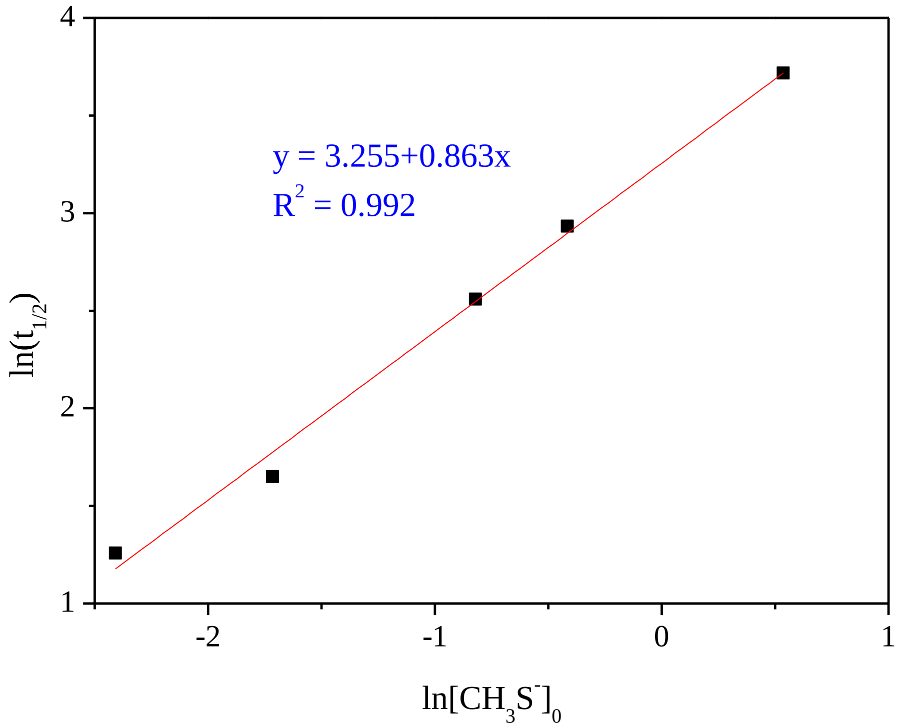

Figure 6-12 The plot between the ln($t_{1/2}$) and ln[CH_3S^-]$_0$

6.4 Summary

This chapter introduced a new treatment process named "In-situ Ferrate(VI) Oxidation (IFO)" in which gaseous odour such as methyl mercaptan (CH_3SH) can be rapidly absorbed by aqueous alkaline solution and quickly degraded by in-situ freshly generated ferrate(VI) through electrolysis. Two kinetic models to describe the in-situ ferrate(VI) generation and its reaction with CH_3SH were established mathematically by considering the three main reaction mechanisms of ferrate(VI) electrochemical generation, ferrate(VI) self-decomposition and CH_3SH degradation in aqueous strong alkaline solution. The effects of three key factors: (i) NaOH concentration, (ii) applied current density, and (iii) initial CH_3S^- concentration on the performance of the IFO process were investigated by conducting three sets of experiments and the kinetic models were validated by the fitting of the experimental data. The goodness of the fits demonstrated that the new models can describe well both the kinetics of ferrate(VI) generation reaction and CH_3S^- degradation reaction. The experimental results confirmed that the higher the NaOH concentration and the current density applied the more beneficial to the electrochemical generation of ferrate(VI) and also elimination of its self-decomposition. The experiments also demonstrated an optimum NaOH concentration at 10 M achieved the best CH_3S^- degradation performance in such an IFO system. However, the new models have only been validated in the case of CH_3S^- degradation so far. Further studies to apply this kinetic model in relation to the degradation of other pollutants is necessary.

CHAPTER 7 Gaseous CH_3SH Removal by an Absorption/Oxidation Scrubber in a Continuous Gas Flow Model

7.1 Introduction

Regulators and government bodies receive more and more complaints concerning odour problems nowadays (Gostelow et al. 2001). Wastewater treatment plants (WWTPs), usually located near residential areas, are responsible for unpleasant odour emissions, since odorous gases are produced in the course of wastewater treatment (Capelli et al. 2009, Frechen 1988). Typically, the species most responsible for odours in sewage treatment works have been identified to be reduced sulphur, nitrogen, fatty organic acids, aldehydes or ketones compounds. Among these, methyl mercaptan (CH_3SH) is a representative member of the sulphur species with a very low odour threshold of around 0.4 ppb/v (Bashkova et al. 2002). The daily average concentrations of CH_3SH produced directly from sewage treatment processes were measured in the range of 6.5-30 ppm/v from the beginning of spring to the end of summer (Charron et al. 2004). Thus, odour treatment at sewage treatment works has become essential.

In order to control these odorous gases, two types of techniques are implemented aiming at high efficiency, low running cost, easy operation properties, a small footprint and making use of simple equipments, including: (1) dry processes such as activated carbon adsorption (Bashkova et al. 2002, Tanada and Boki 1979), thermal oxidation (Chu et al. 2001), and newly developed non-thermal oxidation processes called "cold oxidation techniques" such as plasma (Tsai et al. 2001, Tsai et al. 2003, Yan et al. 2006), UV (Li et al. 2006, Liu et al. 2008), and microwave techniques (Sun et al. 2010); and (2) wet processes such as water absorption (chemical scrubbers) (Charron et al. 2006) and biological processes (biofilters or bioscrubbers) (Kanagawa and Mikami 1989, Myung et al. 1999, Tanji et al. 1989). Comparatively, the scrubbing technique has proven to be one of the most effective and reliable for odour treatment in wastewater treatment plants, since the high water content (moisture) in these odorous gases greatly reduces the efficiency of most dry processes.

In a wet chemical scrubber, the odorants should be quickly absorbed by liquid media such as water and then oxidized by some oxidizing reagents including chlorine, sodium hypochlorite, calcium hypochlorite, hydrogen peroxide, ozone, and potassium permanganate. Therefore, the contact time and pH of the scrubbing solution are two key parameters affecting odorants removal in this process. For example, in a compact scrubber with a NaClO/NaOH washing solution, CH_3SH removal with an initial concentration of 2 ppm/v proved difficult at a high gas velocity (a short contact time), even at a high pH of 11, while pH level had no influence on H_2S removal with the same situation (Sanchez et al. 2006). In the photocatalytic wet scrubbing process, CH_3SH absorption by the solution is a rate-determining step at $pH < 11.5$ (Liu et al. 2010). The pKa of CH_3SH is equal to 9.7. The crucial step is that the pH of the scrubbing solution is not basic enough to dissociate CH_3SH into ionized species and then enhance its mass transfer rate from gas phase to liquid phase (by moving the gas-liquid equilibrium) (Hentz and Balchunas 2000). To enhance gas-liquid mass transfer, three improvements can be made. The solution needs higher pH, longer contact time and higher oxidation potential of the chemical concerned. Indeed, conventional scrubbing processes have also revealed high investment and capital costs on the construction for high and wide towers, since a long residence time is necessary for gas-liquid contact and distribution.

Up to now, different concepts of electrochemical gas purification have increased the interest in electrochemical abatement strategies. Electrochemical techniques offer several advantages including the facts that there is no requirement for the continuous supply of large amounts of chemical reagents and no consideration is necessary concerning the transport and storage of hazardous and unstable chemicals. In the electrochemical gas purification process, the initial step is absorption of the gas pollutants into the electrolyte and the final step is the reaction between the liquid pollutants. The above reaction is either directly via conversion at the electrode of an electrochemical cell or indirectly via chemical reaction with a redox mediator, which can be electrochemically regenerated in continuous mode after the reaction.

In a previous study, a continuous flow process for odorous gas treatment by in-situ electro-generation of ferrate(VI) was developed (Ding et al. 2012). In our process, gaseous CH_3SH can be completely removed. Moreover, using fresh ferrate(VI) can not only save time and cost on ferrate(VI) purification, but also avoid the transportation and storage of ferrate(VI) chemical.

In order to optimize the best operating conditions and design parameters for a scale-up design, the efficiency of CH_3SH removal was characterized in a laboratory-scale pilot unit during this study. Experimental investigations were conducted on the removal of CH_3SH form synthetic odorous gas by in-situ electro-generation of ferrate(VI) in an absorption-oxidation scrubbing system. The influencing factors of NaOH electrolyte concentration, applied current density, CH_3SH loading and CH_3SH compositions, were investigated. As a new effective CH_3SH control strategy, this work has great academic significance and application value.

7.2 Gaseous CH_3SH Removal in the First Reactor

To investigate the feasibility of continuous CH_3SH removal from odorous gases, several sets of experiments were conducted in a wet scrubbing/oxidation reactor in Fig. 3-3 and 3-5 with in-situ generation of ferrate(VI) as a standalone odour treatment process at room temperature.

7.2.1 Effect of NaOH Concentration

The first set of experiments was performed to search out the optimum NaOH concentration for CH_3SH removal. The synthetic CH_3SH gas with an inlet concentration of 43 ppm/v was continuously fed into the reactor at 600 mL min^{-1} and the absorbed CH_3SH in aqueous NaOH solution was then immediately oxidized by ferrate(VI) freshly and continuously produced from the iron anode at the current density of 2.22 mA cm^{-2}. CH_3SH concentrations in both gas and liquid phases were monitored. In addition, a set of control experiments without the application of electricity was also conducted in NaOH solutions to monitor CH_3SH absorption only. The experiments were conducted for 240 min, in which electricity was not applied during the first 30 min as pre-treatment to build up the concentration of dissolved CH_3SH in the solution and then electricity was continuously applied for further 210 min.

In all experiments, it was found that the CH_3SH concentrations in the outlet gases were well below the detection limit of the CH_3SH sensor (< 1 ppm/v), which means the removal of CH_3SH from the gas phase was almost complete. From Eq. (2), it can be seen that mass transfer was promoted through the dissociation of CH_3SH into CH_3S^-, resulting in an increase of CH_3SH apparent solubility and in a mass transfer acceleration between the gas and the liquid phases. CH_3SH was then oxidized into its by-products by the in-situ generated ferrate, Eq. (3). Both of these mechanisms reduce CH_3SH accumulation in the liquid phase, and thus, improves its ability to remove gases.

At the gas–liquid interface:

$$CH_3SH_{(G)} \leftrightarrow CH_3SH_{(L)} \qquad (1)$$

In the liquid phase:

$$CH_3SH + OH^- \leftrightarrow CH_3S^- + H_2O \quad pKa = 9.7 \qquad (2)$$

$$14FeO_4^{2-} + 3CH_3SH + 23H_2O \rightarrow 14Fe(OH)_3 + 3SO_4^{2-} + 3CO_3^{2-} + 16OH^- \qquad (3)$$

Furthermore, in the control experiments without ferrate(VI) generation, the amount of absorbed CH_3SH in all NaOH solutions (3-14 M) was almost equivalent to its dose from gaseous phase, which means that the CH_3SH absorption by NaOH solution was rapid and complete in such a simple bubbling reactor system. In order to operate this reactor continuously, it is important to determine the saturated concentrations of CH_3SH in aqueous solutions with different NaOH concentrations. Therefore, experiments on the absorption of gaseous CH_3SH by different NaOH concentrations were carried out and the results are shown in Table 1. The saturation concentration of CH_3SH at 6 M NaOH solution was found to be 2,250 mM, which concentration was 5 orders of magnitude of aqueous CH_3SH concentration remaining in the NaOH solutions with in-situ generation of ferrate(VI). This result indicates that the driving force for CH_3SH absorption by NaOH solution is dramatically strong. Moreover, the saturation concentrations of CH_3SH from 1 M to 6 M NaOH increased linearly. Considering the chemical absorption mechanism, the saturation concentrations of

CH_3SH would further increase with increased NaOH concentrations. Therefore, it is believed that the overall process of CH_3SH removal is not limited at all by absorption rate from gaseous phase into liquid phase.

Table 7-1 Saturation concentrations of CH_3SH at different NaOH concentrations

NaOH (M)	1	3	6
CH_3SH (mM)	472	1,275	2,250

After electrical current was switched on, the dissolved CH_3SH concentration first dropped significantly due to the CH_3SH degradation by the freshly generated ferrate(VI), and then gradually recovered to eventually approach a balanced level, when the degradation rate is equal to the absorption rate. The concentration of dissolved CH_3SH in the aqueous solution was monitored and the results are shown in Fig. 7-1. It can further be observed that the CH_3SH concentration in the 6 M NaOH solution eventually stabilized the lowest level.

The dissolved CH_3SH concentration at 120 min vs. NaOH concentration in all experiments declined significantly compared to that in the control experiments, as shown in Fig. 7-2. Especially, the experiments in 5-8 M NaOH solutions showed a shock fall of CH_3SH concentration due to the faster rate of CH_3SH reduction by ferrate(VI) than that of CH_3SH intake rate. In the meantime, other experiments in the NaOH solutions either below 5 M or above 8 M showed higher concentrations of dissolved CH_3SH, indicating the reaction rates of CH_3SH reduction by ferrate(VI) in these solutions were not as fast as those in 5-8 M NaOH solutions. Ferrate(VI) was generated from the iron anode in the NaOH electrolyte. As indicated by Eq. (4), increasing the NaOH concentration results in an increase in the amount of ferrate(VI). However, the ferrate(VI) oxidation potential decreases, when the concentration of OH^- ions increases. Therefore, an optimum condition for CH_3SH removal should be achieved when there is a good balance between these two factors. Under our experimental conditions, an optimum NaOH concentration was found to be at around 6 M.

$$Fe + 2OH^- + 2H_2O \rightarrow FeO_4^{2-} + 3H_2 \qquad (4)$$

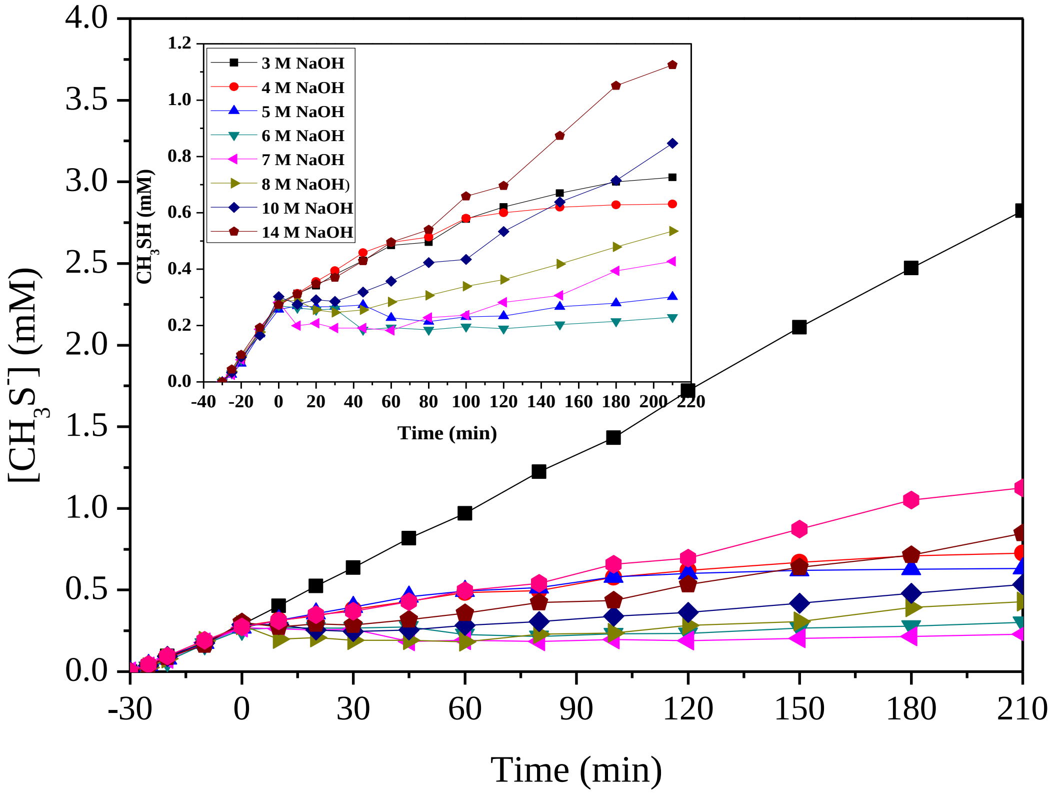

Figure 7-1 Effect of NaOH concentration on gaseous CH_3SH removal in the in-situ ferrate(VI) generation reactor Insert: Variation of CH_3SH concentration vs. reaction time in 3-14 M NaOH solutions (Current density = 2.22 mA cm^{-2})

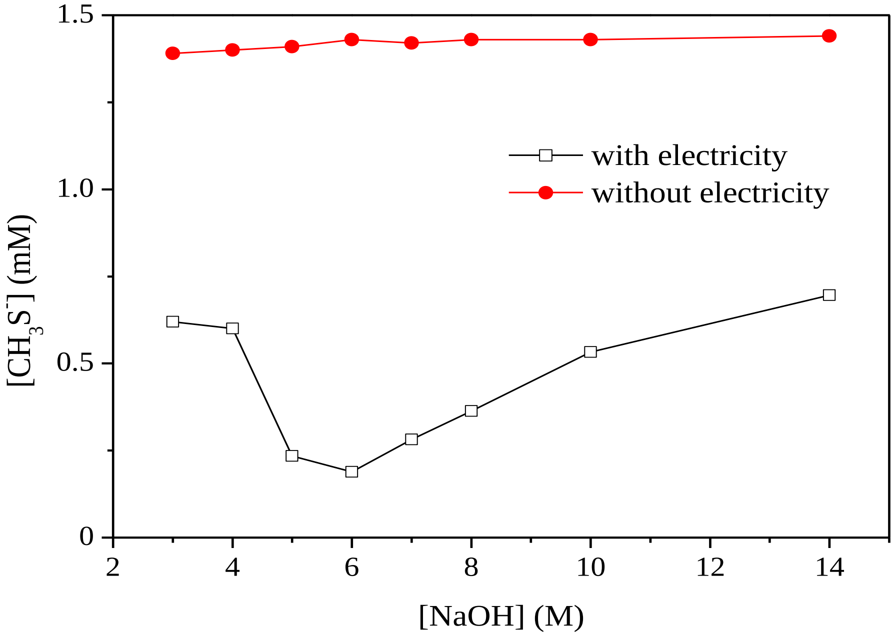

Figure 7-2 Aqueous CH_3SH concentration in different NaOH solutions after 120 min reaction in the in-situ ferrate(VI) generation reactor (current density= 2.22 mA cm^{-2}; $[CH_3SH]_{inlet-gas}$= ~43 ppm/v; gas flow rate= 600 mL min^{-1})

7.2.2 Effect of Current Density

The experiments on the effect of current density were conducted in 6 M NaOH solution with initial CH_3SH concentration of 43 ppm/v and gas flow rate of 600 mL min^{-1} for 180 min. Electricity was not supplied during the first 30 min as pre-treatment to build up the concentration of dissolved CH_3SH in the solution, Electricity was then continuously supplied for 150 min. The variation of the aqueous CH_3SH concentration at different current densities is shown in Fig. 7-3. After electricity was switched on, the dissolved CH_3SH concentration vs. NaOH concentration in all experiments declined significantly compared to that in the control experiment. Especially, the CH_3SH concentration at the current density of 4.44 mA cm^{-2} almost approached zero due to the rapid generation of ferrate(VI) at high current density. The insert showed a relationship between the aqueous CH_3SH concentration in alkaline solution at 150 min and the applied current densities from 0.56 to 4.44 mA cm^{-2}. The aqueous CH_3SH concentration at 150 min decreased quickly with increased current densities from 0.56 to 2.22 mA cm^{-2} and then gradually declined beyond 2.22 mA cm^{-2}. This indicates that the CH_3SH reduction is a rapid process and increasing the current density does not result in significantly higher CH_3SH removal rates.

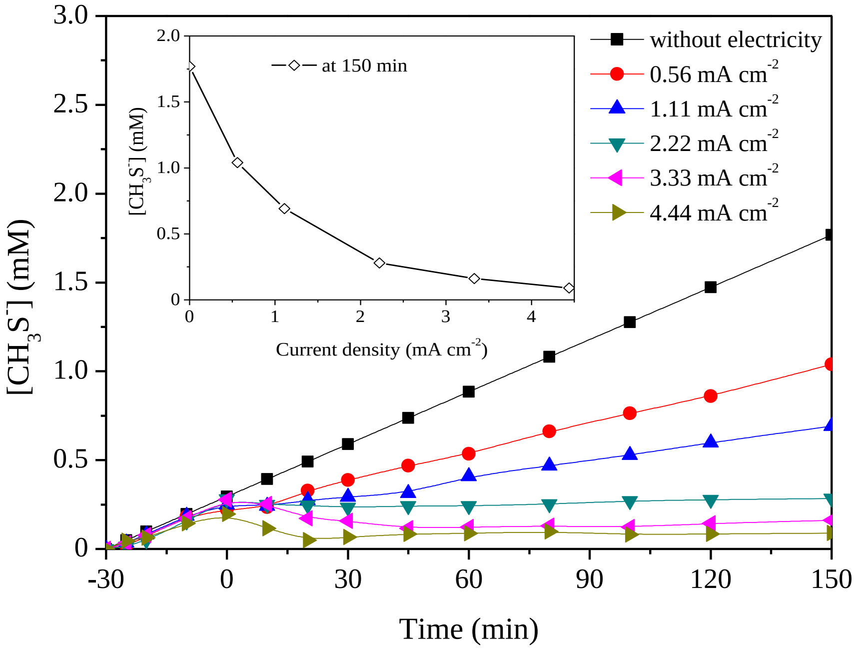

Figure 7-3 Variation of aqueous CH_3SH concentration at 150 min vs. current density;

Insert: Effect of current density on gaseous CH_3SH removal in the in-situ ferrate(VI) generation reactor (NaOH concentration=6 M; $[CH_3SH]_{inlet-gas}$=43 ppm/v; gas flow rate=600 mL min^{-1})

From an energy consumption point of view, the specific energy consumption (SEC) per mole of degraded CH_3SH by ferrate(VI) at various NaOH concentrations with a constant current intensity of 30 mA was calculated in terms of kWh/M using Eq. (5) below:

$$\mathrm{SEC} = \frac{\int I \times U dt}{M} \tag{5}$$

Fig. 7-4. shows the effect of the current density on specific energy consumption related to the CH_3SH removal performance. It is seen that an increase in the current density from 0.56 to 4.44 mA cm^{-2} led to a linear increase in the SEC from 0.047 to 0.172 kWh/M. When the current density was increased from 0.56 to 2.22 mA cm^{-2}, the CH_3SH removal efficiency dramatically increased from 41.2 % to 84.2 %, However, when the current density was further increased from 2.22 to 4.44 mA cm^{-2}, the CH_3SH removal efficiency increased slightly from 84.2% to 94.9%. Therefore, a suitable current density should be selected at 2.22 mA cm^{-2}, which can achieve not only higher CH_3SH removal, but also lower energy consumption with both of technical and economical benefits.

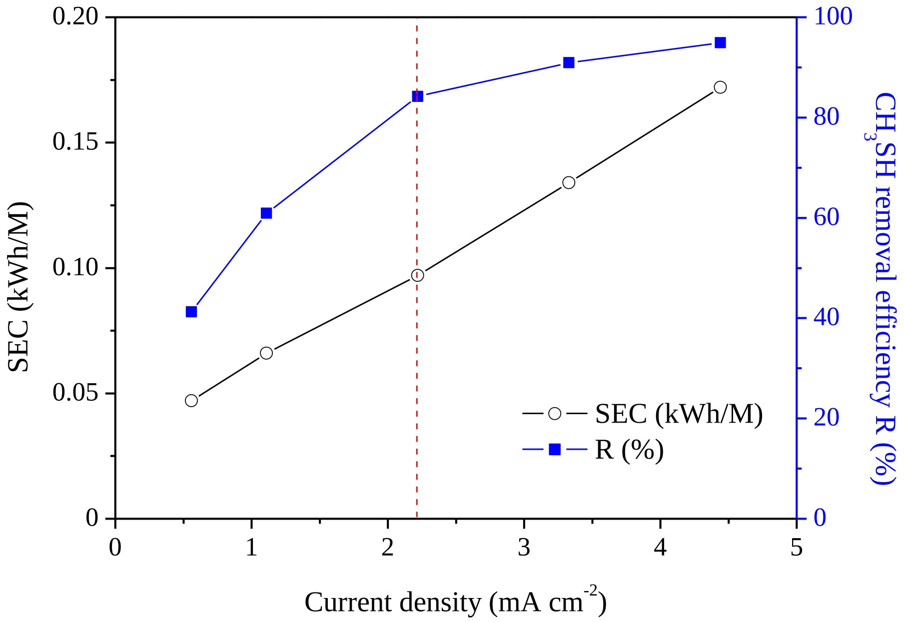

Figure 7-4 Effect of current density on specific energy consumption of gaseous CH_3SH removal and CH_3SH removal efficiency at 150 min in the in-situ Ferrate(VI) generation reactor (NaOH concentration= 6 M; $[CH_3SH]_{inlet\text{-}gas}$=43 ppm/v; gas flow rate=600 mL min^{-1})

In the course of the in-situ ferrate(VI) reaction process, ferrate(VI) concentration was also monitored and the experimental results are shown in Fig. 7-5. It is found that ferrate(VI) concentration in the present of CH_3SH at current densities of 0.56 or 1.11 mA cm^{-2} was below the detection limit of the UV-vis spectrophotometer at 510 nm. The ferrate(VI) concentration with CH_3SH present levelled off at around 0.004 and 0.07 mM with the current density of 2.22 and 3.33 mA cm^{-2}, while the ferrate(VI) concentration quickly increased after 45 min at the current density of 4.44 mA cm^{-2}. To compare the variation of ferrate(VI) concentration in the presence or absence of CH_3SH, control experiments of electrochemical ferrate(VI) generation were also conducted. From Fig. 7-6, it can be seen that the ferrate(VI) concentration in the absence of CH_3SH linearly increased with a relatively high-raising slope at the increased current density from 1.11 to 4.44 mA cm^{-2}. Fig 7-6 also showed a relationship between CH_3SH/ferrate(VI) concentration vs. current density. It was found that, once nearly all aqueous CH_3SH has been degraded at the current density of 4.44 mA cm^{-2}, ferrate(VI) concentration rapidly increased.

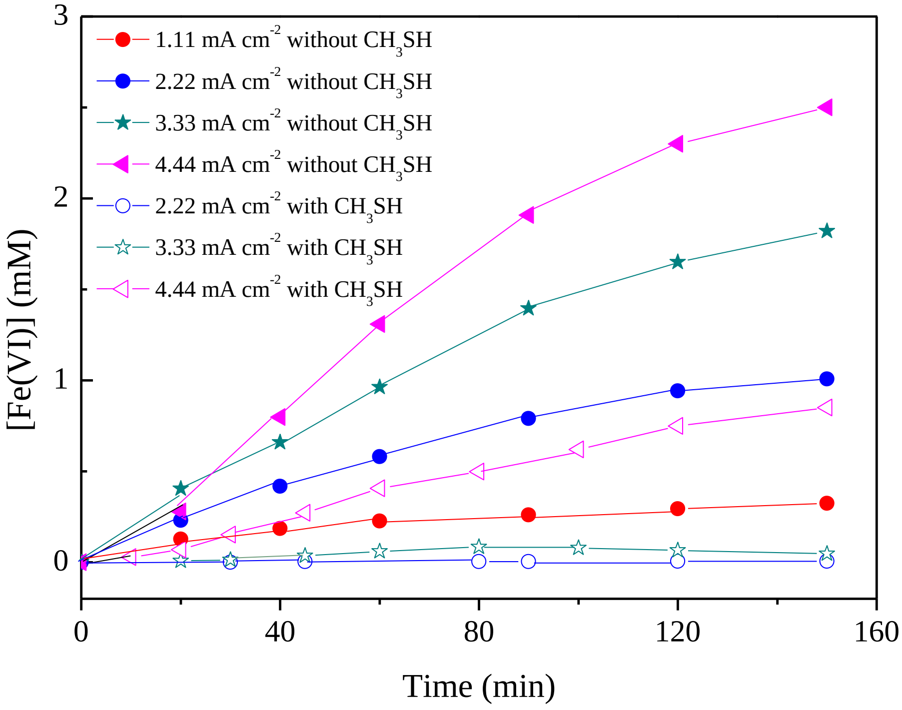

Figure 7-5 Effect of current density on ferrate(VI) concentration in the in-situ ferrate(VI) generation reactor (NaOH concentration=6 M; $[CH_3SH]_{inlet\text{-}gas}$=43 ppm/v; gas flow rate=600 mL min^{-1})

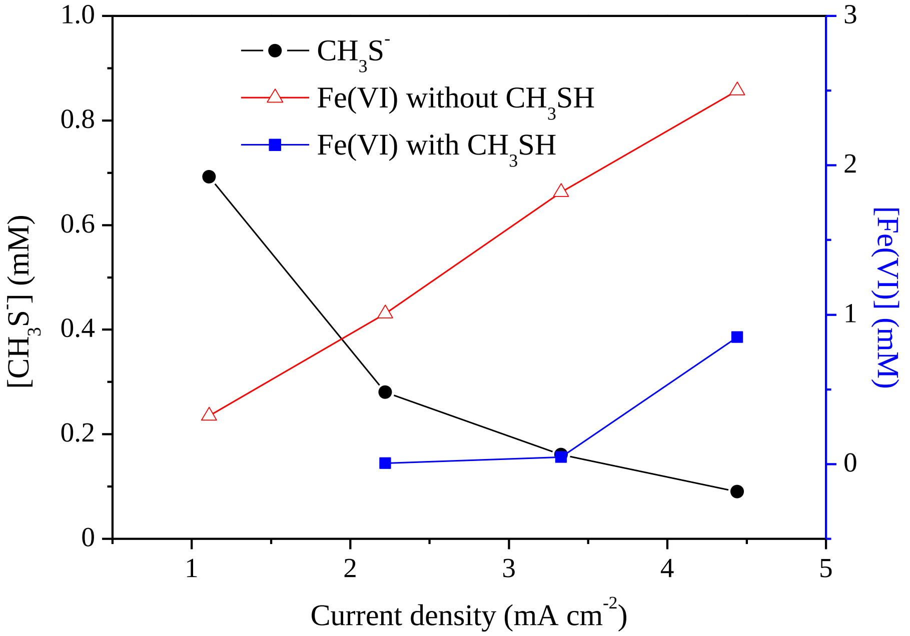

Figure 7-6 Variation of aqueous CH_3SH concentration and ferrate(VI) concentration with or without the presence of CH_3SH at 150 min vs. current density

7.2.3 Effect of CH_3SH Loading

To study the effect of CH_3SH loading on CH_3SH removal characteristics in the in-situ ferrate(VI) reaction process, experiments were conducted in a 6 M NaOH solution at 2.22 mA cm^{-2} but with different CH_3SH loadings. The first set of experiments was performed with a fixed gas flow rate of 600 mL min^{-1} but with variable CH_3SH concentrations in the inlet gas, whereas the second set of experiments was performed with a fixed CH_3SH concentration of ~44 ppm/ but with different gas flow rates. During the experiments, the CH_3SH concentrations in the gas and liquid phases were both monitored to evaluate the performance of CH_3SH removal.

The experimental results are shown in Figure 7-7a and b and Table 7-2, 7-3 and further summarized in Fig. 7-8. It can be seen that, when the CH_3SH loading was below 30 g m^{-3} h^{-1}, the rate of CH_3SH degradation in the aqueous solution was exactly as same as its rate of intake. When the CH_3SH loading was further increased, the rate of CH_3SH degradation levelled off. Furthermore, the gaseous CH_3SH concentrations at the outlet determined by the CH_3SH sensor were still zero at CH_3SH loading up to 46 g m^{-3} h^{-1}, which indicates that the rate of gaseous CH_3SH removal equals the stoichiometric rate of CH_3SH input up to 46 g m^{-3} h^{-1}.

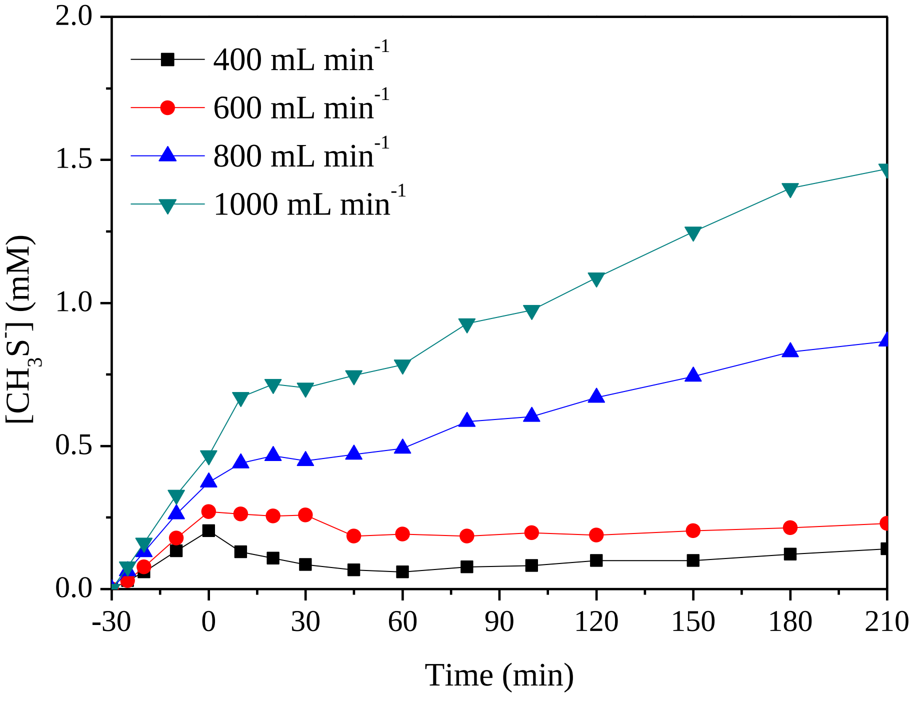

(a)

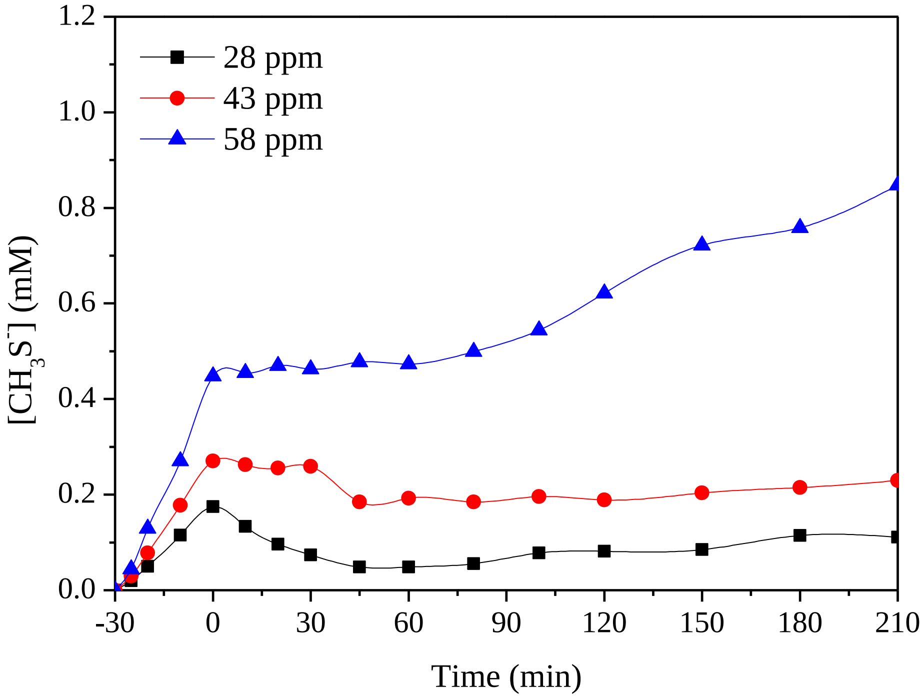

(b)

Figure 7-7 (a). Effect of CH_3SH flow rate in the in-situ ferrate generation reactor; (b) Effect of CH_3SH concentration in the in-situ ferrate generation reactor

Table 7-2 Effect of gas flow rate on gaseous CH_3SH loading after 150 min reaction in the in-situ ferrate(VI) generation reactor (Current density = 2.22 mA cm^{-2}; $[CH_3SH]_{inlet-gas}$, ~43 ppm/v; gas flow rate, 400-1000 mL min^{-1})

CH_3SH loading (g m^{-3} h^{-1})	Total aqueous CH_3SH (mM)	Residual CH_3SH (mM)	Removed CH_3SH (mM)	Rate of CH_3SH removal (g m^{-3} h^{-1})
18.43	1.15	0.1	1.05	16.83
27.64	1.73	0.21	1.52	24.36
36.86	2.30	0.74	1.56	25.02
46.07	2.88	1.30	1.59	25.36

Table 7-3 Effect of initial CH_3SH concentration on gaseous CH_3SH loading after 150 min reaction in the in-situ ferrate(VI) generation reactor (Current density = 2.22 mA cm^{-2}; $[CH_3SH]_{inlet\text{-}gas}$, ~28-58 ppm/v; gas flow rate, 600 mL min^{-1})

CH_3SH loading ($g\ m^{-3}\ h^{-1}$)	Total aqueous CH_3SH (mM)	Residual CH_3SH (mM)	Removed CH_3SH (mM)	Rate of CH_3SH removal ($g\ m^{-3}\ h^{-1}$)
18	1.152	0.0999	1.0521	16.8336
27.64	1.728	0.2053	1.5227	24.3632
37.29	2.304	0.74	1.564	25.024

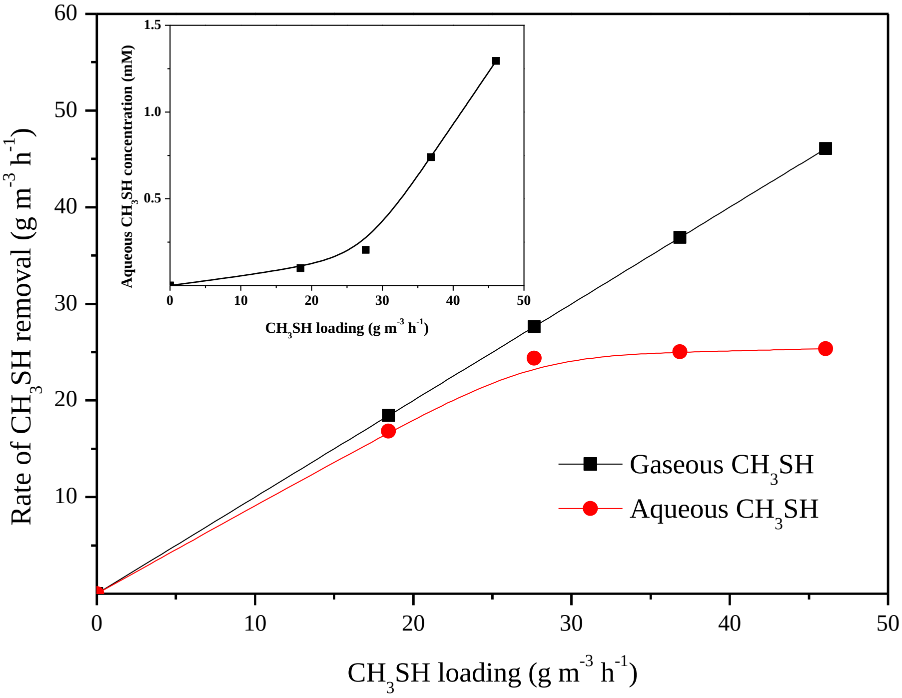

Figure 7-8 Dependence on CH_3SH loading ($[CH_3SH]_{inlet\text{-}gas}Q/V$) of the overall CH_3SH removal at 150 min (NaOH concentration=6 M; $[CH_3SH]_{inlet\text{-}gas}$=43 ppm/v; gas flow rate=0.4~1.0 mL min^{-1}) Insert: Variation of aqueous CH_3SH concentration at 150 min

vs. CH_3SH loading rate

7.2.4 Effect of CH_3SH Gas Composition

The influence of the gas components, O_2, N_2 and air, on the CH_3SH removal in the in-situ ferrate(VI) generation reactor was investigated at the current density of 2.22 mA cm^{-2}, initial CH_3SH concentration of 43 ppm/v and gas flow rate of 600 mL min^{-1}. Variation of the remaining CH_3SH concentration with gas composition as a function of time was shown in Fig. 7-9.

It was interesting to find that the aqueous CH_3S^- concentrations were almost the same when the synthetic CH_3SH gas were prepared with N_2 and O_2 gas, although the aqueous CH_3S^- concentration was slightly higher when the synthetic CH_3SH gas was prepared with air at the same experimental conditions. The CH_3SH removal in the gas phase was still complete among the three experiments, which indicated that the higher aqueous CH_3S^- concentration when mixing with air may result from the lower reaction between CH_3S^- and ferrate(VI). As the same amount of CH_3S^- dissolved in the liquid solution under the three conditions, the possible reason may be caused by less ferrate(VI) generated in NaOH electrolyte when CH_3SH gas was prepared with air. This was proved by the results of ferrate(VI) concentration simultaneously measured under the same experimental conditions in Fig. 7-10. Ferrate(VI) concentration was only 0.006 mM at 150 min when CH_3SH gas was prepared with air, while ferrate(VI) concentration was up to 0.02 mM and 0.021 mM when CH_3SH gases were separately prepared with N_2 gas and O_2 gas. It was also interesting to find that ferrate(VI) concentration at the condition of O_2 gas was slightly higher than the condition of N_2 gas. This result may be attributed to the formation of O_2^- ions from the reaction of dissolved O_2 with OH^- ions ($3O_2 + 4OH^- \rightarrow 2H_2O + 4O_2^-$) (Hives et al. 2006), which benefits for ferrate(VI) conversion from intermediate iron-oxo species (FeO_2^- and FeO_2^{2-}) (Shao et al. 2005). However, this slight improvement on ferrate(VI) generation did not influence the efficiency of CH_3S^- removal.

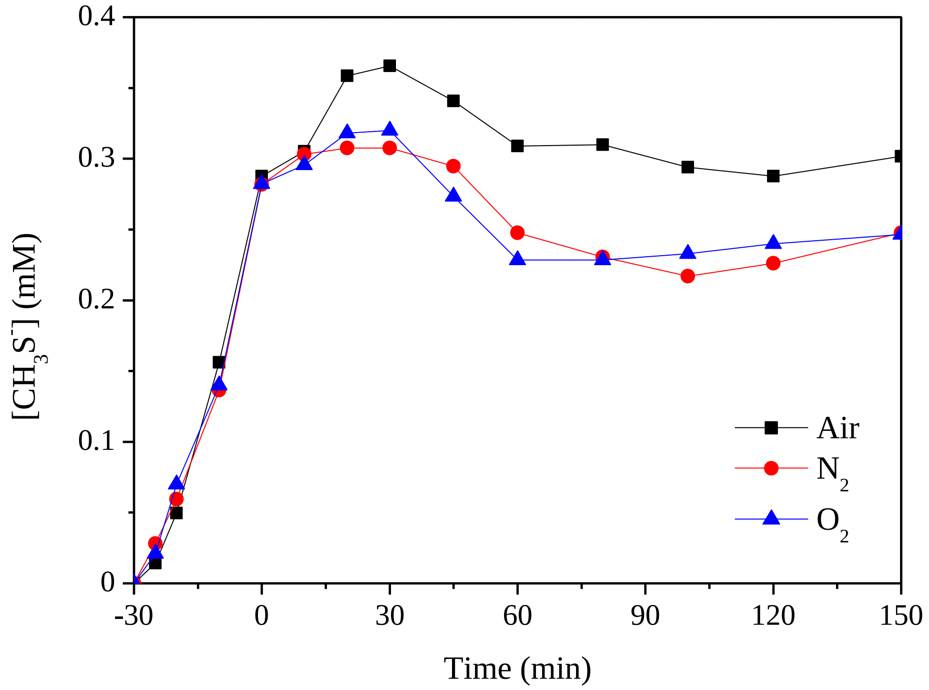

Figure 7-9 Effect of CH_3SH compositions on gaseous CH_3SH removal in the in-situ ferrate(VI) generation reactor (NaOH concentration=6 M; $[CH_3SH]_{inlet\text{-}gas}$=43 ppm/v; gas flow rate=600 mL min^{-1})

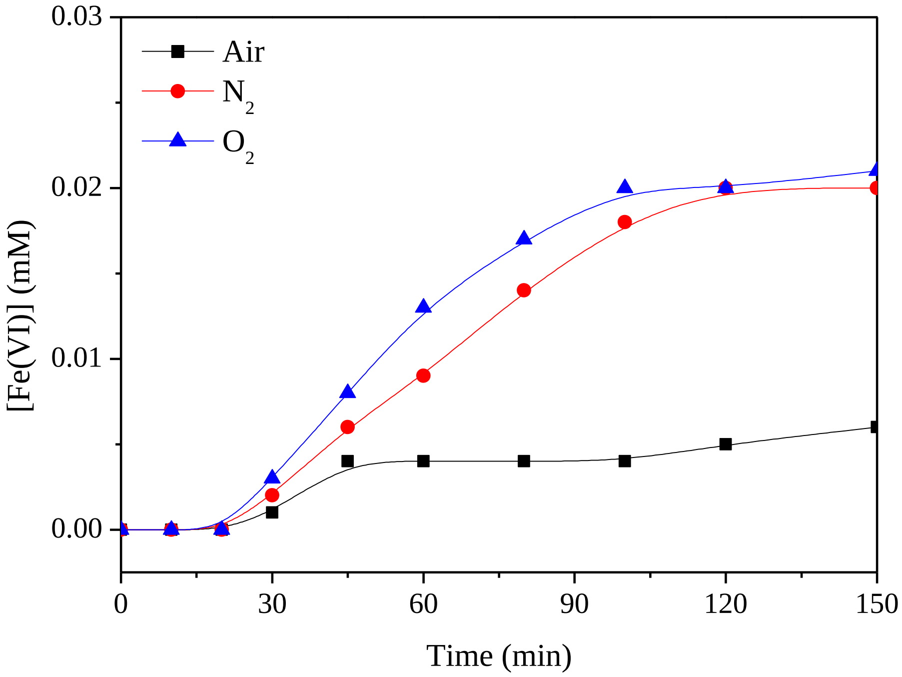

Figure 7-10 Effect of CH_3SH compositions on ferrate(VI) concentration in the in-situ ferrate(VI) generation reactor (NaOH concentration=6 M; $[CH_3SH]_{inlet-gas}$ =43 ppm/v; gas flow rate = 600 mL min^{-1})

Since CO_2 from air was simultaneously introduced into the NaOH solution. And the contact time of the gas and the liquid phase in our reactor as shown in Fig. 3-3a was 12 s, which is sufficient to complete the CO_2 absorption and its reaction with NaOH (Couvert et al. 2008). Thus, sodium carbonate was accumulated in the reacting solution. It was reported that the presence of sodium carbonate might decrease the rate of ferrate(VI) generation by inhibition of the active dissolution sites at the electrode surface (De Koninck et al. 2003). Moreover, the presence of CO_2 actually led to consume extra NaOH electrolyte. From the point of practical application of this new process, the presence of CO_2 in foul gas will not only decrease the process efficiency but also increase the operating cost. However, if we reduce the contact time between foul gas and NaOH solution down to a very low level, the effect of CO_2 on NaOH consumption can be greatly eliminated to its minimum. Therefore, the experimental setup of the in-situ ferrate(VI) generation reactor as shown in Fig. 3-5 for gaseous CH_3SH removal was developed by equipping an absorption scrubber with a very small volume of scrubbing solution before the oxidizing reactor. Thus the contact time between the gas and the liquid phase was reduced from 12 to 0.06 s only, which was the lowest contact time of the system.

In this experimental set-up, the aqueous NaOH solution was continuously circulated between the absorption scrubber and the oxidation reactor. No residual odour was released from outlet gas even with such a small volume of scrubbing solution at a high gas velocity of 5 L min^{-1}. From Fig. 7-11, it can be found that the developed experimental set-up resolved the CO_2 absorption problem successfully. The added absorption scrubber benefited for a very short gas-liquid phase residence time, which can effectively limit an effective CO_2 mass transfer from gas to liquid to avoid the CO_2 absorption and extra consumption the NaOH solution.

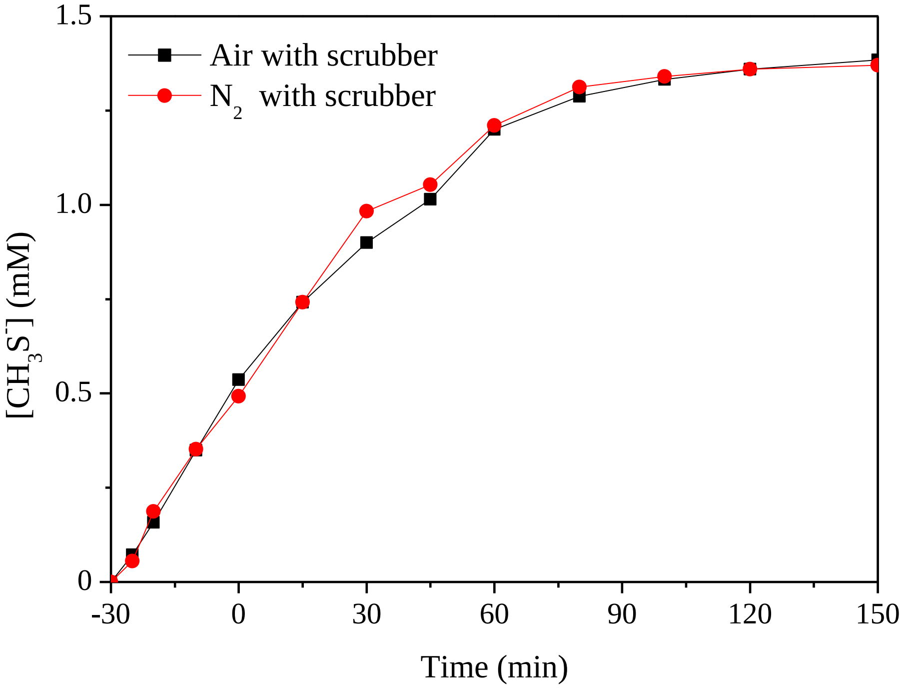

Figure 7-11 Effect of CH_3SH compositions on gaseous CH_3SH removal in the in-situ ferrate(VI) generation reactor (NaOH concentration=6 M; $[CH_3SH]_{inlet\text{-}gas}$=13 ppm/v; gas flow rate=5000 mL min^{-1})

7.3 Gaseous CH_3SH Removal in the Second Reactor

7.3.1 Effect of NaOH Concentration

In the second reactor, the first set of experiments was also performed to search out the optimum NaOH concentration for CH_3SH removal. Since we knew that an optimum NaOH concentration was obtained at around 6 M in the first reactor, the range of trail NaOH concentrations was narrowed to the range 4 M to 7 M. The synthetic CH_3SH gas with an inlet concentration of 13 ppm/v was continuously fed into the absorption column at 5000 mL min^{-1} and the scrubbing solution was simultaneously circulating between the absorption scrubber and the oxidation reactor. Thus, the absorbed CH_3SH in the aqueous NaOH solution was immediately oxidized by the freshly and continuously produced ferrate(VI) from the iron anode at a current density of 3.33 mA cm^{-2}. The CH_3SH concentrations both in gas and liquid phases were monitored. The experiments were conducted for 180 min and the results are presented in Fig. 7-12. In all experiments, the removal of CH_3SH from the gas phase was also almost total.

After electrical current was switched on, the dissolved CH_3SH concentration first dropped significantly due to the CH_3SH degradation by the freshly generated ferrate(VI), before it gradually recovered to eventually approach the balanced level, where the degradation rate equals the absorption rate. It can also be observed that the CH_3SH concentration in the 6 M NaOH solution eventually stabilized at the lowest level, which means that the optimum NaOH concentration was found at 6 M.

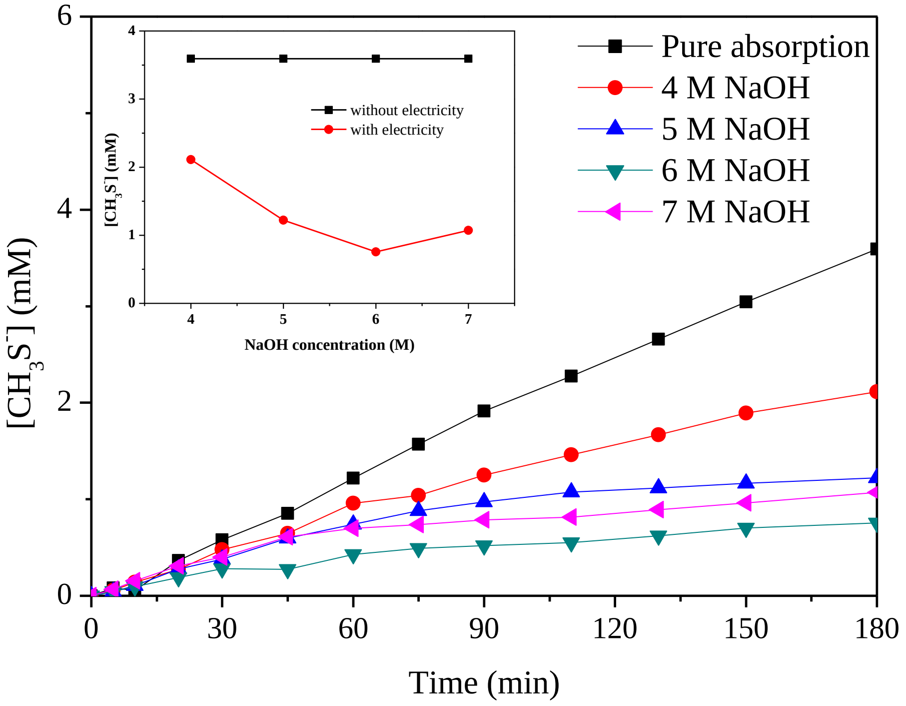

Figure 7-12 Effect of NaOH concentration on gaseous CH_3SH removal in the in-situ ferrate(VI) generation reactor (Current density = 3.33 mA cm^{-2})

7.2.2 Effect of Current Density

The experiments on the effect of current density were conducted in 6 M NaOH solution with an initial CH_3SH concentration of 13 ppm/v and gas flow rate of 5 L min^{-1} for 180 min. The variation in the aqueous CH_3SH concentration at different current densities is shown in Fig. 7-13.

During the first 20 min, the dissolved CH_3SH concentration vs. current density seems to be the same as that of the control experiment in all cases. After 20 min reaction, the dissolved CH_3SH concentration declined significantly, especially, at the current density of 5.55 mA cm^{-2}, where it most reached zero due to the rapid generation of ferrate(VI) at high current density. The insert shows the relationship between the aqueous CH_3SH concentration in alkaline solution at 180 min and the applied current density from 1.11 to 5.55 mA cm^{-2}. The aqueous CH_3SH concentration at 180 min decreased rapidly as current density increased from 1.11 to 4.44 mA cm^{-2} and then gradually declined beyond 5.55 mA cm^{-2}. This indicates that the CH_3SH reduction was a rapid process and increasing the current density did not result in significantly higher CH_3SH removal rates.

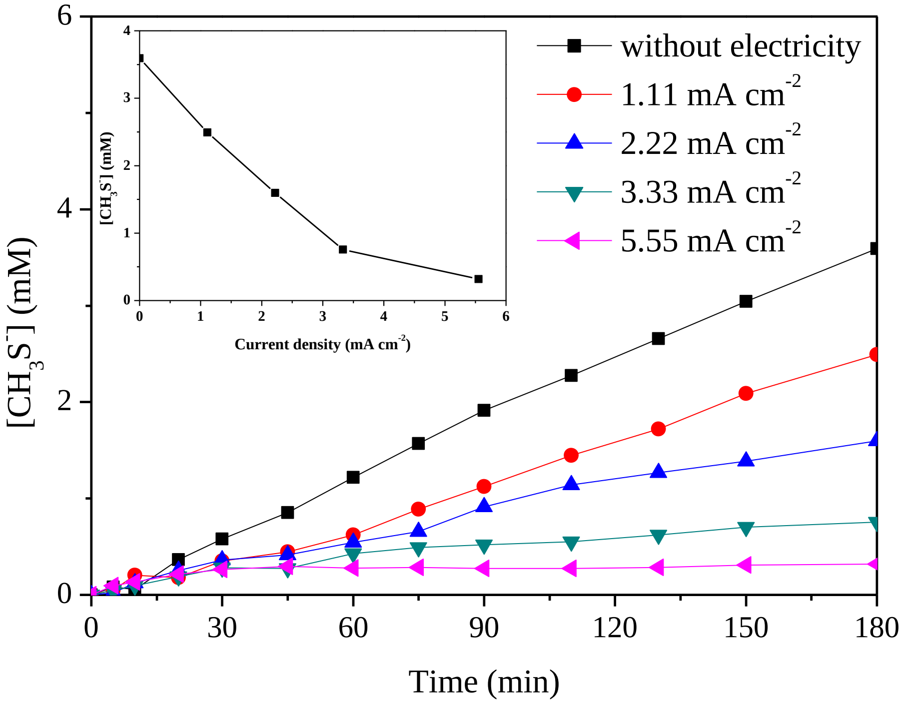

Figure 7-13 Effect of current density on gaseous CH_3SH removal in the in-situ ferrate(VI) generation reactor ([NaOH] = 6 M)

Fig. 7-14 shows the effect of current density on specific energy consumption on the performance of CH_3SH removal. It is seen that the SEC increases gradually from 1.11 to 3.33 mA cm^{-2}, and at a faster rate when the current density is above 3.33 mA cm^{-2}. When current density increases from 1.11 to 3.33 mA cm^{-2}, the CH_3SH removal efficiency dramatically increased from 30.6 % to 79%. However, when the current density further increases from 3.33 to 5.55 mA cm^{-2}, the CH_3SH removal efficiency increases slightly from 79% to 91.1%. Therefore, a suitable current density to be selected is 3.33 mA cm^{-2}, which not only achieves a higher CH_3SH removal, but also lower energy consumption with both of technical and economic benefits.

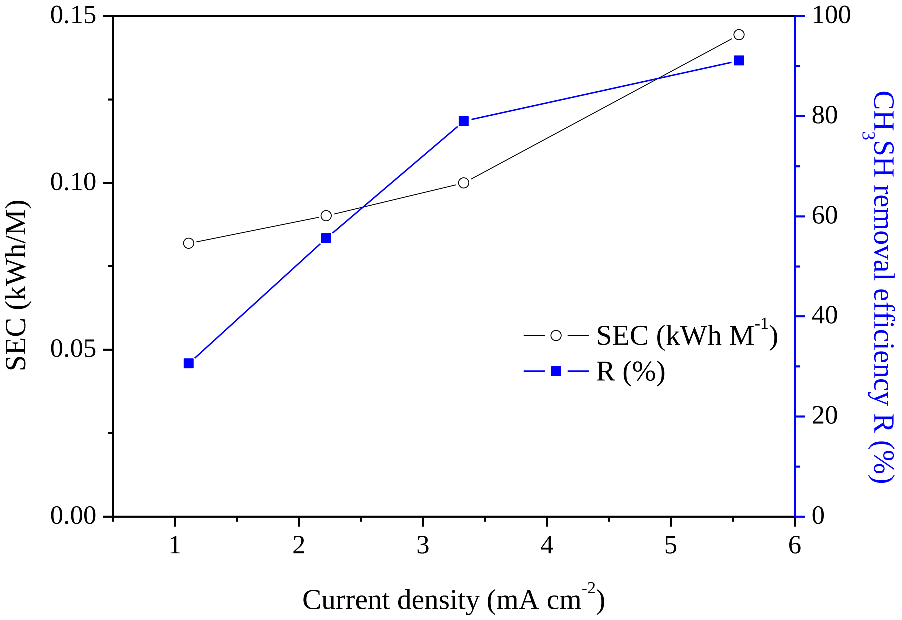

Figure 7-14 Effect of current density on specific energy consumption of gaseous CH_3SH removal and CH_3SH removal efficiency at 180 min in the in-situ Ferrate(VI) generation reactor ([NaOH]= 6 M; $[CH_3SH]_{inlet\text{-}gas}$=13 ppm/v; gas flow rate=5 L min^{-1})

7.2.3 Effect of CH_3SH Loading

To study the effect of CH_3SH loading on CH_3SH removal in the in-situ ferrate(VI) reaction process, experiments were conducted in 6 M NaOH solution at 3.33 mA cm^{-2} with a fixed gas flow rate of 5 L min^{-1} but variable CH_3SH concentrations in the inlet gas. During the experiments, the CH_3SH concentrations in the gas and liquid phases were both monitored to evaluate the performance of CH_3SH removal. The experiments lasted 180 min and the results are shown in Fig. 7-15 and are further summarized in Fig. 7-16 and Table 7-4.

It can be seen that, when CH_3SH loading was below 56 g m^{-3} h^{-1}, the rate of CH_3SH degradation in aqueous solution was balanced with the rate of its intake. When the CH_3SH loading was further increased, the rate of CH_3SH degradation leveled off. Furthermore, the gaseous CH_3SH concentrations in outlet determined by CH_3SH sensor were still zero at the CH_3SH loading up to 116 g m^{-3} h^{-1}, which indicates that the rate of gaseous CH_3SH removal equals to the stoichiometric rate of CH_3SH input up to 116 g m^{-3} h^{-1}.

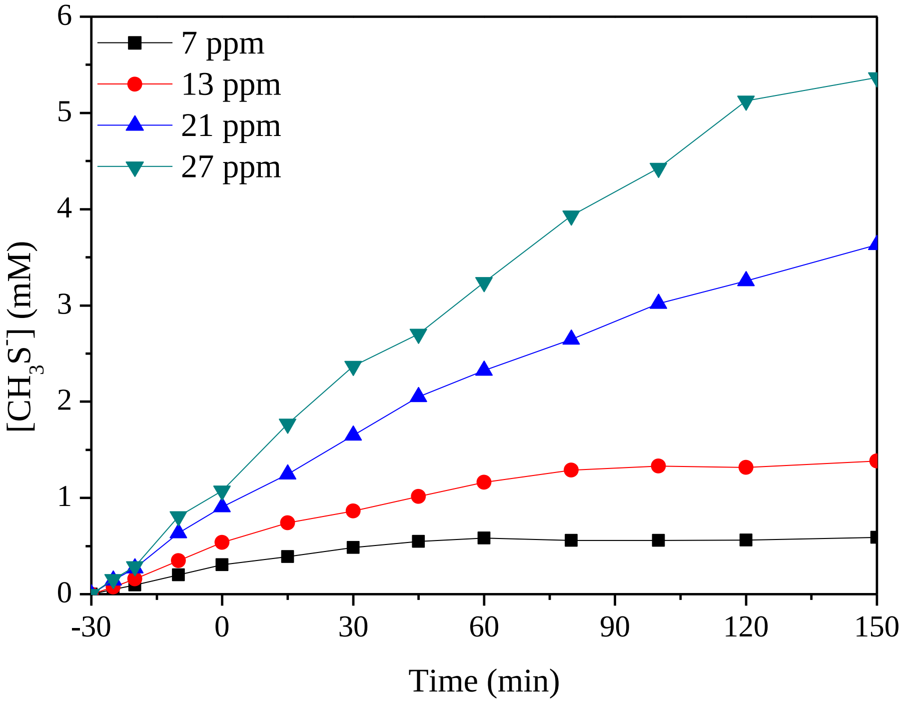

Figure 7-15 Effect of CH_3SH concentration in the in-situ ferrate generation reactor

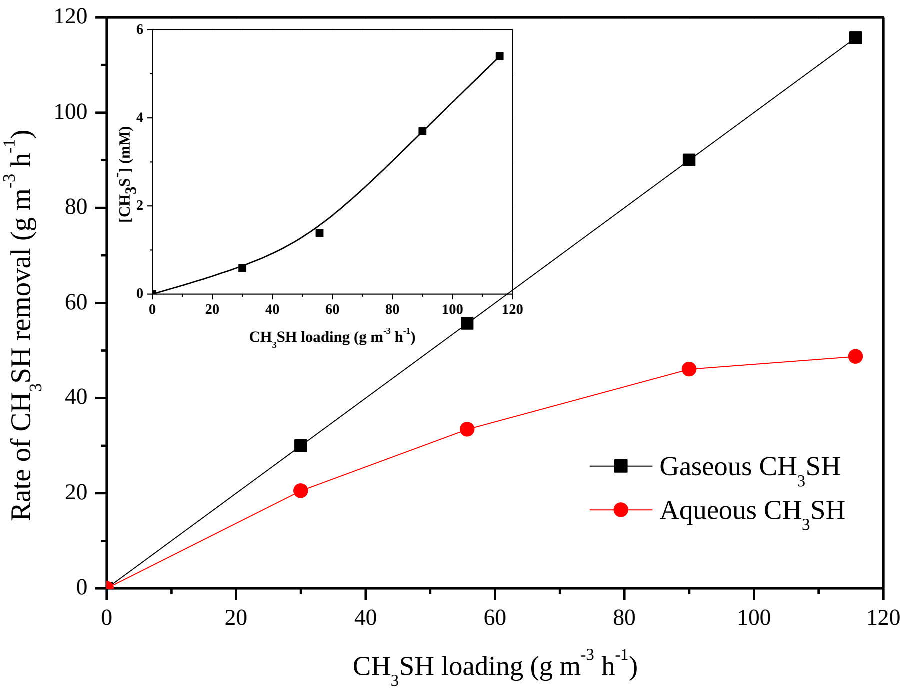

Figure 7-16 Dependence on CH_3SH loading ($[CH_3SH]_{inlet\text{-}gas}Q/V$) of the overall CH_3SH removal at 150 min (NaOH concentration=6 M; $[CH_3SH]_{inlet\text{-}gas}$=7~27 ppm/v; gas flow rate=5 L min^{-1}) Insert: Variation of aqueous CH_3SH concentration at 180

min vs. CH_3SH loading rate.

Table 7-4 Effect of initial CH_3SH concentration on gaseous CH_3SH loading after 180 min reaction in the in-situ ferrate(VI) generation reactor (Current density = 3.33 mA cm^{-2}; $[CH_3SH]_{inlet\text{-}gas}$, ~7-27 ppm/v; gas flow rate, 5 L min^{-1})

CH_3SH loading ($g\ m^{-3}\ h^{-1}$)	Total aqueous CH_3SH (mM)	Residual CH_3SH (mM)	Removed CH_3SH (mM)	Rate of CH_3SH removal ($g\ m^{-3}\ h^{-1}$)
30	1.87	0.47	1.40	22.45
56	3.47	1.38	2.09	33.44
90	6.57	3.69	2.88	46.06
116	8.44	5.40	3.05	48.75

7.4 Environmental Significance for Odour Control

In relation to the performance of gaseous CH_3SH removal by an absorption/oxidation scrubber in continuous gas flow mode, the overall reactions should be counted for its mass balance. Therefore an overall reaction equation by combination of Eq. (1) in Chapter 4 and Eq. (10) in Chapter 5 is established as Eq. (6).

$$14Fe + 12OH^{-} + 3CH_3SH + 51H_2O \rightarrow 14Fe(OH)_3 + 3SO_4^{2-} + 3CO_3^{2-} + 42H_2 \quad (6)$$

In operation, it is necessary to maintain NaOH concentration by continuously adding

NaOH chemical into the reacting solution. It can be calculated that degradation of 1 mol of CH_3SH needs to consume 4 mol of NaOH and produce 1 mol of Na_2SO_4 plus 1 mol of Na_2CO_3. This stoichiometic ratio obtained in Chapter 5.2 can be applied to calculate the NaOH makeup dosage in such a process. Furthermore, a build-up of Na_2SO_4 and Na_2CO_3 concentrations in the solution will eventually affect the performance of the process. Luckily, the solubilities of Na_2SO_4 and Na_2CO_3 are much lower than that of NaOH in aqueous solution and two precipitates of Na_2SO_4 and Na_2CO_3 would form after saturation.

7.5 Summary

In this chapter, a wet scrubbing process with in-situ electro-generation of ferrate(VI) has been developed for removing odour from foul gas in sewage treatment works. In this process, methyl mercaptan (CH_3SH) in synthetic gas is removed through absorption and oxidation by contacting the gaseous stream with aqueous NaOH electrolyte that provides in-situ generation of ferrate(VI). The process parameters including electrolyte concentration, applied current density, initial CH_3SH concentration, gas flow rate and gaseous CH_3SH compositions were investigated to discover the best operating conditions and design parameters suitable for a scale-up design. Under the experimental conditions, 100% removal efficiency of gaseous CH_3SH was achieved by the wet scrubbing process at room temperature and atmospheric pressure. In the first reactor, the process proved to be quite effective for aqueous CH_3SH removal under the research revealed optimum NaOH concentration of 6 M in electrolyte, current density of 2.22 mA cm^{-2} and CH_3SH loading below 30 g m^{-3} h^{-1}. A very short contact time of 0.06 s between the gas and the liquid phases was achieved in the second reactor, where the optimum experimentally discovered conditions consists of NaOH electrolyte of 6 M, current density of 3.33 mA cm^{-2} and CH_3SH loading below 56 g m^{-3} h^{-1}.

CHAPTER 8 Conclusions and Recommendation

8.1 Conclusions

This thesis focuses on the study of odour control with in-situ electrochemically generation of ferrate(VI) in a wet scrubbing process. Firstly, the electrochemical generation of ferrate(VI) was explored to obtain the optimal production of ferrate(VI) . Secondly, the reactivity of ferrate(VI) with CH_3S^- in aqueous highly alkaline solution was investigated. To better study the reaction between ferrate(VI) and CH_3SH, kinetic models were established. Finally, gaseous CH_3SH removal by an absorption/oxidation scrubber in a continuous flow mode was carried out on the basis of the laboratory scale. The efficiency of these processes has been validated by examining the degradation of selected synthetic CH_3SH gas. Achievements of the above phases are as follows:

In the first stage, the electrochemical generation of ferrate(VI) in aqueous NaOH solution was conducted in a two-unit electrolysis cell with a commercial iron steel sheet as the anode and a stainless steel rod as the cathode. The experiments demonstrated that a maximum current efficiency of 90% to generate ferrate(VI) occurred at 14 M NaOH concentration with an current density of 14.06 mA cm^{-2} applied. The presence of SO_4^{2-} in the electrolyte solution shows a significant inhibiting effect on the ferrate(VI) formation rate but a weak effect on that of SO_4^{2-} concentrations. In addition, the experimental result showed that dissolved oxygen slightly enhanced electrochemical ferrate(VI) generation. The self-decomposition of ferrate(VI) in strong alkaline solutions was also studied, and the results showed that the behaviour of ferrate(VI) was more stable in the stronger alkaline solution.

In the second phase of this study, the reactivity of ferrate(VI) with CH_3S^- in aqueous highly alkaline solution was investigated. The experimental results indicated that the second-order reaction model is suitable to describe the kinetics of CH_3S^- reaction with ferrate(VI) in strong alkaline solution. The experimental results demonstrated that the ratio of $[Fe(VI)]/[CH_3S^-] = 2.20$ is a minimum addition dosage to enable ferrate(VI) to destroy CH_3S^-. The dosage ratio of 4.53 is sufficient to completely convert CH_3S^- to sulphate ions. Considering the CH_3S^- degradation efficiency and energy consumption, an optimum NaOH concentration at which a breakeven balance between the oxidation potential of ferrate (VI) and ferrate(VI) generation rate reaches the maximum reaction rate with CH_3S^- was achieved. This part of the study provided essential understanding of the reactivity of ferrate(VI) with CH_3S^- and as useful knowledge for the development of a new process with in-situ electrochemical production of ferrate(VI) for removal of gaseous sulphur-containing odours. This finding could enhance the efficiency of odour control.

In the third phase of this study, two new kinetic models for the in-situ electrochemical generation of ferrate(VI) and its reaction with dissolved CH_3SH in aqueous strong alkaline solution were established mathematically by considering the ferrate(VI) generation rate, ferrate(VI) self-decomposition rate and the reaction rate between ferrate(VI) and CH_3SH. The kinetic models were a good fit for the experimental data enabling the determination of the effects of three key factors: (i) NaOH concentration, (ii) applied current density, and (iii) initial CH_3SH concentration on the CH_3SH reaction with ferrate(VI). The experimental results confirmed that higher application of NaOH concentration and current density would be beneficial to the electrochemical generation of ferrate(VI) and also the elimination of its self-decomposition. The experiments, however, also revealed that the optimum NaOH concentration at 10 M achieved the best CH_3S^- degradation performance of in such an IFO system.

Lastly, an absorption/oxidation scrubbing reactor, where gaseous CH_3SH was first absorbed in the electrolyte and then oxidized by in-situ generated ferrate(VI). Experimental results showed that gaseous CH_3SH could be completely removed by the wet scrubbing process at room temperature and atmospheric pressure. In the first reactor, the optimum experimental conditions for the CH_3SH removal were concluded at NaOH electrolyte of 6 M, current density of 2.22 mA cm^{-2} and CH_3SH loading below 30 g m^{-3} h^{-1}. In the second reactor, the contact time between the gas and the liquid phase can be achieved at 0.06 s. Meanwhile, the optimum experimental conditions were also concluded at NaOH electrolyte of 6 M, current density of 3.33 mA cm^{-2} and CH_3SH loading below 56 g m^{-3} h^{-1}.

8.2 Limitation and Recommendations

The findings of this study of CH_3SH removal for odour control with in-situ electrogenerated ferrate(VI) can only be regarded as a preliminary achievement. Limitations and recommendations arising from the work are given below:

1. The commercial iron steel as the anode material is important for ferrate(VI) generation. More research is needed to analyse the composition of the anode and to clarify the detailed mechanism of the enhancement on ferrate(VI) generation than other anode materials.

2. In this study, the new kinetic models were successfully validated by the experiments of CH_3SH degradation. Further studies to apply this kinetic models in degradation of other pollutants are necessary.

3. A large pilot study should be carried out. The influence of environmental parameters, such as temperature, pressure on the performance of in-situ ferrate(VI) oxidation need to be identified.

4. The results of the present study have proved that CH_3SH can be effectively degraded by in-situ ferrate(VI) in the absorption/oxidation scrubbing reactor. However, the real odour has other compositions. Therefore, this study should be extended by applying this reactor to real odour gas treatment.

5. By applying the electrical current to water the hydroxyl radical is formed, which is a strong radical to reduce CH_3SH. It was reported that the deprotonation of OH radical resulted in O_{aq}^- in alkaline solution (Lian et al. 2004). The newly formed radicals may not only influence ferrate(VI) generation, but also CH_3SH degradation. Therefore, more work should be conducted on the mechanism of ferrate(VI) generation and CH_3SH degradation.

References

Agency, U.E.P. (1985) Process design manual for sulfide control in sanitary sewage systems, USEPA Technology Transfer, Washington, DC.

Agency, U.E.P. (1991) Hydrogen sulphide corrosion in wastewater collection and treatment system.

Agency, U.E.P. (1992) Detection, control, and correction of hydrogen sulfide corrosion in existing wastewater system, Office of Wastewater Enforcement and Compliance, Washington, DC.

Alberici, R.M. and Jardim, W.F. (1997) Photocatalytic destruction of VOCs in the gas-phase using titanium dioxide. Applied Catalysis B: Environmental 14(1–2), 55-68.

Allam, N.K. and Grimes, C.A. (2008) Effect of cathode material on the morphology and photoelectrochemical properties of vertically oriented TiO_2 nanotube arrays. Solar Energy Materials and Solar Cells 92(11), 1468-1475.

Allen, L.A. (1949) The effect of nitro-compounds and some other substances on production of hydrogen-sulphide by sulphatereducing bacteria in sewage, pp. 26-38.

Alsheyab, M., Jiang, J.Q. and Stanford, C. (2009) On-line production of ferrate with an electrochemical method and its potential application for wastewater treatment - A review. J. Environ. Manage. 90(3), 1350-1356.

Alsheyab, M., Jiang, J.Q. and Stanford, C. (2010) Engineering aspects of electrochemical generation of ferrate: A step towards its full scale application for water and wastewater treatment. Water Air and Soil Pollution 210(1-4), 203-210.

Anderson, R. (1984) Sewage treatment processes: the solution to the odour problem. In: Characterization and control of odoriferous pollutants in process industrie (Vigneron, S., Hermia, J., and Chaouki, J., Eds.) Amsterdam Elsevier Science B.V., 471.

Anquandah, G.A.K., Sharma, V.K., Knight, D.A., Batchu, S.R. and Gardinali, P.R. (2011) Oxidation of Trimethoprim by ferrate(VI): kinetics, products, and antibacterial activity. Environmental Science and Technology.

APHA (1985) Standard methods for the examination of water and wastewater, American Public Health Association/American Water Works Association/Water Environment Federation, Washington DC, USA.

Audette, R.J., Quail, J.W. and Smith, P.J. (1972) Oxidation of substituted benzyl alcohols with ferrate(VI) ion. Journal of the Chemical Society, Chemical Communications (2), 38-39.

Ayers, K.E. and White, N.C. (2005) Characterization of iron(VI) compounds and their discharge products in strongly alkaline electrolyte. Journal of the Electrochemical Society 152(2), A467-A473.

Bagreev, A., Menendez, J.A., Dukhno, I., Tarasenko, Y. and Bandosz, T.J. (2005) Oxidative adsorption of methyl mercaptan on nitrogen-enriched bituminous coal-based activated carbon. Carbon 43, 195-213.

Bansal, R.C., Donnet, J.B. and Stoeckli, F. (1988) Active Carbon, Marcel Dekker, New York.

Bartzatt, R. and Nagel, D. (1991) Removal of Nitrosamines from Waste Water by Potassium Ferrate Oxidation. Archives of Environmental Health: An International Journal 46(5), 313-315.

Bartzatt, R., Cano, M., Johnson, L. and Nagel, D. (1992) Removal of toxic metals and nonmetals from contaminated water. Journal of Toxicology and Environmental Health 35(4), 205-210.

Bashkova, S., Bagreev, A. and Bandosz, T.J. (2002) Adsorption of methyl mercaptan on activated carbons. Environ. Sci. Technol. 36(12), 2777-2782.

Beardslay, C.W., Krotinger, N.J. and Rigdon, J.H. (1958) Removal of sewer odours by scrubbing with alkaline solutions. Sewage and Industrial Wastes 30(2), 220-225.

Beck, F., Kaus, R. and Oberst, M. (1985) Transpassive dissolution of iron to ferrate(VI) in concentrated alkali hydroxide solutions. Electrochimica Acta 30(2), 173-183.

Beynon, R.J. and Easterby, J.S. (1996) Buffer solutions. IRL press at oxford university.

Bielski, B.H.J., Sharma, V.K. and Czapski, G. (1994) Reactivity of ferrate(V) with carboxylic acids: A pre-mix pulse radiolysis study. Radiation Physics and Chemistry 44(5), 479-484.

Bonnin, C., Coriton, G. and Martin, G. (1994) Biodeodorization processes: from organic media filters to mineral beds. VDI Berichte 1104, 217-230.

Boon, A.G. and Lister, A.R. (1975) Formation of sulfide in rising main sewer and its prevention by injection of oxygen. Progress in Water Technology 7, 289-300.

Bouzek, K. and Roušar, I. (1993) Current efficiency during anodic dissolution of iron to ferrate(vi) in concentrated alkali hydroxide solutions. Journal of Applied Electrochemistry 23(12), 1317-1322.

Bouzek, K. and Roušar, I. (1996) Influence of anode material on current yields during ferrate(VI) production by anodic iron dissolution Part I: Current efficiency during anodic dissolution of grey cast iron to ferrate(vi) in concentrated alkali hydroxide solutions. J. Appl. Electrochem. 26(9), 919-923.

Bouzek, K. and Roušar, I. (1997) Influence of anode material on current yield during ferrate(VI) production by anodic iron dissolution Part III: Current efficiency during anodic dissolution of pure iron to ferrate(VI) in concentrated alkali hydroxide solutions. J. Appl. Electrochem. 27(6), 679-684.

Bouzek, K., Roušar, I. and Taylor, M.A. (1996a) Influence of anode material on current yield during ferrate(VI) production by anodic iron dissolution Part II: Current efficiency during anodic dissolution of white cast iron to ferrate(vi) in concentrated alkali hydroxide solutions. J. Appl. Electrochem. 26(9), 925-931.

Bouzek, K., Schmidt, M.J. and Wragg, A.A. (1999a) Influence of electrolyte composition on current yield during ferrate(VI) production by anodic iron dissolution. Electrochemistry Communications 1(9), 370-374.

Bouzek, K., Schmidt, M.J. and Wragg, A.A. (1999b) Influence of anode material composition on the stability of electrochemically-prepared ferrate(VI) solutions. Journal of Chemical Technology & Biotechnology 74(12), 1188-1194.

Bouzek, K., Palmer, J., Rousar, I. and Wragg, A.A. (1996b) Mass transfer to wall electrodes in a fluidised bed of inert particles. Electrochimica Acta 41(4), 583-589.

Bouzek, K., Lipovska, M., Schmidt, M., Rousar, I. and Wragg, A.A. (1998) Electrochemical production of ferrate(VI) using sinusoidal alternating current superimposed on direct current: grey and white cast iron electrodes. Electrochim. Acta 44(4), 547-557.

Bryers, J.D. and Characklis, W.G. (1990) Biofilms in water and waste water treatment. . CHARACKLIS, W.G.a.M., K.C. eds. (ed), Wiley, NY.

Canela, M.C., Alberici, R.M., Sofia, R.C.R., Eberlin, M.N. and Jardim, W.F. (1999) Destruction of malodorous compounds using heterogeneous photocatalysis. Environmental Science and Technology 33(16), 2788-2792.

Capelli, L., Sironi, S., Del Rosso, R. and Céntola, P. (2009) Predicting odour emissions from wastewater treatment plants by means of odour emission factors. Water Res. 43(7), 1977-1985.

Carpenter, W.T. (1932) Sodium nitrate used to control nuisance. Water Works Sewerage 79, 175-176.

Carr James, D. (2008) Ferrates, pp. 189-196, American Chemical Society.

Castle, J.E. (1954) Process for coating metals and product thereof.

Charron, I., Féliers, C., Couvert, A., Laplanche, A., Patria, L. and Requieme, B. (2004) Use of hydrogen peroxide in scrubbing towers for odor removal in wastewater treatment plants. Water Sci. Technol. 50(4), 267-274.

Charron, I., Couvert, A., Laplanche, A., Renner, C., Patria, L. and Requieme, B. (2006) Treatment of odorous sulphur compounds by chemical scrubbing with hydrogen peroxide - stabilisation of the scrubbing solution. Environ. Sci. Technol. 40(24), 7881-7885.

Chen, G.H. and Leung, D.H.-W. (2000) Utilization of oxygen in a sanitary gravity sewer. Water Research 34(15), 3813-3821.

Cho, K.S., Hirai, M. and Shoda, M. (1992) Degradation of hydrogen sulfide by Xanthomonas sp. strain DY44 isolated from peat. Applied and Environmental Microbiology 58(4), 1183-1189.

Chu, H., Chiou, Y.Y., Horng, K.H. and Tseng, T.K. (2001) Catalytic incineration of C_2H_5SH and its mixture with CH_3SH over a Pt/Al_2O_3 catalyst. J. Environ. Eng. 127(5), 438-442.

Chu, W. and Ma, C.-W. (2000) Quantitative prediction of direct and indirect dye ozonation kinetics. Water Research 34(12), 3153-3160.

Colodette, J.L., Rothenberg, S. and Dence, C.W. (1988) Factors affecting hydrogen peroxide stability in the brightening of mechanical and chemimechanical pulps. Part 1. Hydrogen peroxide stability in the absence of stabilizing systems. Journal of Pulp and Paper Science 14(6), 126-132.

Couvert, A., Sanchez, C., Laplanche, A. and Renner, C. (2008) Scrubbing intensification for sulphur and ammonia compounds removal. Chemosphere 70(8), 1510-1517.

Dalai, A.K., Tollefson, E.L., Yang, A. and Sasaoka, E. (1997) Oxidation of methyl mercaptan over an activated carbon in a fixed-bed reactor. Industrial and Engineering Chemistry Research 36(11), 4726-4733.

De Guardia, A., Bouzaza, A., Martin, G., Laplanche, A., Barbaza, P., Lescuyer, J.L., Camps, R. and Boch, J.P. (1995) Treatment of gas containing VOC. Absorption of the pollutants in a silicon oil followed by the chemical regeneration of the oil. Odours VOC's J 1, 84.

De Koninck, M. and Belanger, D. (2003) The electrochemical generation of ferrate at pressed iron powder electrode: comparison with a foil electrode. Electrochimica Acta 48(10), 1435-1442.

De Koninck, M., Brousse, T. and Belanger, D. (2003) The electrochemical generation of ferrate at pressed iron powder electrodes: effect of various operating parameters. Electrochim. Acta 48(10), 1425-1433.

Deininger, J.P. (1993) Process for producing ferrate employing beta-ferric oxide
Olin Corporation (Stamford, CT), United States.

Delaude, L. and Laszlo, P. (1996) A novel oxidizing reagent based on potassium ferrate(VI). J. Org. Chem. 61(18), 6360-6370.

Delgado, S., Alvarez, M., Aguiar, E. and Rodríguez-Gómez, L.E. (1998) Effect of dissolved oxygen in reclaimed wastewater transformation during transportation. Case study: Tenerife, Spain. Water Science and Technology 37(1), 123-130.

DeLuca, S.J., Idle, C.N. and Chao, A.C. (1996) Quality improvement of biosolids by ferrate(VI) oxidation of offensive odour compounds. Water Science and Technology 33(3), 119-130.

Denvir, A. and Pletcher, D. (1996) Electrochemical generation of ferrate .2. Influence of anode composition. Journal of Applied Electrochemistry 26(8), 823-827.

Ding, L., Liang, H.C. and Li, X.Z. (2012) Oxidation of CH_3SH by in situ generation of ferrate(VI) in aqueous alkaline solution for odour treatment. Sep. Purif. Technol. 91(0), 117-124.

Ding, Z., Yang, C.C. and Wu, Q. (2004) The electrochemical generation of ferrate at porous magnetite electrode. Electrochimica Acta 49(19), 3155-3159.

Do, J.S. and Chen, C.P. (1993) In situ oxidative degradation of formaldehyde with electrogenerated hydrogen peroxide. Journal of the Electrochemical Society 140(6), 1632-1637.

Do, J.S., Yeh, W.C. and Chao, I.Y. (1997) Kinetics of the oxidative degradation of formaldehyde with electrogenerated hypochlorite ion. Industrial and Engineering Chemistry Research 36(2), 349-356.

DSD (2009) Sewerage and flood protection - drainage services 1841-2008. Drainage-Services-Department (ed), pp. 166-167, The Government of Hong Kong

Special Administrative Region.

Feliers, C., Patria, L., Morvan, J. and Laplanche, A. (2001) Kinetics of oxidation of odorous sulfur compounds in aqueous alkaline solution with H_2O_2. Environmental Technology 22(10), 1137 - 1146.

Frechen, F.B. (1988) Odour emissions and odour control at wastewater treatment plants in West Germany. Water Sci. Technol. 20(4-5), 261-266.

Galbács, Z.M. and Csányi, L.J. (1983) Alkali-induced decomposition of hydrogen peroxide. Journal of the Chemical Society, Dalton Transactions (11), 2353-2357.

Gilbert, M.B., Waite, T.D. and Hare, C. (1976) Analytical notes-Fan investigation of the applicability of ferrate ion for disinfection. Journal of the American Water Works Association 68(495-497).

Gostelow, P., Parsons, S.A. and Stuetz, R.M. (2001) Odour measurements for sewage treatment works. Water Res. 35(3), 579-597.

Graham, N., Chu, W. and Lau, C. (2003) Observations of 2,4,6-trichlorophenol degradation by ozone. Chemosphere 51(4), 237-243.

Graham, N., Jiang, C.C., Li, X.Z., Jiang, J.Q. and Ma, J. (2004) The influence of pH on the degradation of phenol and chlorophenols by potassium ferrate. Chemosphere 56(10), 949-956.

Gray, K.A. and Waite, T.D. (1983) Coagulation and precipitation studies of the ferrate(VI) ion. Abstracts of Papers American Chemical Society 186, 48.

Gulyas, H. (1997) Processes for the removal of recalcitrant organics from industrial wastewaters. Water Science and Technology 36(2–3), 9-16.

Haaning Nielsen, A., Lens, P., Vollertsen, J. and Hvitved-Jacobsen, T. (2005) Sulfide–iron interactions in domestic wastewater from a gravity sewer. Water

Research 39(12), 2747-2755.

He, C., Li, X.Z., Sharma, V.K. and Li, S.Y. (2009) Elimination of sludge odor by oxidizing sulfur-containing compounds with ferrate(VI). Environ. Sci. Technol. 43(15), 5890-5895.

He, W.C., Wang, J.M., Yang, C.C. and Zhang, J.Q. (2006) The rapid electrochemical preparation of dissolved ferrate(VI): effects of various operating parameters. Electrochim. Acta 51(10), 1967-1973.

Hentz, L.H. and Balchunas, B.M. (2000) Chemical and physical processes associated with mass transfer in odor control scrubbers, pp. 1013-1030, Cincinnati, US.

Hives, J., Benova, M., Bouzek, K. and Sharma, V.K. (2006) Electrochemical formation of ferrate(VI) in a molten NaOH-KOH system. Electrochem. Commun. 8(11), 1737-1740.

Hives, J., Macova, Z., Benova, M. and Bouzek, K. (2008) Comparison of ferrate(VI) synthesis in eutectic NaOH-KOH melts and in aqueous solutions. Journal of the Electrochemical Society 155(9), E113-E119.

Hoffmann, M.R., Martin, S.T., Choi, W. and Bahnemann, D.W. (1995) Environmental applications of semiconductor photocatalysis. Chemical Reviews 95(1), 69-96.

Hoigné, J. and Bader, H. (1983a) Rate constants of reactions of ozone with organic and inorganic compounds in water—II: Dissociating organic compounds. Water Research 17(2), 185-194.

Hoigné, J. and Bader, H. (1983b) Rate constants of reactions of ozone with organic and inorganic compounds in water—I: Non-dissociating organic compounds. Water Research 17(2), 173-183.

Hoppe, M.L., Schlemper, E.O. and Murmann, R.K. (1982) Structure of dipotassium ferrate(VI). Acta Crystallographica Section B 38, 2237-2239.

Huang, H., Sommerfeld, D., Dunn, B.C., Eyring, E.M. and Lloyd, C.R. (2001) Ferrate(VI) oxidation of aqueous phenol: Kinetics and mechanism. Journal of Physical Chemistry A 105(14), 3536-3541.

Hwang, Y., Matsuo, T., Hanaki, K. and Suzuki, N. (1994) Removal of odorous compounds in wastewater by using activated carbon, ozonation and aerated biofilter. Water Research 28(11), 2309-2319.

I, Y.-P., Liu, Y.-C., Han, K.-Y. and She, T.-C. (2004) Construction of a low-pressure microwave plasma reactor and its application in the treatment of volatile organic compounds. Environmental Science & Technology 38(13), 3785-3791.

Iranpour, R., Cox, H.H.J., Deshusses, M.A. and Schroeder, E.D. (2005) Literature review of air pollution control biofilters and biotrickling filters for odor and volatile organic compound removal. Environmental Progress 24(3), 254-267.

Jain, A., Sharma, V.K. and Mbuya, O.S. (2009) Removal of arsenite by Fe(VI), Fe(VI)/Fe(III), and Fe(VI)/Al(III) salts: Effect of pH and anions. Journal of Hazardous Materials 169(1-3), 339-344.

Jameel, P. (1989) The use of ferrous chloride to control dissolved sulfides in interceptor sewers. Water Pollution Control Federation 61(2), 230-236.

Jensen, A.B. and Webb, C. (1995) Treatment of H_2S-containing gases: A review of microbiological alternatives. Enzyme and Microbial Technology 17(1), 2-10.

Jiang, J.Q. and Lloyd, B. (2002) Progress in the development and use of ferrate(VI) salt as an oxidant and coagulant for water and wastewater treatment. Water Res. 36(6), 1397-1408.

Jiang, J.Q., Stanford, C. and Alsheyab, M. (2009) The online generation and application of ferrate(VI) for sewage treatment--A pilot scale trial. Sep. Purif. Technol. 68(2), 227-231.

Jiang, J.Q., Yin, Q., Zhou, J.L. and Pearce, P. (2005) Occurrence and treatment trials of endocrine disrupting chemicals (EDCs) in wastewaters. Chemosphere 61(4), 544-550.

Johnson, M.D. and Hornstein, B.J. (1996) Unexpected selectivity in the oxidation of arylamines with ferrate-preliminary mechanistic considerations. Chemical Communications (8), 965-966.

Johnson, M.D. and Hornstein, B.J. (2003) The kinetics and mechanism of the ferrate(VI) oxidation of hydroxylamines. Inorganic Chemistry 42(21), 6923-6928.

Johnson Michael, D., Hornstein Brooks, J. and Wischnewsky, J. (2008) Ferrates, pp. 177-188, American Chemical Society.

Kachina, A., Preis, S. and Kallas, J. (2006) Catalytic TiO_2 oxidation of ethanethiol for environmentally begnin air pollution control of sulphur compounds. Environmental Chemistry Letters 4(2), 107-110.

Kanagawa, T. and Mikami, E. (1989) Removal of methanethiol, dimethyl sulfide, dimethyl disulfide, and hydrogen sulfide from contaminated air by Thiobacillus thioparus TK-m. Applied and Environmental Microbiology 55(3), 555-558.

Kasakura, T. and Tatsukawa, K. (1995) On the scent of a good idea for odour removal. Water Quality International (2), 24-27.

Kastner, J.R., Das, K.C., Buquoi, Q. and Melear, N.D. (2003) Low temperature catalytic oxidation of hydrogen sulfide and methanethiol using wood and coal fly ash. Environmental Science and Technology 37(11), 2568-2574.

Katoh, H., Kuniyoshi, I., Hirai, M. and Shoda, M. (1995) Studies of the oxidation mechanism of sulphur-containing gases on wet activated carbon fibre. Applied Catalysis B: Environmental 6(3), 255-262.

Kazama, F. (1995) Viral inactivation by potassium ferrate. Water Science and

Technology 31(5–6), 165-168.

Khataee, A.R., Vatanpour, V. and Amani Ghadim, A.R. (2009) Decolorization of C.I. Acid Blue 9 solution by UV/Nano-TiO_2, Fenton, Fenton-like, electro-Fenton and electrocoagulation processes: A comparative study. Journal of Hazardous Materials 161(2–3), 1225-1233.

Lapicque, F. and Valentin, G. (2002) Direct electrochemical preparation of solid potassium ferrate. Electrochemistry Communications 4(10), 764-766.

Laplanche, A., Bonnin, C. and Darmon, D. (1994) Studies in Environmental Science, pp. 277-294, Elsevier.

Lee, Y., Cho, M., Kim, J.Y. and Yoon, J. (2004) Chemistry of ferrate (Fe(VI)) in aqueous solution and its applications as a green chemical. Journal of Industrial and Engineering Chemistry 10(1), 161-171.

Lescuras-Darrou, V., Lapicque, F. and Valentin, G. (2002) Electrochemical ferrate generation for waste water treatment using cast irons with high silicon contents. Journal of Applied Electrochemistry 32(1), 57-63.

Li, C., Li, X.Z. and Graham, N. (2005a) A study of the preparation and reactivity of potassium ferrate. Chemosphere 61(4), 537-543.

Li, F.B., Li, X.Z. and Hou, M.F. (2004) Photocatalytic degradation of 2-mercaptobenzothiazole in aqueous La 3+-TiO2 suspension for odor control. Applied Catalysis B: Environmental 48(3), 185-194.

Li, F.B., Li, X.Z. and Ng, K.H. (2005b) Photocatalytic degradation of an odorous pollutant: 2-Mercaptobenzothiazole in aqueous suspension using Nd^{3+}–TiO_2 catalysts. Industrial and Engineering Chemistry Research 45(1), 1-7.

Li, X.Z. and Li, F.B. (2001) Study of Au/Au^{3+}-TiO_2 photocatalysts toward visible photooxidation for water and wastewater treatment. Environmental Science and

Technology 35(11), 2381-2387.

Li, X.Z., Hou, M.F., Li, F.B. and Chua, H. (2005c) Photocatalytic oxidation of methyl mercaptan in foul gas for odor control. Industrial and Engineering Chemistry Research 45(2), 487-494.

Li, X.Z., Hou, M.F., Li, F.B. and Chua, H. (2006) Photocatalytic oxidation of methyl mercaptan in foul gas for odor control. Ind. Eng. Chem. Res. 45(2), 487-494.

Lian, R., Crowell, R.A., Shkrob, I.A., Bartels, D.M., Oulianov, D.A. and Gosztola, D. (2004) Recombination of geminate (OH, e(aq)(-)) pairs in concentrated alkaline solutions: lack of evidence for hydroxyl radical deprotonation. Chemical Physics Letters 389(4-6), 379-384.

Licht, S. (1985) pH measurement in concentrated alkaline solutions. Analytical chemistry 57(2), 514-519.

Licht, S. and Yu, X.W. (2005) Electrochemical alkaline Fe(VI) water purification and remediation. Environ. Sci. Technol. 39, 8071-8076.

Licht, S., Wang, B. and Ghosh, S. (1999) Energetic iron(VI) chemistry: The super-iron battery. Science 285(5430), 1039-1042.

Licht, S., Naschitz, V. and Wang, B. (2002a) Rapid chemical synthesis of the barium ferrate super-iron Fe (VI) compound, $BaFeO_4$. Journal of Power Sources 109(1), 67-70.

Licht, S., Tel-Vered, R. and Halperin, L. (2002b) Direct electrochemical preparation of solid Fe(VI) ferrate and super-iron battery compounds. Electrochem. Commun. 4(11), 933-937.

Licht, S., Naschitz, V. and Ghosh, S. (2002c) Silver mediation of Fe(VI) charge transfer: Activation of the K_2FeO_4 super-iron cathode. The Journal of Physical Chemistry B 106(23), 5947-5955.

Licht, S., Tel-Vered, R. and Halperin, L. (2004) Toward efficient electrochemical synthesis of Fe(VI) ferrate and super-iron battery compounds. J. Electrochem. Soc. 151(1), A31-A39.

Licht, S., Naschitz, V., Halperin, L., Halperin, N., Lin, L., Chen, J.J., Ghosh, S. and Liu, B. (2001) Analysis of ferrate(VI) compounds and super-iron Fe(VI) battery cathodes: FTIR, ICP, titrimetric, XRD, UV/VIS, and electrochemical characterization. Journal of Power Sources 101(2), 167-176.

Liu, T.X., Li, X.Z. and Li, F.B. (2008) $AgNO_3$-induced photocatalytic degradation of odorous methyl mercaptan in gaseous phase: Mechanism of chemisorption and photocatalytic reaction. Environ. Sci. Technol. 42(12), 4540-4545.

Liu, T.X., Li, X.Z. and Li, F.B. (2010) Development of a photocatalytic wet scrubbing process for gaseous odor treatment. Ind. Eng. Chem. Res. 49(8), 3617-3622.

Luo, Z., Strouse, M., Jiang, J.Q. and Sharma, V.K. (2011) Methodologies for the analytical determination of ferrate(VI): A review. J. Environ. Sci. Heal. A 46(5), 453-460.

Mácová, Z., Bouzek, K. and Sharma, V.K. (2008) Ferrates: synthesis, properties, and applications in water and wastewater treatment, American Chemical Society.

Macova, Z., Bouzek, K., Hives, J., Sharma, V.K., Terryn, R.J. and Baum, J.C. (2009a) Research progress in the electrochemical synthesis of ferrate(VI). Electrochimica Acta 54(10), 2673-2683.

Macova, Z., Bouzek, K., Hives, J., Sharma, V.K., Terryn, R.J. and Baum, J.C. (2009b) Research progress in the electrochemical synthesis of ferrate(VI). Electrochim. Acta 54(10), 2673-2683.

Mansfield, L.A., Melnyk, P.B. and Richardson, G.C. (1992) Selection and full-Scale use of a chelated iron absorbent for odor control. Water Environment Research 64(2), 120-127.

Masgrau, L., González-Lafont, À. and Lluch, J.M. (2003) Variational transition-state theory rate constant calculations of the OH + CH_3SH reaction and several isotopic variants. The Journal of Physical Chemistry A 107(22), 4490-4496.

Murmann, R.K. and Robinson, P.R. (1974) Experiments utilizing FeO_4^{2-} for purifying water. Water Research 8(8), 543-547.

Myung, C.J., Suk, C.W. and Lee, J.H. (1999) Removal of organo-sulphur odour compounds by Thiobacillus novellus SRM, sulphur-oxidizing microorganisms. Process Biochem. 34(6-7), 659-665.

Newcombe, G., Morrison, J. and Hepplewhite, C. (2002) Simultaneous adsorption of MIB and NOM onto activated carbon. I. Characterisation of the system and NOM adsorption. Carbon 40(12), 2135-2146.

Nielsen, A.H., Yongsiri, C., Hvitved-Jacobsen, T. and Vollertsen, J. (2005) Simulation of sulfide buildup in wastewater and atmosphere of sewer networks. Water Science and Technology 52, 201–208.

Norcross, B.E., Lewis, W.C., Gai, H., Noureldin, N.A. and Lee, D.G. (1997) The oxidation of secondary alcohols by potassium tetraoxoferrate(VI). Canadian Journal of Chemistry 75(2), 129-139.

Ockerman, L.T. and Schreyer, J.M. (1951) Preparation of sodium ferrate(VI). J. Am. Chem. Soc. 73(11), 5478-5478.

Osathaphan, K., Tiyanont, P., Yngard, R.A. and Sharma, V.K. (2009) Progress in Environmental Science and Technology, pp. 966-970.

Padival, N.A., Weiss, J.S. and Arnold, R.G. (1995) Control of Thiobacillus by means of microbial competition: Implications for corrosion of concrete sewers. Water Environment Research 67(2), 201-205.

Paillard, H. and Blondeau, F. (1988) Les nuisances olfactives en assainissement: causes et remèdes. T.S.M.-L'EAU 2, 79-88.

Perfiliev, Y.D., Benko, E.M., Pankratov, D.A., Sharma, V.K. and Dedushenko, S.K. (2007) Formation of iron(VI) in ozonalysis of iron(III) in alkaline solution. Inorganica Chimica Acta 360(8), 2789-2791.

Phae, C.G. and Shoda, M. (1991) A new fungus which degrades hydrogen sulfide, methanethiol, dimethyl sulfide and dimethyl disulfide. Biotechnology Letters 13(5), 375-380.

Pichat, P., Disdier, J., Hoang-Van, C., Mas, D., Goutailler, G. and Gaysse, C. (2000) Purification/deodorization of indoor air and gaseous effluents by TiO2 photocatalysis. Catalysis Today 63(2–4), 363-369.

Poduska, R.A. and Anderson, B.D. (1981) Successful storage lagoon odor control. Water Pollution Control Federation 53(3), 299-310.

Potts, M.E. and Churchwell, D.R. (1994) Removal of radionuclides in wastewaters utilizing potassium ferrate(VI). Water Environment Research 66(2), 107-109.

Rabald (1954) Oxidation of metals and alloys. Von O. Kubaschewski und B. E. Hopkins. London: Butterworths Scientific Publications 1953. 239 S., 84 Abb., 18 Zahlentafeln, 35.

Read, J.F., John, J., MacPherson, J., Schaubel, C. and Theriault, A. (2001) The kinetics and mechanism of the oxidation of inorganic oxysulfur compounds by potassium ferrate. Part I. Sulfite, thiosulfate and dithionite ions. Inorganica Chimica Acta 315(1), 96-106.

Rideh, L., Wehrer, A., Ronze, D. and Zoulalian, A. (1997) Photocatalytic degradation of 2-chlorophenol in TiO_2 aqueous suspension: Modeling of reaction rate. Industrial and Engineering Chemistry Research 36(11), 4712-4718.

Riener, C., Kada, G. and Gruber, H. (2002) Quick measurement of protein sulfhydryls with Ellman's reagent and with 4,4'-dithiodipyridine. Anal. Bioanal. Chem. 373(4), 266-276.

Sanchez, C., Couvert, A., Laplanche, A. and Renner, C. (2006) New compact scrubber for odour removal in wastewater treatment plants. Water Sci. Technol. 54(9), 45-52.

Schink, T. and Waite, T.D. (1980) Inactivation of f2 virus with ferrate (VI). Water Research 14(12), 1705-1717.

Schroth, M.H., Oostrom, M., Wietsma, T.W. and Istok, J.D. (2001) In-situ oxidation of trichloroethene by permanganate: effects on porous medium hydraulic properties. Journal of Contaminant Hydrology 50(1-2), 79-98.

Shao, H.B., Wang, J.M., He, W.C., Zhang, J.Q. and Cao, C.N. (2005) EIS analysis on the anodic dissolution kinetics of pure iron in a highly alkaline solution. Electrochem. Commun. 7(12), 1429-1433.

Shao, M.-h., Liu, P. and Adzic, R.R. (2006) Superoxide anion is the intermediate in the oxygen reduction reaction on platinum electrodes. Journal of the American Chemical Society 128(23), 7408-7409.

Sharma, V.K. (2002) Potassium ferrate(VI): an environmentally friendly oxidant. Advances in Environmental Research 6(2), 143-156.

Sharma, V.K. (2010a) Oxidation of nitrogen-containing pollutants by novel ferrate(VI) technology: A review. Journal of Environmental Science and Health Part a-Toxic/Hazardous Substances & Environmental Engineering 45(6), 645-667.

Sharma, V.K. (2010b) Oxidation of inorganic compounds by ferrate(VI) and ferrate(V): One-electron and two-electron transfer steps. Environ. Sci. Technol. 44(13), 5148-5152.

Sharma, V.K. (2011) Oxidation of inorganic contaminants by ferrates (VI, V, and

IV)–kinetics and mechanisms: A review. Journal of Environmental Management 92(4), 1051-1073.

Sharma, V.K. and Bielski, B.H.J. (1991) Reactivity of ferrate(VI) and ferrate(V) with amino-acids. Inorganic Chemistry 30(23), 4306-4310.

Sharma, V.K. and Cabelli, D. (2009) Reduction of oxyiron(V) by sulfite and thiosulfate in aqueous solution. Journal of Physical Chemistry A 113(31), 8901-8906.

Sharma, V.K., Obrien, B. and Smith, J.O. (1997a) Removal of cyanide in rinse water by ferrate(VI). Abstracts of Papers of the American Chemical Society 213, 238-ENVR.

Sharma, V.K., Smith, J.O. and Millero, F.J. (1997b) Ferrate(VI) oxidation of hydrogen sulfide. Environmental Science and Technology 31(9), 2486-2491.

Sharma, V.K., Bloom, J.T. and Joshi, V.N. (1998a) Oxidation of ammonia by ferrate(VI). Journal of Environmental Science and Health Part a-Toxic/Hazardous Substances & Environmental Engineering 33(4), 635-650.

Sharma, V.K., Luther, G.W. and Millero, F.J. (2011) Mechanisms of oxidation of organosulfur compounds by ferrate(VI). Chemosphere 82(8), 1083-1089.

Sharma, V.K., Rivera, W., Smith, J.O. and O'Brien, B. (1998b) Ferrate(VI) oxidation of aqueous cyanide. Environmental Science and Technology 32(17), 2608-2613.

Sharma, V.K., Rendon, R.A., Millero, F.J. and Vazquez, F.G. (2000) Oxidation of thioacetamide by ferrate(VI). Marine Chemistry 70(1-3), 235-242.

Sharma, V.K., Rivera, W., Joshi, V.N., Millero, F.J. and O'Connor, D. (1999) Ferrate(VI) oxidation of thiourea. Environmental Science and Technology 33(15), 2645-2650.

Sioukri, E. and Bandosz, T.J. (2005) Enhancement of the performance of activated carbons as municipal odor removal media by addition of a sewage-sludge-derived phase. Environmental Science and Technology 39(16), 6225-6230.

Smet, E., Lens, P. and Van Langenhove, H. (1998) Treatment of waste gases contaminated with odorous sulfur compounds. Critical Reviews in Environmental Science and Technology 28(1), 89-117.

Smet, E., Chasaya, G., Van Langenhove, H. and Verstraete, W. (1996) The effect of inoculation and the type of carrier material used on the biofiltration of methyl sulphides. Applied Microbiology and Biotechnology 45(1-2), 293-298.

Solo, H.M. and Waite, T.D. (1989) Direct-filtration of ground-water using iron(VI) ferrateFa pilot-study. Abstracts of Papers American Chemical Society 198, 119.

Špalek, O., Balej, J. and Paseka, I. (1982) Kinetics of the decomposition of hydrogen peroxide in alkaline solutions. Journal of the Chemical Society, Faraday Transactions 1: Physical Chemistry in Condensed Phases 78(8), 2349-2359.

Stahl, G.E. (1715) Opusculum chymico-physico-medicum halae-magdeburgiae. str. 742

Stanford, C., Jiang, J.Q. and Alsheyab, M. (2010) Electrochemical production of ferrate (Iron VI): application to the wastewater treatment on a laboratory scale and comparison with Iron (III) coagulant. Water Air and Soil Pollution 209(1-4), 483-488.

Stephanson, C.J. and Flanagan, G.P. (2003) Antioxidant capacity of silica hydride: a combinational photosensitization and fluorescence detection assay. Free Radical Biol. Med. 35(9), 1129-1137.

Stupin, D.Y. and Ozernoi, M.I. (1995) Coprecipitation of {sup 152}Eu with Iron(III) hydroxide formed upon reduction of sodium ferrate(VI) in aqueous medium. Radiochemistry 37(4), 329-332.

Sun, X., Zhang, B., He, L.A., Hou, H.Q. and Zhang, R.X. (2010) Photolysis of H_2S

with interior microwave discharge electrodeless lamps. Chinese Chem. Lett. 21(8), 968-972.

Tanada, S. and Boki, K. (1979) Adsorption of various kinds of offensive odor substances on activated carbon and zeolite. Bulletin of Environmental Contamination and Toxicology 23(1), 524-530.

Tanaka, N. and Takenaka, K. (1995) Control of hydrogen sulfide and degradation of organic matter by air injection into a wastewater force main. Water Science and Technology 31(7), 273-282.

Tanaka, N., Hvitved-Jacobsen, T., Ochi, T. and Sato, N. (2000) Aerobic–anaerobic microbial wastewater transformations and reaeration in an air-injected pressure sewer. Water Environment Research 72(6), 665-674.

Tanji, Y., Kanagawa, T. and Mikami, E. (1989) Removal of dimethyl sulfide, methyl mercaptan, and hydrogen sulfide by immobilized Thiobacillus thioparus TK-m. Journal of Fermentation and Bioengineering 67(4), 280-285.

Thompson, G.W., Ockerman, L.T. and Schreyer, J.M. (1951) Preparation and purification of potassium ferrate(VI). J. Am. Chem. Soc. 73(3), 1379-1381.

Thompson, J.A. (1983) Process for producing alkali metal ferrates.

Thompson, J.A. (1985) Process for producing alkali metal ferrates utilizing hematite and magnetite.

Thompson, T.L. and Yates, J.T. (2006) Surface science studies of the photoactivation of TiO_2—new photochemical processes. Chemical Reviews 106(10), 4428-4453.

Tiwari, D., Kim, H.U., Choi, B.J., Lee, S.M., Kwon, O.H., Choi, K.M. and Yang, J.K. (2007) Ferrate(VI): A green chemical for the oxidation of cyanide in aqueous/waste solutions. Journal of Environmental Science and Health Part a-Toxic/Hazardous Substances & Environmental Engineering 42(6), 803-810.

Tomar, M. and Abdullah, T.H.A. (1994) Evaluation of chemicals to control the generation of malodorous hydrogen sulfide in waste water. Water Research 28(12), 2545-2552.

Toušek, J. (1962) Collect. Czech. Chem. Commun. 27, 914.

Tsai, C.H., Lee, W.J., Chen, C.Y. and Liao, W.T. (2001) Decomposition of CH_3SH in a RF plasma reactor: Reaction products and mechanisms. Ind. Eng. Chem. Res. 40(11), 2384-2395.

Tsai, C.H., Lee, W.J., Chen, C.Y., Tsai, P.J., Fang, G.C. and Shih, M. (2003) Difference in conversions between dimethyl sulfide and methanethiol in a cold plasma environment. Plasma Chem. Plasma P. 23(1), 141-157.

Tsuda, Y. and Nakajima, S. (1978) Potassium ferrate, a new selective oxidating agent. Chemistry Letters 7(12), 1397-1398.

Turk, A., Sakalis, E., Lessuck, J., Karamitsos, H. and Rago, O. (1989) Ammonia injection enhances capacity of activated carbon for hydrogen sulfide and methyl mercaptan. Environmental Science and Technology 23(10), 1242-1245.

Van Durme, G.P., McNamara, B.F. and McGinley, C.M. (1992) Bench-scale removal of odor and volatile organic compounds at a composting facility. Water Environment Research 64(1), 19-27.

Waite, T.D. (1979) Feasibility of wastewater treatment with ferrate. Journal of Environmental Engineering-Asce 105, 1023-1034.

Westerhoff, P., Aiken, G., Amy, G. and Debroux, J. (1999) Relationships between the structure of natural organic matter and its reactivity towards molecular ozone and hydroxyl radicals. Water Research 33(10), 2265-2276.

Williams, D.H. and Riley, J.T. (1974) Preparation and alcohol oxidation studies of the ferrate(VI) ion, FeO_4^{2-}. Inorganica Chimica Acta 8(0), 177-183.

Wood, R.H. (1958) The heat, free energy and entropy of the ferrate(VI) ion. Journal of the American Chemical Society 80(9), 2038-2041.

Wulfsberg, G. (ed) (2000) Inorganic chemistry, Sausalito, California, USA.

Xia, D., He, C., Zhu, L., Huang, Y., Dong, H., Su, M., Asi, M.A. and Bian, D. (2011) A novel wet-scrubbing process using Fe(vi) for simultaneous removal of SO_2 and NO. Journal of Environmental Monitoring 13(4), 864-870.

Yan, N.Q., Qu, Z., Jia, J.P., Wang, X.P. and Wu, D. (2006) Removal characteristics of gaseous sulfur-containing compounds by pulsed corona plasma. Ind. Eng. Chem. Res. 45(19), 6420-6427.

Yang, E.l., Shi, J.j. and Liang, H.c. (2012) On-line electrochemical production of ferrate (VI) for odor control. Electrochimica Acta 63(0), 369-374.

Yang, W., Vollertsen, J. and Hvitved-Jacobsen, T. (2005) Anoxic sulfide oxidation in wastewater of sewer networks. Water Science and Technology 52(30), 191–199.

Yu, X.W. (2008) Advances in electrochemical Fe synthesis and analysis. J. Appl. Electrochem. 38, 731-742.

Zhang, L., De Schryver, P., De Gusseme, B., De Muynck, W., Boon, N. and Verstraete, W. (2008) Chemical and biological technologies for hydrogen sulfide emission control in sewer systems: A review. Water Research 42(1–2), 1-12.

Zhao, Y., Han, Y.H., Ma, T.Z. and Guo, T.X. (2011) Simultaneous desulfurization and denitrification from flue gas by ferrate(VI). Environmental Science and Technology 45(9), 4060-4065.

Ziolek, M. and Decyk, P. (1999) Relation between chemisorption and catalytic transformation of R_2S compounds on Faujasite-Type Zeolites. Langmuir 15(18), 5781-5784.